RESEARCH DEPARTMENT REPORT SERIES No. 2-2008 ISSN 1749-8775

PALAEOLITHIC RIVERS OF SOUTH-WEST BRITAIN

OPTICALLY STIMULATED LUMINESCENCE DATING OF RESIDUAL DEPOSITS OF THE PROTO-AXE, EXE, OTTER, AND DONIFORD

SCIENTIFIC DATING REPORT

Phillip Toms, Tony Brown, Laura Basell, and Rob Hosfield

ENGLISH HERITAGE

Research Department Report Series 2-2008

PALAEOLITHIC RIVERS OF SOUTH-WEST BRITAIN: OPTICALLY STIMULATED LUMINESCENCE DATING OF RESIDUAL DEPOSITS OF THE PROTO-AXE, EXE, OTTER, AND DONIFORD

Dr P S Toms[1], Prof A G Brown[2], Dr L S Basell,[3] and Dr R T Hosfield[4]

© English Heritage

ISSN 1749-8775

The Research Department Report Series incorporates reports from all the specialist teams within the English Heritage Research Department: Archaeological Science; Archaeological Archives; Historic Interiors Research and Conservation; Archaeological Projects; Aerial Survey and Investigation; Archaeological Survey and Investigation; Architectural Investigation; Imaging, Graphics and Survey; and the Survey of London. It replaces the former Centre for Archaeology Reports Series, the Archaeological Investigation Report Series, and the Architectural Investigation Report Series.
Many of these are interim reports, which make available the results of specialist investigations in advance of full publication. They are not usually subject to external refereeing, and their conclusions may sometimes have to be modified in the light of information not available at the time of the investigation. Where no final project report is available, readers are advised to consult the author before citing these reports in any publication. Opinions expressed in Research Department Reports are those of the author(s) and are not necessarily those of English Heritage.

Requests for further hard copies, after the initial print run, can be made by emailing:
Res.reports@english-heritage.org.uk.
or by writing to English Heritage, Fort Cumberland, Fort Cumberland Road, Eastney, Portsmouth PO4 9LD
Please note that a charge will be made to cover printing and postage.

SUMMARY

This study contributes to the Palaeolithic Rivers of South-West Britain project, which aims to synthesise the open air archaeological evidence for the Lower and Middle Palaeolithic occupation of south west Britain. Such evidence is dominated by stone tool assemblages found in secondary contexts, within river terrace deposits. Dating these sediments offers an opportunity to delimit periods of hominin occupation. The purpose of this study is to provide an outline of the temporal range of artefact-bearing terraces of the Rivers Axe, Exe, Otter, and Doniford by means of optically stimulated luminescence (OSL) dating. In total, 26 sediment samples were dated. The reliability of age estimates was assessed on the basis of analytical acceptability and, where possible, the degree of age convergence from samples of divergent dosimetry obtained from equivalent stratigraphic units. It is surmised that the Axe was aggrading at intervals between at least 86 and 401ka (Marine Isotope Stages 5 to 10), the Exe before 10ka and perhaps further back than 86ka (MIS >1 to >5), the Otter before 66ka and by at least 209ka (MIS >3 to 7), and the Doniford at intervals between at least 22 and 71ka (MIS 2 to 4). The age estimates of sediments from the Exe, Otter, and Doniford indicate that some Palaeolithic finds in these catchments have been reworked; nonetheless the chronology greatly facilitates comparison with the cave sequences in the region by providing a preliminary spatio-temporal model for open sites.

ARCHIVE LOCATION

University of Southampton

CONTACT DETAILS

[1]Geochronology Laboratories, Department of Natural and Social Sciences, University of Gloucestershire, Swindon Road, Cheltenham GL50 4AZ. Tel: 01242 714708.
Email: ptoms@glos.ac.uk

[2]School of Geography, University of Southampton, Highfield, Southampton SO17 1BJ

[3]Research Laboratory for Archaeology and the History of Art, University of Oxford, Dyson Perrins Building, South Parks Road, Oxford OX1 3QY

[4]Department of Archaeology, School of Human and Environmental Science, University of Reading, Whiteknights, PO Box 227, Reading RG6 6AB

CONTENTS

1.0 Introduction 1

2.0 Optical dating: mechanisms and principles 8

3.0 Sample collection and preparation 8

4.0 Acquisition and accuracy of D_e value 9

4.1 Laboratory factors 9

4.1.1 Feldspar contamination 9

4.1.2 Preheating 10

4.1.3 Irradiation 11

4.1.4 Internal consistency 11

4.2 Environmental factors 11

4.2.1 Incomplete zeroing 11

4.2.2 Turbation 12

5.0 Acquisition and accuracy of D_r value 12

6.0 Estimation of age 13

7.0 Analytical uncertainty 13

8.0 Intrinsic assessment of reliability 14

9.0 Discussion 14

10.0 References 18

Appendices 22

1.0 INTRODUCTION

This study contributes to the Palaeolithic Rivers of Southwest Britain (PRoSWeB) project, funded through the Aggregates Levy Sustainability Fund, administered by English Heritage (EH project number: 3847MAIN). The aim of PRoSWeB is to synthesise the open-air archaeological evidence for the Lower and Middle Palaeolithic occupation of southwest Britain (*c* 500–40ka). The majority of evidence for hominin presence within this period consists of assemblages of stone tools deposited by hominins on floodplains, or entrained by ancient rivers and archived within terrace deposits. Through dating these secondary contexts, the timing of occupation can be delimited.

Phase 1 of PRoSWeB focused on assessing the known Lower and Middle Palaeolithic finds from river gravels, the fluvial deposits and terrace landforms of south west Britain. It revealed the archaeological record, mass of fluvial deposits and number of terrace landforms were significantly greater than had been previously reported (eg Wymer 1999). Archaeologically, the number of findspots in fluvial contexts was some 48% greater than that previously documented and, whilst confirming the Axe Valley as a focus of hominin activity, new, yet infrequent findspots were uncovered to the west (Fig 1). Geomorphologically, the Axe comprises thick sequences of sands and gravels: it is a fill terrace system, and lacks an altitudinally distinct terrace system. In contrast, the Exe and Otter are characterised by staircase terrace systems; their archaeology-bearing deposits are also more extensive than hitherto recorded. Phase 1 also highlighted the lack of chronological control within these fluvial sequences, restricting the contextualisation of the archaeology. Considering the revised assessment of findspots and terrace deposits, along with the location of current /potential aggregate extraction, Phase 2 focused on the valleys of the Axe (at Chard, Kilmington, and Broom), Exe (at Princesshay, Yellowford Farm, Fortescue Farm), Otter (at Monkey Lane, Budleigh Salterton) and Doniford (at Doniford) (Figs 2-8).

In support of Phase 2, the aim of this study is to provide the first estimates of the chronological spread in residual deposits of the proto-Axe, Exe, Otter, and Doniford Rivers, within which artefacts are dispersed. Optically stimulated luminescence (OSL) dating is used as the chronometer. This investigation builds on the earlier luminescence study of Toms *et al* (2005) at Broom on deposits of the River Axe, which were optically dated to Marine Isotope Stage (MIS) 7 to >MIS 9 (195ka to >297ka).

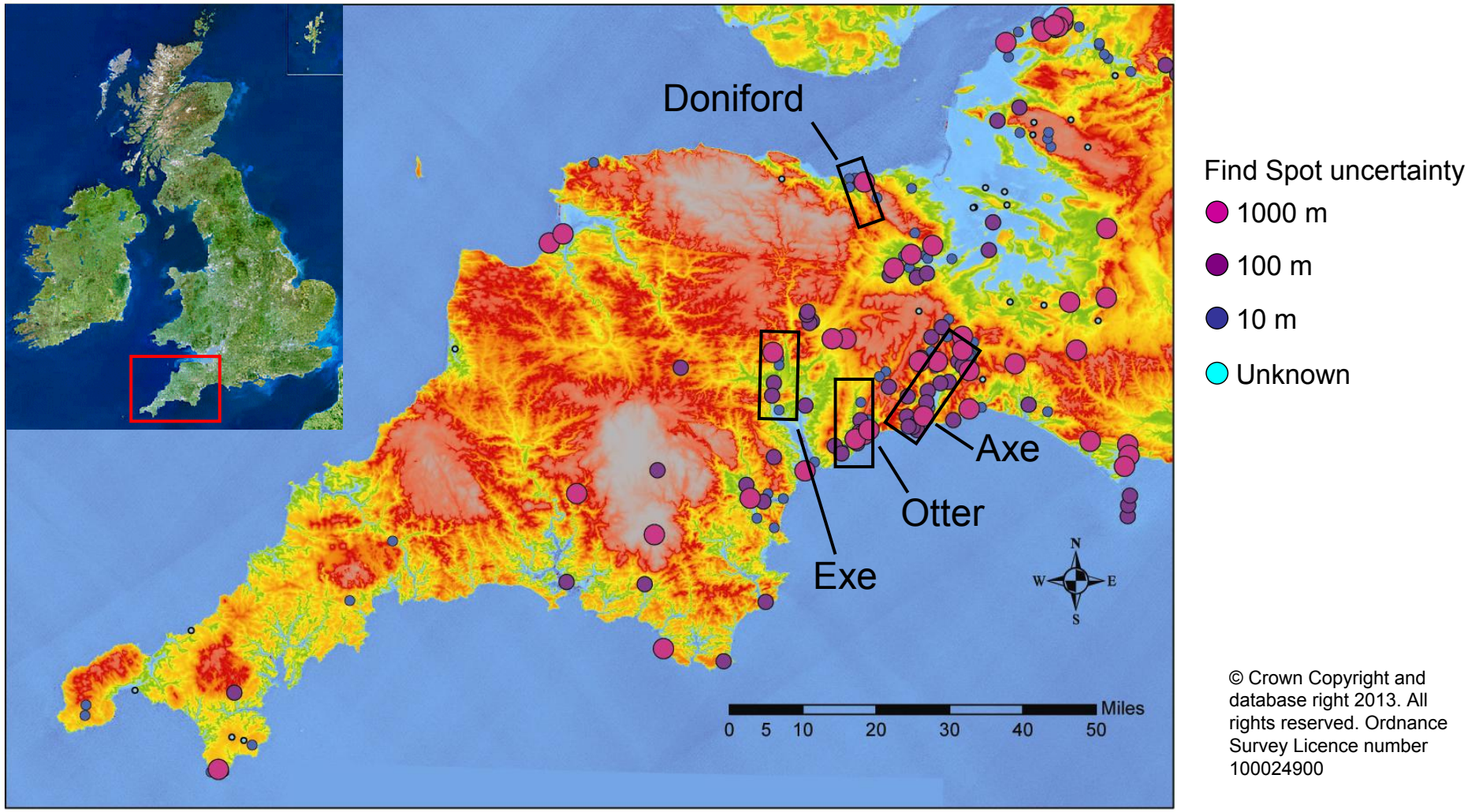

© Crown Copyright and database right 2013. All rights reserved. Ordnance Survey Licence number 100024900

Figure 1: Study area highlighting the river valleys of the Axe, Exe, Otter and Doniford and associated (open) Palaeolithic findspots

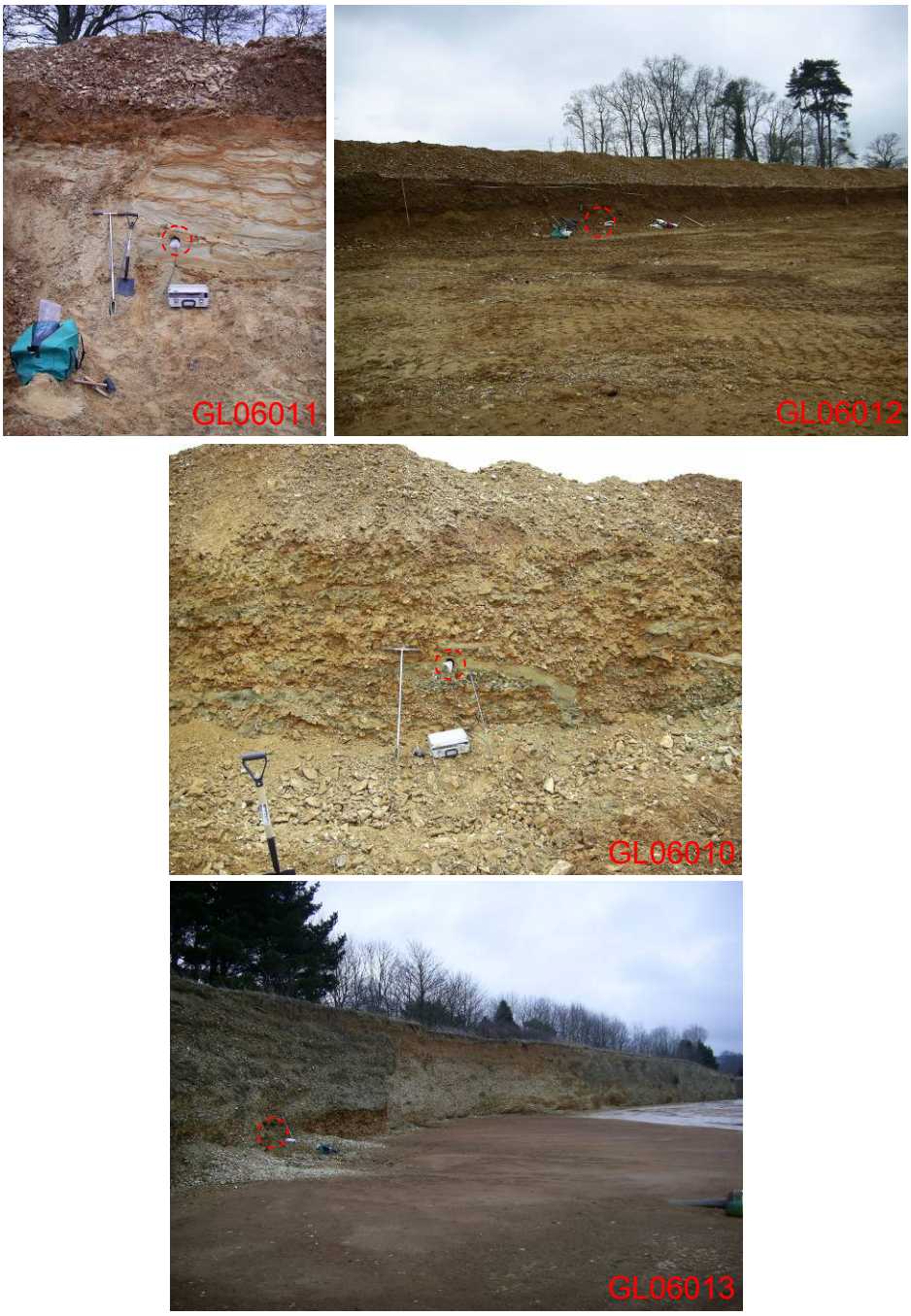

Figure 2: Images of sampling locations at Chard Junction (proto-Axe, ST 346 046)

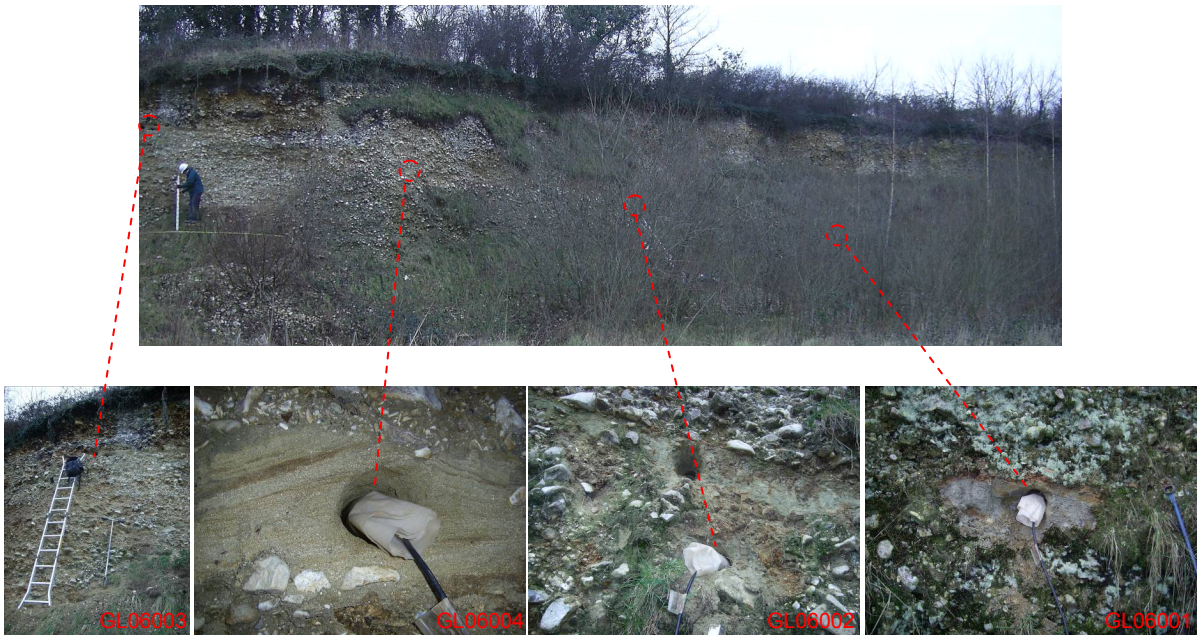

Figure 3: Images of sampling locations at Kilmington (proto-Axe, SY 275 978);

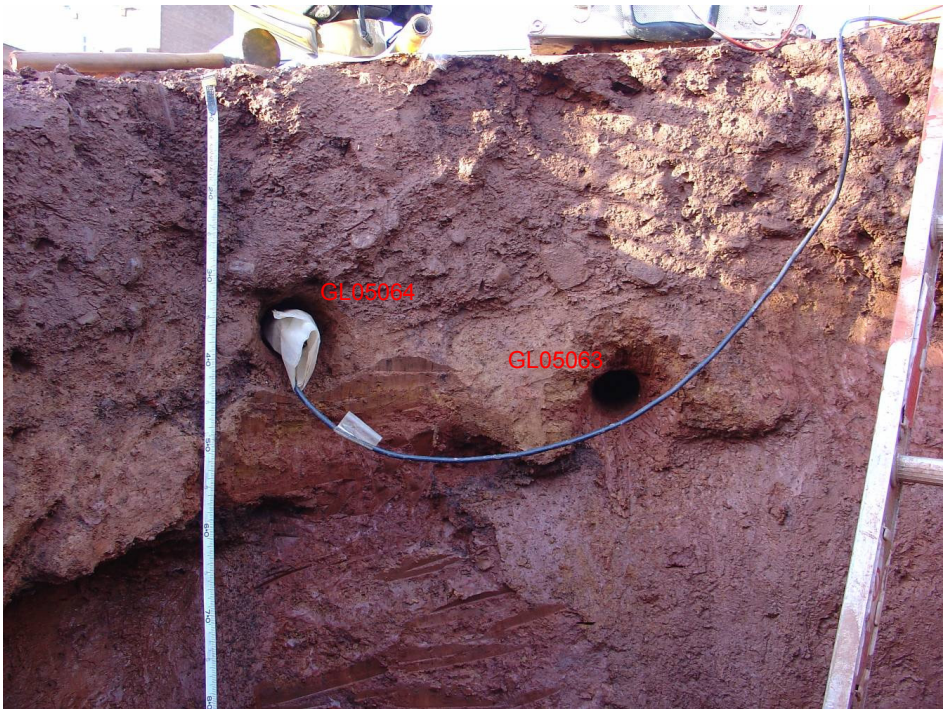

Figure 4: Image of sampling locations at Princesshay (proto-Exe, SX 922 927)

Figure 5: Images of sampling locations at Monkey Lane (proto-Otter, SY 080 887)

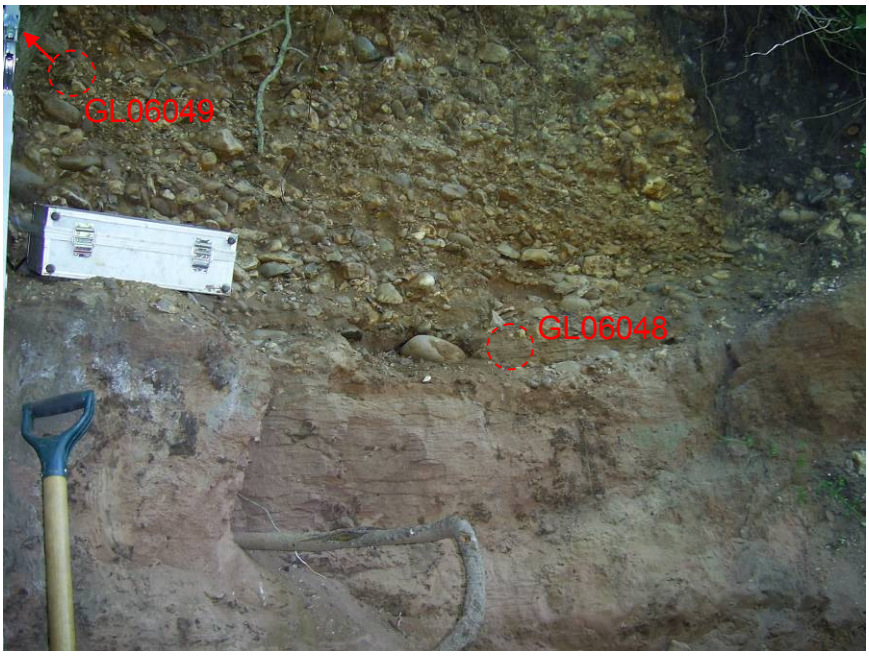

Figure 6: Image of sampling locations at Budleigh Salterton (proto-Otter, SY 071 822)

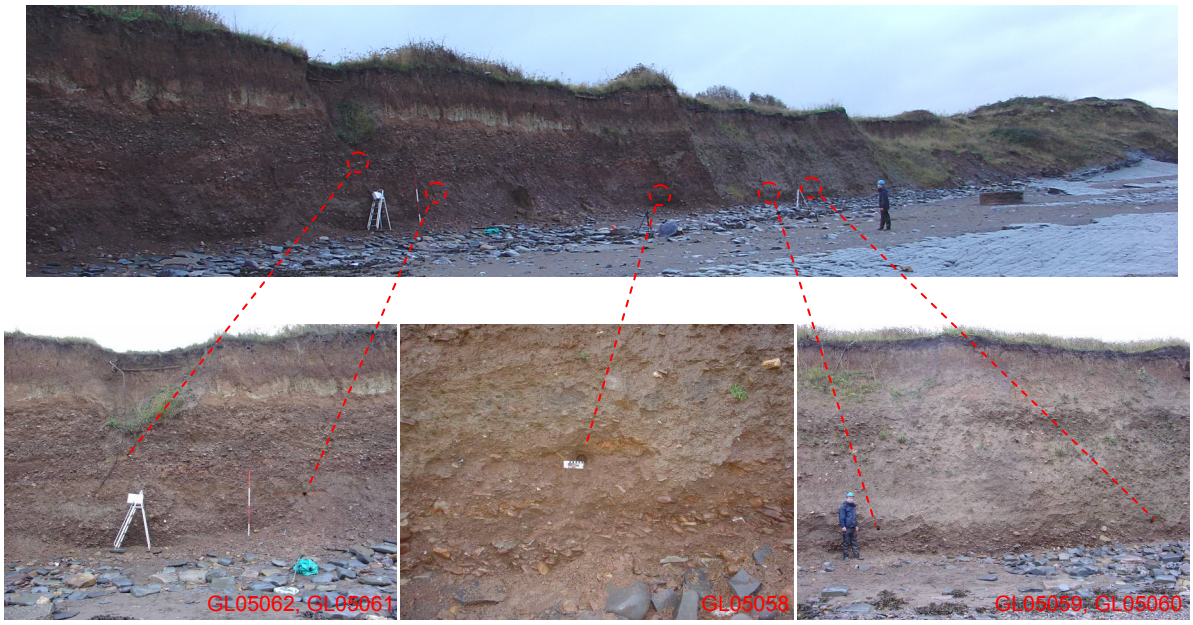

Figure 7: Images of sampling locations at Doniford (proto-Doniford, ST 084 430)

©ENGLISH HERITAGE

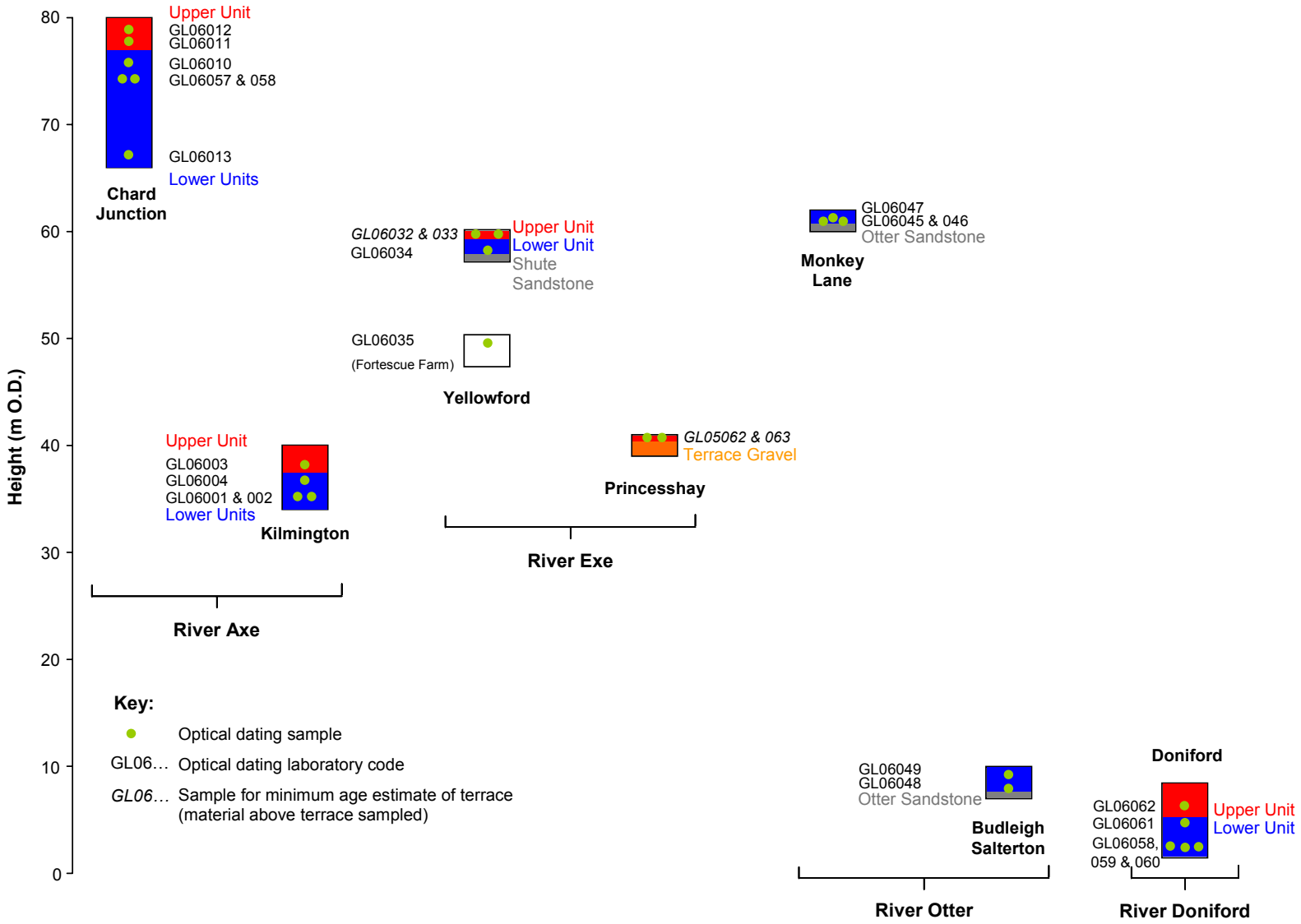

Figure 8: Relative position of sections and optical dating samples

2.0 OPTICAL DATING: MECHANISMS AND PRINCIPLES

Upon exposure to ionising radiation, electrons within the crystal lattice of insulating minerals are displaced from their atomic orbits. Whilst this dislocation is momentary for most electrons, a portion of charge is redistributed to meta-stable sites (traps) within the crystal lattice. In the absence of significant optical and thermal stimuli, this charge can be stored for extensive periods. The quantity of charge relocation and storage relates to the magnitude and period of irradiation. When the lattice is optically or thermally stimulated, charge is evicted from traps and may return to a vacant orbit position (hole). Upon recombination with a hole, an electron's energy can be dissipated in the form of light-generating crystal luminescence, providing a measure of dose absorption.

Herein, quartz is segregated for dating. The utility of this minerogenic dosimeter lies in the stability of its datable signal over the mid to late Quaternary period, predicted through isothermal decay studies (eg Smith *et al* 1990; retention lifetime 630Ma at 20° C) and evidenced by optical age estimates concordant with independent chronological controls (eg Murray and Olley 2002). This stability is in contrast to the anomalous fading of comparable signals commonly observed for other ubiquitous sedimentary minerals, such as feldspar and zircon (Wintle 1973; Templer 1985; Spooner 1993).

Optical age estimates of sedimentation (Huntley *et al* 1985) are premised upon reduction of the minerogenic time dependent signal (OSL) to zero through exposure to sunlight and, once buried, signal reformulation by absorption of litho- and cosmogenic radiation. The signal accumulated post-burial acts as a dosimeter recording total dose absorption, converting to a chronometer by estimating the rate of dose absorption quantified through the assay of radioactivity in the surrounding lithology and streaming from the cosmos.

$$\text{Age} = \frac{\text{Mean Equivalent Dose } (D_e, \text{ Gy})}{\text{Mean Dose Rate } (D_r, \text{ Gy.ka}^{-1})}$$

Aitken (1998) and Bøtter-Jensen *et al* (2003) offer a detailed review of optical dating.

3.0 SAMPLE COLLECTION AND PREPARATION

Twenty-five conventional sediment samples – those located within matrix-supported units composed predominantly of sand and silt – were collected in daylight from sections, by means of opaque plastic tubing (150x45mm) forced into each face, or carved as lithified blocks (75x75x50mm). In addition, one non-conventional sample (GL06035), located within a clast-supported unit, was collected as an aggregated mass (500x500x250mm). In order to attain an intrinsic metric of reliability, where possible, multiple samples were obtained from stratigraphically equivalent units, targeting positions which were likely to be divergent in dosimetry on the basis of textural and colour differences (see section 8.0). Each sample was wrapped in cellophane and parcel tape in order to preserve moisture content and integrity until ready for laboratory preparation. For each sample, an additional *c* 100g of sediment was collected for laboratory-based assessment of radioactive disequilibrium. The locations of the optical dating samples are shown in Figures 2–8.

To preclude optical erosion of the datable signal prior to measurement, all samples were prepared under controlled laboratory illumination provided by Encapsulite RB-10 (red) filters. To isolate that material potentially exposed to daylight during sampling, sediment located within 20mm of each tube-end or the outermost 10mm of each block face was removed.

The remaining sample was dried and then sieved. Depending upon each sample's modal grain size, quartz within the fine sand (63–90μm, 90–125μm, 125–180μm) fraction was then segregated (Table 1). Samples were subjected to acid and alkaline digestion (10% HCl, 15% H_2O_2) to attain removal of carbonate and organic components respectively.

A further acid digestion in HF (40%, 60min for 125–180μm; 40%, 40min for 90–125μm; 20% 15min for 63-90μm) was used to etch the outer 10-15μm layer affected by α radiation and degrade each sample's feldspar content. During HF treatment, continuous magnetic stirring is used to effect isotropic etching of grains. 10% HCl was then added to remove acid soluble fluorides. Each sample was dried and resieved and quartz was isolated from the remaining heavy mineral fraction using sodium polytungstate density separation at 2.68g.cm^{-3}. Twelve multi-grain aliquots (*c* 3–6mg) of quartz from each sample were then mounted on aluminium discs for determination of D_e values.

All drying was conducted at 40° C to prevent thermal erosion of the signal. All acids and alkalis were Analar grade. All dilutions (removing toxic-corrosive and non-minerogenic luminescence-bearing substances) were conducted with distilled water to prevent signal contamination by extraneous particles.

4.0 ACQUISITION AND ACCURACY OF D_e VALUE

All minerals naturally exhibit marked inter-sample variability in luminescence per unit dose (sensitivity). Therefore, the estimation of D_e acquired since burial requires calibration of the natural signal using known amounts of laboratory dose. D_e values were quantified using a single-aliquot regenerative-dose (SAR) protocol (Murray and Wintle 2000; 2003) facilitated by a Risø TL-DA-15 irradiation-stimulation-detection system (Markey *et al* 1997; Bøtter-Jensen *et al* 1999). Within this apparatus, optical signal stimulation of each sample was provided by one of two light sources: an assembly of blue diodes (five packs of six Nichia NSPB500S), filtered to 470±80nm, conveying 15mW.cm^{-2} using a 3mm Schott GG420 positioned in front of each diode pack, or a 150W tungsten halogen lamp, filtered to a broad blue-green light, 420-560nm conveying 16mWcm^{-2}, using three 2mm Schott GG420 and a broadband interference filter. Infrared (IR) stimulation, provided by 6 IR diodes (Telefunken TSHA 6203) stimulating at 875±80nm delivering ~5mW.cm^{-2}, was used to indicate the presence of contaminant feldspars (Hütt *et al* 1988). Stimulated photon emissions from quartz aliquots are in the ultraviolet (UV) range and were filtered from stimulating photons by 7.5mm HOYA U-340 glass and detected by an EMI 9235QA photomultiplier fitted with a blue-green sensitive bialkali photocathode. Aliquot irradiation was conducted using a 1.48GBq ^{90}Sr/^{90}Y β source calibrated for multi-grain aliquots of each isolated quartz fraction against the 'Hotspot 800' ^{60}Co γ source located at the National Physical Laboratory (NPL), UK.

SAR by definition evaluates D_e through measuring the natural signal (Fig 1 in each Appendix) of a single aliquot and then regenerating that aliquot's signal by using known laboratory doses to enable calibration. For each aliquot, at least four different regenerative doses were administered, so as to image dose response. D_e values for each aliquot were then interpolated, and associated counting and fitting errors calculated, by way of exponential or exponential plus linear regression (Fig 1 in each Appendix). Weighted (geometric) mean D_e values were calculated, given sufficient mass, from 12 aliquots using the central age model outlined by Galbraith *et al* (1999), and are quoted at 1σ confidence. The accuracy with which D_e equates to total absorbed dose and that dose absorbed since burial is assessed. The former can be considered a function of laboratory factors, the latter, one of environmental issues. Diagnostics were deployed to estimate the influence of these factors and criteria instituted to optimise the accuracy of D_e values.

4.1 Laboratory factors

4.1.1 Feldspar contamination

The propensity of feldspar signals to fade and underestimate age, coupled with their higher sensitivity relative to quartz, makes it imperative to qualify feldspar contamination. At room temperature, feldspars generate a signal (IRSL) upon exposure to IR, whereas quartz does not (Fig 1 in each Appendix). The feldspar index (Table 1) was used to evaluate the presence of this contaminant. A regenerative dose equivalent in magnitude to the mean D_e value of a sample was administered to aliquots, and IR response measured. The feldspar index is a ratio of (initial 0.2s) measured IRSL to 3σ background IRSL; the presence of feldspar is confirmed where this index exceeds unity. The source of feldspar contamination is rarely

rooted in sample preparation; it predominantly results from the occurrence of feldspars as inclusions within quartz.

Where significant feldspar content was detected, samples were immersed in 35% H_2SiF_6 for two weeks in an attempt to etch inclusions that may be partially exposed at grain surfaces. Samples were then resieved. The influence upon D_e of any remaining contamination was estimated by two methods. The D_e value was measured from 12 aliquots; if feldspar contamination had been reduced and the original content affected the D_e value, then a statistically greater D_e might evolve from that sub-sample that had undergone additional acid digestion. The repeat dose ratio of OSL to post-IR OSL was also quantified (Duller 2003). The signal from feldspars contributing to OSL can be depleted by prior exposure to IR. If the addition to OSL by feldspars is significant, then the repeat-dose ratio of OSL to post-IR OSL should be greater than unity. Samples from the River Otter (GL06045 to GL06049) exhibited minor to substantial feldspar contamination and were the subject of these further tests. Each sample exhibited an insignificant adjustment in mean D_e value, and OSL to post-IR OSL repeat dose ratios were statistically consistent. There was limited depletion of IR signal in response to a standard regenerative dose, rendering the comparison of mean D_e values of little utility. Given the lack of a significant difference between OSL and post-IR OSL signals, and that there appears to be little relationship between the magnitude of IRSL and age, it is suggested that in these samples the presence of feldspars has limited influence upon D_e values. These terrace samples come from two sites separated by several terraces. The similarity of their optical age estimates suggests either the age estimates are anomalous at one/both sites, or that the terrace-forming events on the River Otter operated over finite periods, indistinguishable by optical dating.

4.1.2 Preheating

Preheating aliquots between irradiation and optical stimulation is necessary to ensure comparability between natural and laboratory-induced signals. However, the multiple irradiation and preheating steps that are required to define single-aliquot regenerative-dose response leads to signal sensitisation, rendering calibration of the natural signal inaccurate. The SAR protocol (Murray and Wintle 2000; 2003) enables this sensitisation to be monitored and corrected using a test dose, here set at *c* 20Gy preheated to 220° C for 10s, to track signal sensitivity between irradiation-preheat steps. However, the accuracy of sensitisation correction for both natural and laboratory signals can be preheat-dependent. Three diagnostics were used to assess the optimal preheat temperature for accurate correction and calibration.

Irradiation-preheat cycling (Fig 2 in each Appendix) quantifies the preheat dependence of sensitisation correction for laboratory-induced signals. If sensitisation is accurately corrected, then the same regenerative dose should yield an equivalent sensitivity-corrected value, irrespective of the number of times it is applied and its associated signal measured. The ratio of subsequent to initial corrected regenerative-dose signals should be statistically concordant with unity. Alternatively, this ratio may differ from unity yet attain consistency after one or more cycles, evidencing that accurate sensitivity correction exists if the sample is primed by irradiation-preheat cycles. For this diagnostic, 18 aliquots were divided into sets of three, and assigned a 10s preheat between 180° C and 280° C.

D_e preheat dependence (Fig 3 in each Appendix) quantifies the combined effects of thermal transfer and sensitisation on the natural signal. Insignificant adjustment in $\mathbf{D_e}$ values in response to differing preheats may reflect limited influence of these effects. Samples generating D_e values <10Gy and exhibiting a systematic, statistically significant adjustment in D_e value with increasing preheat temperature may indicate the presence of significant thermal transfer; in such instances low temperature (<220° C) preheats may provide the apposite measure of D_e. For this diagnostic, the $\mathbf{D_e}$ value of each of the same 18 aliquots and their assigned preheat was assessed.

Dose recovery (Fig 4 in each Appendix) attempts to replicate the above diagnostic, yet provide improved resolution of thermal effects through removal of variability induced by heterogeneous dose absorption in the environment, using a precise laboratory dose to simulate natural dose. The ratio between the applied dose and recovered $\mathbf{D_e}$ value should be statistically concordant with unity. For this diagnostic, a further six aliquots were each assigned a 10s preheat between 180° C and 280° C.

That preheat treatment fulfilling the criterion of accuracy for all three diagnostics was selected to refine the final D_e value from a further nine aliquots. Further thermal treatments, prescribed by Murray and Wintle (2000; 2003), were applied to optimise accuracy and precision. Optical stimulation occured at 125° C, in order to minimise effects associated with photo-transferred thermoluminescence and maximise signal-to-noise ratios. Inter-cycle optical stimulation was conducted at 280° C to minimise recuperation.

4.1.3 Irradiation

For all samples having D_e values in excess of 100Gy, matters of signal saturation and laboratory irradiation effects are of concern. As regards the former, the rate of signal accumulation generally adheres to a saturating exponential form, and it is this that limits the precision and accuracy of D_e values for samples having absorbed large doses. For such samples, the functional range of D_e interpolation is defined from log-linear plots of dose response (Fig 1 in each Appendix). Within these plots, the maximum D_e value is delimited by the cessation of statistically significant increases in signal response.

Laboratory irradiation effects may evolve from the contrasting rates of natural dose exposure and the calibrating laboratory dose, the latter delivered to each aliquot at nine orders of magnitude faster than the former. Bailey (2004) has suggested that for doses in excess of ~40Gy, an overestimation of age may arise due to competing mechanisms of signal accumulation within the crystal lattice of quartz. Bailey (2004) suggests this effect can be countered by using pulsed irradiation-preheats (10Gy, 240° C cycles) rather than single large doses. Dose response to this revised irradiation procedure was quantified for a portion of the sample suite having D_e >40Gy (Fig 1 in each Appendix). Where pulsed irradiation D_e values are significantly less than those generated from continuous irradiation, Bailey (2004) advises that the mean D_e generated from the former be used to define age. However, of those samples examined, only two samples (GL06001 and GL06047) exhibited a significant contrast in dose response. Of these, GL06047 did not perform as predicted, producing a higher D_e value from pulsed rather than continuous irradiation. Given the embryonic stages of pulsed irradiation research and the lack of distinction between continuous and pulsed dose responses in this study, the D_e value of the remainder of the sample suite was derived from continuous irradiation.

4.1.4 Internal consistency

Quasi-radial plots (Fig 5 in each Appendix; *cf* Galbraith 1990) are used to illustrate inter-aliquot D_e variability for natural and regenerated signals. D_e values are standardised relative to the central D_e value for natural signals and applied dose for regenerated signals. D_e values are described as over-dispersed when >5% lie beyond $\pm 2\sigma$ of the standardising value, resulting from a heterogeneous absorption of burial dose and/or response to the SAR protocol. For multi-grain aliquots, over-dispersion for natural signals does not necessarily imply inaccuracy. However, where over-dispersion is observed for regenerated signals, the age estimate for that sample should be accepted tentatively.

4.2 Environmental factors

4.2.1 Incomplete zeroing

Post-burial OSL signals residual of pre-burial dose absorption can result where pre-burial sunlight exposure is limited in spectrum, intensity, and/or period, leading to age over-estimation. This effect is particularly acute for material eroded and redeposited sub-aqueously (Olley *et al* 1998, 1999; Wallinga 2002) and exposed to a burial dose of <20Gy (eg Olley *et al* 2004) and can have some influence in sub-aerial contexts, but is rarely of consequence where aerial transport has occurred.

Within single-aliquot regenerative-dose optical dating, there are two diagnostics of partial resetting (or bleaching); signal analysis (Agersnap Larsen *et al* 2000; Bailey *et al* 2003) and inter-aliquot D_e distribution studies (Murray *et al* 1995).

Within this study, signal analysis is used to quantify the change in D_e value with respect to optical stimulation time for multi-grain aliquots. This exploits the existence of traps within minerogenic dosimeters

that bleach with different efficiency for a given wavelength of light. D_e (t) plots (Fig 6 in each Appendix; Bailey *et al* 2003) are constructed from separate integrals of signal decay as laboratory optical stimulation progresses. A statistically significant increase in natural D_e (t) is indicative of partial bleaching, assuming three conditions are fulfilled. Firstly, that a statistically significant increase in D_e (t) is observed when partial bleaching is simulated within the laboratory. Secondly, that there is no significant rise in D_e (t) when full bleaching is simulated. Finally, there should be no significant augmentation in D_e (t) when zero dose is simulated. Where partial bleaching is detected, the age derived from the sample should be considered a maximum estimate only. However, the utility of signal analysis is strongly dependent upon a sample's pre-burial experience of sunlight's spectrum and its residual to post-burial signal ratio. Given that, in the majority of cases, the spectral exposure history of a deposit is uncertain, the absence of an increase in natural D_e (t) does not necessarily testify to the absence of partial bleaching.

Although not investigated in this study, the insensitivities of multi-grain single-aliquot signal analysis may be circumvented by inter-aliquot D_e distribution studies. This analysis uses aliquots of single sand grains to quantify inter-grain D_e distribution. At present, it is contended that asymmetric inter-grain D_e distributions are symptomatic of partial bleaching and/or pedoturbation (Murray *et al* 1995; Olley *et al* 1999; Olley *et al* 2004; Bateman *et al* 2003). For partial bleaching at least, it is further contended that the D_e acquired during burial is located in the minimum region of such ranges. The mean and breadth of this minimum region is the subject of current debate, as it is additionally influenced by heterogeneity in microdosimetry, variable inter-grain response to SAR and residual to post-burial signal ratios. Presently, the apposite measure of age is that defined by the D_e interval delimited by the minimum and central age models of Galbraith *et al* (1999).

4.2.2 Turbation

The accuracy of sedimentation ages can further be affected by post-burial trans-strata grain movements forced by pedo- or cryoturbation. Berger (2003) contends that pedogenesis prompts a reduction in the apparent sedimentation age of parent material through bioturbation and illuviation of younger material from above, and/or by biological recycling and resetting of the datable signal of surface material. Berger (2003) proposes that the chronological products of this remobilisation are A-horizon age estimates reflecting the cessation of pedogenic activity, Bc/C-horizon ages delimiting the maximum age for the initiation of pedogenesis, with estimates obtained from Bt-horizons providing an intermediate age 'close to the age of cessation of soil development'. Singhvi *et al* (2001), in contrast, suggest that B and C-horizons closely approximate the age of the parent material, the A-horizon, that of the 'soil forming episode'. At present there is no post-sampling mechanism for the direct detection of, and correction for, post-burial sediment remobilisation. However, intervals of palaeosol evolution can be delimited by a maximum age derived from parent material and a minimum age obtained from a unit overlying the palaeosol. Pedogenic effects are not considered significant within this study, owing to the lack of visible soil development and dominance of clast-supported units. Inaccuracy forced by cryoturbation may be bidirectional, heaving older material upwards or drawing younger material downwards into the level to be dated. All but one of the samples in this study were obtained from matrix-supported material; these sediments exhibited little evidence of cryogenic deformation.

5.0 ACQUISITION AND ACCURACY OF D_r VALUE

Lithogenic D_r values were defined through measurement of U, Th, and K radionuclide concentration, and conversion of these quantities into β and γ D_r values (Table 1). β contributions were estimated from sub-samples by Neutron Activation Analysis (NAA) delivered by Becquerel Canada. γ dose rates were estimated from *in situ* NaI gamma spectrometry or, where direct measurements were not possible, laboratory-based Ge gamma spectrometry of sub-samples. *In situ* measurements were conducted using an EG&G μNomad portable NaI gamma spectrometer (calibrated using the block standards at RLAHA, University of Oxford); these reduce uncertainty relating to potential heterogeneity in the γ dose field surrounding each sample. Estimates of radionuclide concentration were converted into D_r values (Adamiec and Aitken 1998), accounting for D_r modulation forced by grain size (Mejdahl 1979) and present moisture

content (Zimmerman 1971). Cosmogenic D_r values are calculated on the basis of sample depth, geographical position, and matrix density (Prescott and Hutton 1994).

The spatiotemporal validity of D_r values can be considered as five variables. Firstly, age estimates devoid of *in situ* γ spectrometry data should be accepted tentatively if the sampled unit is heterogeneous in texture or if the sample is located within 0.3m of strata consisting of differing texture and/or mineralogy. However, where samples are obtained throughout a vertical profile, consistent values of γ D_r based solely on, for example, NAA may evidence the homogeneity of the γ field and hence accuracy of γ D_r values. Secondly, disequilibrium can force temporal instability in U and Th emissions. The impact of this infrequent phenomenon (Olley *et al* 1996) upon age estimates is usually insignificant, given their associated margins of error, but this effect is pronounced for at least one sample (GL06034) in this study (Fig 7 in each Appendix). For this sample, ongoing or recent migration of U from the underlying Shute sandstone has generated disequilibrium and a D_r significantly higher than that that may have dominated since deposition of GL06034, producing an age under-estimate for this sample. Thirdly, pedogenically-induced variations in matrix composition of B and C-horizons, such as radionuclide and/or mineral remobilisation, may alter the rate of energy emission and/or absorption. If D_r is invariant through a dated profile and samples encompass primary parent material, then element mobility is probably limited in effect. In this study, there is limited evidence of pedogenesis for any unit sampled. Fourthly, spatiotemporal deviations from present moisture content are difficult to assess directly, requiring knowledge of the magnitude and timing of differing contents. However, the maximum influence of moisture content variations can be delimited by recalculating D_r for minimum (zero) and maximum (saturation) content. Finally, temporal alteration in the thickness of overburden alters cosmic D_r values. Cosmic D_r often forms a negligible portion of total D_r. It is possible to quantify the maximum influence of overburden flux by recalculating D_r for minimum (zero) and maximum (surface sample) cosmic D_r.

6.0 ESTIMATION OF AGE

Age estimates reported in Table 1 provide an estimate of sediment burial period based on mean D_e and D_r values and their associated analytical uncertainties. Uncertainty in age estimates is reported as a product of systematic and experimental errors, with the magnitude of experimental errors alone shown in parentheses (Table 1). Probability distributions indicate the inter-aliquot variability in age (Fig 8 in each Appendix). The maximum influence of temporal variations in D_r forced by minima-maxima variation in moisture content and overburden thickness is illustrated in Figure 8 in each Appendix. Where uncertainty in these parameters exists, this age range may prove instructive, but the combined extremes represented should not be construed as preferred age estimates.

7.0 ANALYTICAL UNCERTAINTY

All errors are based upon analytical uncertainty and quoted at 1σ confidence. Error calculations account for the propagation of systematic and/or experimental (random) errors associated with D_e and D_r values.

For D_e values, systematic errors are confined to laboratory β source calibration. Uncertainty in this respect is that combined from the delivery of the calibrating γ dose (1.2%; NPL, pers comm), the conversion of this dose for SiO_2 using the respective mass energy-absorption coefficient (2%; Hubbell 1982) and experimental error, totalling 3.5%. Mass attenuation and *Bremsstrahlung* losses during γ dose delivery are considered negligible. Experimental errors relate to D_e interpolation using sensitisation corrected dose responses. Natural and regenerated sensitisation corrected dose points (S_i) are quantified by

$$S_i = (D_i - x.L_i) / (d_i - x.L_i) \qquad \text{Eq.1}$$

where D_i = Natural or regenerated OSL, initial 0.2s
L_i = Background natural or regenerated OSL, final 5s
d_i = Test dose OSL, initial 0.2s

x = Scaling factor, 0.08

The error on each signal parameter is based on counting statistics, reflected by the square-root of measured values. The propagation of these errors within Eq. 1 generating σS_i follows the general formula given in Eq. 2. σS_i are then used to define fitting and interpolation errors within linear or exponential regressions (Green and Margerison 1978; Ixaru *et al* 2004).

For D_r values, systematic errors accommodate uncertainty in radionuclide conversion factors (5%), β attenuation coefficients (5%), matrix density (0.20g.cm^{-3}), vertical thickness of sampled section (specific to sample collection device), saturation moisture content (3%), moisture content attenuation (2%), burial moisture content (25% relative, unless direct evidence exists of the magnitude and period of differing content), NaI gamma spectrometer calibration (3%) and/or NAA (2%). Experimental errors are associated with radionuclide quantification for each sample by gamma spectrometry and/or NAA.

The propagation of these errors through to age calculation is quantified using the expression,

$$\sigma y\ (\delta y/\delta x) = (\Sigma\ ((\delta y/\delta x_n).\sigma x_n)^2)^{1/2} \qquad \text{Eq. 2}$$

where y is a value equivalent to that function comprising terms x_n and where σy and σx_n are associated uncertainties.

Errors on age estimates are presented as combined systematic and experimental errors and experimental errors alone. The former (combined) error should be considered when comparing luminescence ages herein with independent chronometric controls. The latter assumes systematic errors are common to luminescence age estimates generated by means equal to those detailed herein and enable direct comparison with those estimates.

8.0 INTRINSIC ASSESSMENT OF RELIABILITY

Here, intrinsic assessment of reliability is divided into two categories, analytical acceptability and inference. Table 2 details the analytical acceptability of age estimates evolved in this study, drawn principally from diagnostics illustrated in Figures 1 to 7 in each Appendix and detailed in sections 4.0 to 5.0. The inference of reliability comes from the level of intra-site stratigraphic consistency and the convergence of age estimates from stratigraphically equivalent units of divergent dosimetry.

All but one sample (GL06001; Kilmington, River Axe) generated age estimates consistent with their relative stratigraphic position at each site. GL06001 may have been obtained from a slipped deposit that is in effect stratigraphically younger than samples from the lower units. Figure 9 shows D_e:D_r plots (Toms *et al* 2005); the gradient of lines from the origin to a data point or through data points of samples from stratigraphically equivalent units represents the age of the sample. The utility of D_e:D_r plots is twofold. Firstly, they readily illustrate the spread of luminescence ages. Secondly, they demonstrate the reliability of age estimates from stratigraphically equivalent units where there is significant bivariation in D_e and D_r yet statistical concordance of data points with the mean isochron (ie a line regressed through the data points to the origin). Hierarchically, as intrinsic measures of reliability, comparable ages derived from stratigraphically equivalent units of differing D_r supersede analytical acceptability, even where the latter is questionable. The D_e:D_r plot for Chard (River Axe) demonstrates the reliability of the ages from the upper unit where a significant variation in D_r was recorded. It is possible that the D_e:D_r plot of data from the lower unit at Kilmington substantiates the accuracy of ages from this level, but the stratigraphic equivalence of these samples is unclear.

9.0 DISCUSSION

This study provides the first estimates of the chronological spread in residual deposits of the proto-Axe, Exe, Otter, and Doniford rivers (incorporating data from Broom, River Axe; Toms *et al* 2005). The age

envelopes in Figure 10 indicate that the Axe was aggrading at intervals between at least 86 and 401ka (MIS 5 to 10), the Exe before 10ka and perhaps further back than 86ka (MIS >1 to >5), the Otter before 66ka and by at least 209ka (MIS >3 to 7), and the Doniford at intervals between at least 22 and 71ka (MIS 2 to 4).

At Doniford, the deposits of the proto-Doniford have yielded numerous flakes, several bifaces and mammoth remains. The antiquity of these finds is incompatible with the relatively young age of the deposits, suggesting substantial reworking of the artefacts. The fill terrace system of the Axe yielded age estimates significantly older than those sampled from the staircase terrace system of the Exe and Otter. This likely reflects the abundance of sediment supply from the Blackdown Hills to the Axe, which, along with limited discharge precluded removal and incision of the deposits. In contrast, lower sediment supply coupled with the erosive power of the Exe and Otter catchments generated a staircase of terrace deposits. The age of the Exe and Otter fluvial sediments relative to the postulated age of the artefacts contained within them, points to substantial reworking. The sediment supply and erosive characteristics of these catchments perhaps may explain this higher degree of reworking and lower concentration findspots relative to the Axe. However, the dearth of finds at Chard and Kilmington relative to Broom warrants further investigation (via deeper excavations) of the Axe.

Whilst not providing a precise chronology for the Lower and Middle Palaeolithic presence in South West England, the chronology outlined here does provide a preliminary spatiotemporal model for open sites, which allows comparison with the better-known cave sequence of South West England.

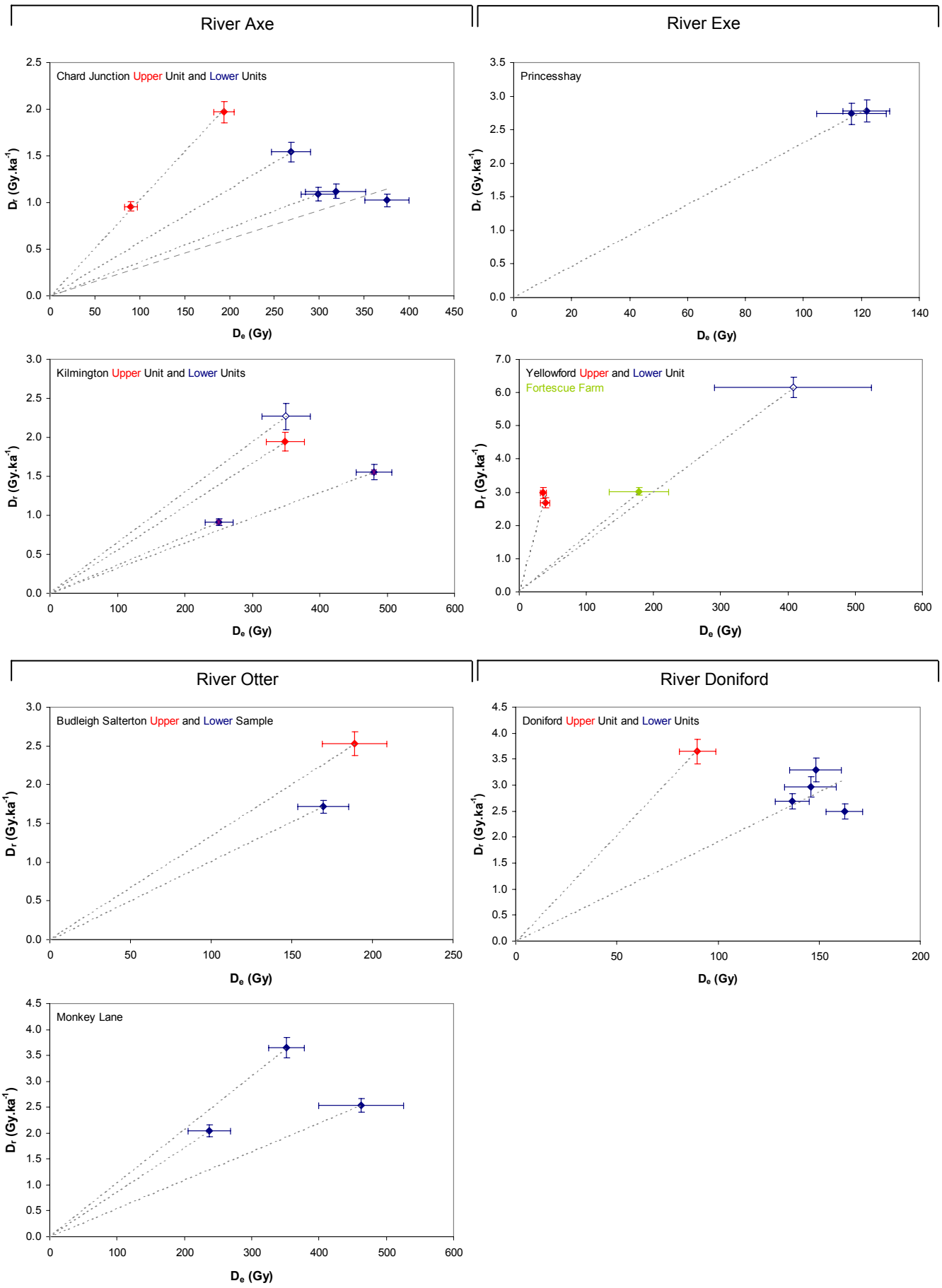

Figure 9: D_e:D_r plots for this study's suite of samples

The gradient of a line drawn from the origin to the data point of any sample represents sample age; the shallower the gradient, the older the age estimate. Samples from a stratigraphically equivalent unit are fitted with a single line representing the isochron for that unit. Unfilled symbols reflect data where qualifications are made within the text

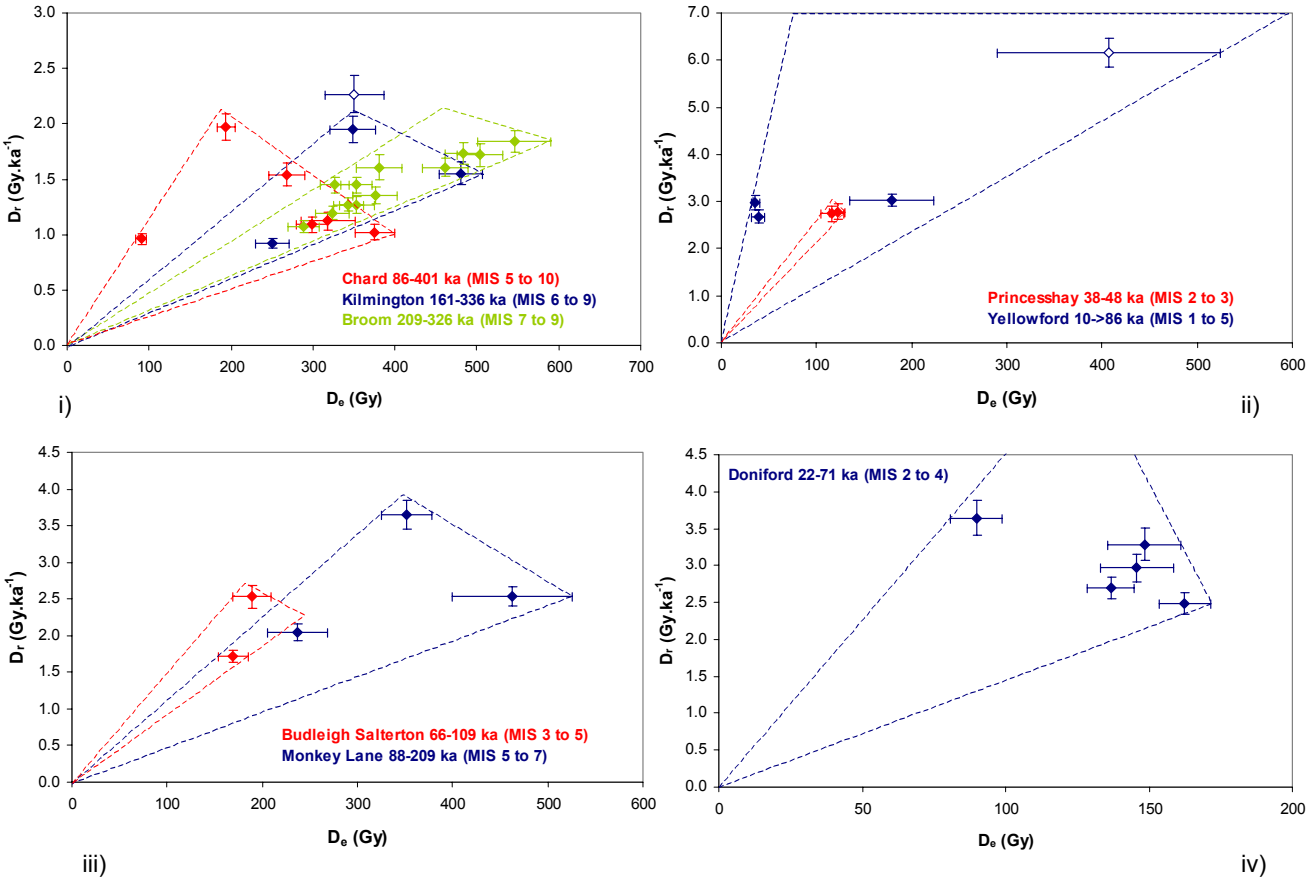

Figure 10: Age envelopes for site deposits of the former i) Axe, ii) Exe, iii) Otter, and iv) Doniford Rivers

10.0 REFERENCES

Adamiec, G, and Aitken, M J, 1998 Dose-rate conversion factors: new data, *Ancient TL*, **16**, 37–50

Agersnap Larsen, N, Bulur, E, Bøtter-Jensen, L, and McKeever, S W S, 2000 Use of the LM-OSL technique for the detection of partial bleaching in quartz, *Radiation Measurements*, **32**, 419–25.

Aitken, M J, 1998 *An Introduction to Optical Dating: the Dating of Quaternary Sediments by the Use of Photon-Stimulated Luminescence*, Oxford (Oxford Univ Press)

Bailey, R M, 2004 Paper I – simulation of dose absorption in quartz over geological timescales and its implications for the precision and accuracy of optical dating, *Radiation Measurements*, **38**, 299–310

Bailey, R M, Singarayer, J S, Ward, S, and Stokes, S, 2003 Identification of partial resetting using D_e as a function of illumination time, *Radiation Measurements*, **37**, 511–18

Banerjee, D, Murray, A S, Bøtter-Jensen, L, and Lang, A, 2001 Equivalent dose estimation using a single aliquot of polymineral fine grains, *Radiation Measurements*, **33**, 73–94

Bateman, M D, Frederick, C D, Jaiswal, M K, and Singhvi, A K, 2003 Investigations into the potential effects of pedoturbation on luminescence dating, *Quat Sci Rev*, **22**, 1169–76

Berger, G W, 2003 Luminescence chronology of late Pleistocene loess-paleosol and tephra sequences near Fairbanks, Alaska, *Quat Res*, **60**, 70–83

Bøtter-Jensen, L, Mejdahl, V, and Murray, A S, 1999 New light on OSL, *Quat Sci Rev*, **18**, 303–10

Bøtter-Jensen, L, McKeever, S W S, and Wintle, A G, 2003 *Optically Stimulated Luminescence Dosimetry*, Amsterdam (Elsevier)

Duller, G A T, 2003 Distinguishing quartz and feldspar in single grain luminescence measurements, *Radiation Measurements*, **37**, 161–5.

Galbraith, R F 1990 The radial plot: graphical assessment of spread in ages. *Nuclear Tracks and Radiation Measurements*, **17**, 207–14

Galbraith, R F, Roberts, R G, Laslett, G M, Yoshida, H, and Olley, J M, 1999 Optical dating of single and multiple grains of quartz from Jinmium rock shelter (northern Australia): Part I, Experimental design and statistical models, *Archaeometry*, **41**, 339–64

Green, J R and Margerison, D, 1978 *Statistical Treatment of Experimental Data*, New York (Elsevier Scientific Publications)

Hubble, J H, 1982 Photon mass attenuation and energy-absorption coefficients from 1keV to 20MeV, *Int J Applied Radioisotopes*, **33**, 1269–90

Huntley, D J, Godfrey-Smith, D I, and Thewalt, M L W, 1985 Optical dating of sediments, *Nature*, **313**, 105–7

Hütt, G, Jaek, I, and Tchonka, J, 1988 Optical dating: K-feldspars optical response stimulation spectra, *Quat Sci Rev*, **7**, 381–6

Ixaru, L, Vandenberghe, G, and Hazewinkel, M, 2004 *Exponential Fitting*, Kluwer

Markey, B G, Bøtter-Jensen, L, and Duller, G A T, 1997 A new flexible system for measuring thermally and optically stimulated luminescence, *Radiation Measurements*, **27**, 83–9

Mejdahl, V, 1979 Thermoluminescence dating: beta-dose attenuation in quartz grains, *Archaeometry*, **21**, 61–72

Murray, A S and Olley, J M, 2002 Precision and accuracy in the Optically Stimulated Luminescence dating of sedimentary quartz: a status review, *Geochronometria*, **21**, 1–16

Murray, A S and Wintle, A G, 2000 Luminescence dating of quartz using an improved single-aliquot regenerative-dose protocol, *Radiation Measurements*, **32**, 57–73

Murray, A S and Wintle, A G, 2003 The single aliquot regenerative dose protocol: potential for improvements in reliability. *Radiation Measurements*, **37**, 377–81

Murray, A S, Olley, J M, and Caitcheon, G G, 1995 Measurement of equivalent doses in quartz from contemporary water-lain sediments using optically stimulated luminescence, *Quat Sci Rev*, **14**, 365–71

Olley, J M, Murray, A S, and Roberts, R G, 1996 The effects of disequilibria in the Uranium and Thorium decay chains on burial dose rates in fluvial sediments. *Quat Sci Rev*, **15**, 751–60

Olley, J M, Caitcheon, G G, and Murray, A S, 1998 The distribution of apparent dose as determined by optically stimulated luminescence in small aliquots of fluvial quartz: implications for dating young sediments, *Quat Sci Rev*, **17**, 1033–40

Olley, J M, Caitcheon, G G, and Roberts R G, 1999 The origin of dose distributions in fluvial sediments, and the prospect of dating single grains from fluvial deposits using -optically stimulated luminescence, *Radiation Measurements,* **30,** 207–17

Olley, J M, Pietsch, T, and Roberts, R G, 2004 Optical dating of Holocene sediments from a variety of geomorphic settings using single grains of quartz, *Geomorphol*, **60**, 337–58

Prescott, J R and Hutton, J T, 1994 Cosmic ray contributions to dose rates for luminescence and ESR dating: large depths and long-term time variations, *Radiation Measurements*, **23**, 497–500

Singhvi, A K, Bluszcz, A, Bateman, M D, and Someshwar Rao, M, 2001 Luminescence dating of loess-palaeosol sequences and coversands: methodological aspects and palaeoclimatic implications, *Earth Sci Rev*, **54**, 193–211

Smith, B W, Rhodes, E J, Stokes, S, and Spooner, N A, 1990 The optical dating of sediments using quartz, *Radiation Protection Dosimetry*, **34**, 75–8

Spooner, N A, 1993 'The validity of optical dating based on feldspar', unpubl DPhil thesis, Oxford Univ

Templer, R H, 1985 The removal of anomalous fading in zircons, *Nuclear Tracks and Radiation Measurements*, **10**, 531–7

Toms, P S, Hosfield, R T, Chambers, J C, Green, C P, and Marshall, P, 2005 Optical dating of the Broom Palaeolithic sites, Devon and Dorset, *Centre for Archaeol Rep* **16/2005**

Wallinga, J, 2002 Optically stimulated luminescence dating of fluvial deposits: a review, *Boreas*, **31**, 303–22

Wintle, A G, 1973 Anomalous fading of thermoluminescence in mineral samples, *Nature*, **245**, 143–4

Wymer, J J, 1999 The Lower Palaeolithic Occupation of Britain. Wessex Archaeology & English Heritage, London

Zimmerman, D W, 1971 Thermoluminescent dating using fine grains from pottery, *Archaeometry*, **13**, 29–52

Table 1: D_r, D_e and Age data of submitted samples. Uncertainties in age, quoted at 1σ confidence, are based on analytical errors and reflect combined systematic and experimental variability and (in parenthesis) experimental variability alone (see 6.0). Blue indicates samples with accepted age estimates, red, age estimates with caveats (see Table 2)

Field Code	Lab Code	Location	Height OD	Over-burden	Grain size	Moisture content	NaI γ-spectrometry (in situ)			γ D_r	Neutron Activation Analysis (†or Ge γ-spectrometry)			α Dr	β Dr	Cosmic D_r	Total D_r	Feldspar index	Preheat, 10s	D_e	Age
			(m)	(m)	(μm)		K (%)	Th (ppm)	U (ppm)	(Gy.ka^{-1})	K (%)	Th (ppm)	U (ppm)	(Gy.ka^{-1})	(Gy.ka^{-1})	(Gy.ka^{-1})	(Gy.ka^{-1})		(°C)	(Gy)	(ka)
DON01	GL05058	51° 10' 44.99" N 3° 18' 39.14" W	7	6.3	125–180	0.15 ± 0.04	1.45 ± 0.03	6.40 ± 0.22	3.32 ± 0.15	1.03 ± 0.04	1.75 ± 0.07	9.84 ± 0.42	3.34 ± 0.15	-	1.58 ± 0.14	0.08 ± 0.01	2.70 ± 0.14	12.0	260	136.7 ± 8.2	50 ± 4 (3)
DON02	GL05059	51° 10' 44.95" N 3° 18' 39.94" W	7	6.3	63–90	0.17 ± 0.04	1.24 ± 0.03	6.52 ± 0.23	2.94 ± 0.15	0.94 ± 0.03	1.77 ± 0.08	8.01 ± 0.35	2.30 ± 0.12	-	1.47 ± 0.14	0.08 ± 0.01	2.49 ± 0.15	0.4	240	162.5 ± 9.1	65 ± 5 (4)
DON03	GL05060	51° 10' 44.90 N 3° 18' 40.22 W	7	6.6	125–180	0.18 ± 0.04	1.41 ± 0.03	6.70 ± 0.21	2.87 ± 0.14	0.99 ± 0.03	2.96 ± 0.12	11.28 ± 0.48	3.07 ± 0.14	-	2.23 ± 0.22	0.08 ± 0.01	3.29 ± 0.22	5.7	240	148.4 ± 12.9	45 ± 5 (4)
DON04	GL05061	51° 10' 45.05" N 3° 18' 37.83" W	7	5.0	125–180	0.18 ± 0.04	1.42 ± 0.03	7.28 ± 0.22	2.62 ± 0.13	0.99 ± 0.03	2.51 ± 0.11	9.80 ± 0.42	2.48 ± 0.12	-	1.88 ± 0.19	0.09 ± 0.01	2.97 ± 0.19	1.8	260	145.7 ± 12.6	49 ± 5 (5)
DON05	GL05062	51° 10' 45.03" N 3° 18' 37.70" W	7	4.0	125–180	0.16 ± 0.04	1.53 ± 0.03	8.13 ± 0.22	2.84 ± 0.14	1.08 ± 0.04	3.17 ± 0.13	13.37 ± 0.56	2.97 ± 0.14	-	2.46 ± 0.23	0.11 ± 0.01	3.65 ± 0.23	2.4	260	89.8 ± 9.0	25 ± 3 (3)
PHAY01	GL05063	51° 43' 25.75" N 3° 31' 40.90" W	40	0.5	125–180	0.17 ± 0.04	1.29 ± 0.03	6.12 ± 0.21	3.11 ± 0.14	0.96 ± 0.03	2.07 ± 0.09	7.57 ± 0.33	2.25 ± 0.11	-	1.59 ± 0.15	0.20 ± 0.02	2.74 ± 0.16	0.7	280	116.6 ± 11.9	43 ± 5 (5)
PHAY02	GL05064	50° 43' 25.75" N 3° 31' 40.90" W	40	0.3	125–180	0.16 ± 0.04	1.16 ± 0.03	5.61 ± 0.21	3.13 ± 0.15	0.90 ± 0.03	2.16 ± 0.09	7.57 ± 0.33	2.47 ± 0.12	-	1.68 ± 0.16	0.20 ± 0.03	2.78 ± 0.16	0.8	260	121.8 ± 8.0	44 ± 4 (3)
KILM01	GL06001	50° 46' 32.59" N 3° 01' 45.41" W	40	5.0	125–180	0.18 ± 0.05	0.49 ± 0.02	3.73 ± 0.13	1.69 ± 0.09	0.49 ± 0.02	2.10 ± 0.09	10.26 ± 0.44	2.85 ± 0.14	-	1.68 ± 0.17	0.10 ± 0.01	2.27 ± 0.17	19.0	260	350.2 ± 35.8	154 ± 19 (18)
KILM03	GL06002	50° 46' 32.29" N 3° 01' 44.36" W	40	5.0	125–180	0.16 ± 0.04	0.51 ± 0.01	2.83 ± 0.12	1.10 ± 0.07	0.38 ± 0.02	1.33 ± 0.06	6.14 ± 0.27	1.56 ± 0.09	-	1.08 ± 0.10	0.10 ± 0.01	1.55 ± 0.10	6.2	260	480.5 ± 26.6	309 ± 26 (21)
KILM05	GL06003	51° 46' 31.99" N 3° 01' 43.41" W	40	2.0	125–180	0.14 ± 0.03	0.57 ± 0.02	3.49 ± 0.16	1.20 ± 0.10	0.44 ± 0.02	1.52 ± 0.07	8.62 ± 0.37	2.42 ± 0.12	-	1.36 ± 0.11	0.15 ± 0.01	1.95 ± 0.12	16.0	260	348.7 ± 28.3	179 ± 18 (16)
KILM06	GL06004	50° 46' 32.36" N 3° 01' 43.79" W	40	4.0	125–180	0.06 ± 0.01	0.38 ± 0.02	1.85 ± 0.13	0.87 ± 0.09	0.28 ± 0.01	0.62 ± 0.03	2.07 ± 0.11	0.52 ± 0.04	-	0.53 ± 0.04	0.11 ± 0.01	0.92 ± 0.04	8.8	240	250.6 ± 20.5	273 ± 26 (22)
CHAR01	GL06010	50° 50' 19.78" N 2° 55' 21.32" W	80	4.3	125–180	0.16 ± 0.04	0.36 ± 0.01	2.28 ± 0.12	1.29 ± 0.08	0.34 ± 0.02	1.27 ± 0.06	6.86 ± 0.29	2.08 ± 0.10	-	1.09 ± 0.10	0.11 ± 0.01	1.54 ± 0.10	12.6	240	268.5 ± 22.0	174 ± 18 (16)
CHAR02	GL06011	50° 50' 19.78"N 2° 55' 21.32" W	80	2.5	125–180	0.13 ± 0.03	0.30 ± 0.01	2.12 ± 0.10	1.01 ± 0.07	0.29 ± 0.01	0.60 ± 0.03	3.10 ± 0.15	0.95 ± 0.06	-	0.53 ± 0.04	0.14 ± 0.01	0.96 ± 0.05	9.7	260	90.2 ± 6.8	94 ± 9 (7)
CHAR03	GL06012	50° 50' 17.55" N 2° 55' 21.26" W	80	1.7	125–180	0.14 ± 0.03	0.68 ± 0.02	3.85 ± 0.17	1.62 ± 0.11	0.53 ± 0.02	1.53 ± 0.07	7.23 ± 0.31	1.90 ± 0.09	-	1.28 ± 0.11	0.16 ± 0.02	1.97 ± 0.11	58.9	260	193.7 ± 11.0	98 ± 9 (6)
CHAR04	GL06013	50° 50' 19.02" N 2° 55' 52.97" W	75	4.5	125–180	0.15 ± 0.04	0.36 ± 0.02	1.82 ± 0.13	0.79 ± 0.08	0.26 ± 0.01	0.99 ± 0.05	2.71 ± 0.13	0.65 ± 0.05	-	0.72 ± 0.07	0.10 ± 0.01	1.09 ± 0.07	11.9	240	298.6 ± 19.2	274 ± 25 (20)
YELL01	GL06032	51° 47' 37.92" N 3° 31' 30.85" W	60	1.2	125–180	0.16 ± 0.04	0.82 ± 0.03	5.98 ± 0.20	4.59 ± 0.15	1.00 ± 0.04	1.89 ± 0.08	7.60 ± 0.32	2.31 ± 0.11	-	1.50 ± 0.14	0.17 ± 0.02	2.68 ± 0.15	1.0	280	39.0 ± 7.0	15 ± 3 (3)
YELL02	GL06033	50° 47' 38.06" N 3° 31' 31.29" W	60	0.8	125–180	0.13 ± 0.04	1.41 ± 0.02	6.31 ± 0.19	3.31 ± 0.13	1.02 ± 0.03	2.10 ± 0.09	9.56 ± 0.40	2.67 ± 0.13	-	1.77 ± 0.15	0.19 ± 0.02	2.98 ± 0.16	19.2	220	35.8 ± 4.2	12 ± 2 (1)
YELL03	GL06034	50° 47' 38.20" N 3° 31' 31.51" W	60	2.5	125–180	0.17 ± 0.04	0.28 ± 0.07	3.46 ± 0.22	25.20 ± 0.35	3.08 ± 0.15	2.15 ± 0.09	9.80 ± 0.41	14.45 ± 0.59	-	2.93 ± 0.26	0.14 ± 0.02	6.15 ± 0.30	0.9	260	407.5±117.4	66 ± 19 (19)
YELL04†	GL06035	51° 46' 58.58" N 3° 31' 19.05" W	50	0.8	180–250	0.01 ± 0.00	-	-	-	1.22 ± 0.09	1.42 ± 0.07	11.39 ± 0.64	3.08 ± 0.15	-	1.62 ± 0.11	0.19 ± 0.02	3.02 ± 0.12	0.4	260	178.6 ± 44.1	59 ± 15 (15)
OML01	GL06045	50° 41' 29.45" N 3° 18' 12.50" W	60	1.6	180–250	0.10 ± 0.03	0.97 ± 0.02	5.22 ± 0.17	2.41 ± 0.11	0.76 ± 0.03	1.96 ± 0.08	7.95 ± 0.32	2.12 ± 0.09	-	1.62 ± 0.13	0.16 ± 0.02	2.54 ± 0.13	5.3	260	462.5 ± 62.9	182 ± 26 (25)
OML02	GL06046	50° 41' 29.48" N 3° 18' 12.55" W	60	1.7	180–250	0.13 ± 0.03	2.39 ± 0.03	7.72 ± 0.22	3.13 ± 0.14	1.30 ± 0.04	2.91 ± 0.12	9.02 ± 0.37	2.38 ± 0.10	-	2.19 ± 0.19	0.16 ± 0.02	3.65 ± 0.20	13.4	280	351.9 ± 26.2	96 ± 9 (7)
OML03	GL06047	50° 41' 29.55" N 3° 18' 12.72" W	60	1.4	180–250	0.08 ± 0.02	0.70 ± 0.02	3.14 ± 0.13	1.68 ± 0.09	0.51 ± 0.02	1.76 ± 0.07	4.73 ± 0.19	1.13 ± 0.05	-	1.37 ± 0.11	0.17 ± 0.02	2.05 ± 0.11	72.6	240	237.2 ± 31.8	116 ± 17 (16)
OBS01	GL06048	50° 3' 58.59" N 3° 18' 50.38" W	10	2.5	180–250	0.02 ± 0.00	0.74 ± 0.02	3.14 ± 0.13	1.68 ± 0.09	0.47 ± 0.02	1.31 ± 0.06	3.56 ± 0.15	0.83 ± 0.03	-	1.11 ± 0.08	0.14 ± 0.01	1.72 ± 0.08	66.2	280	169.5 ± 16.0	99 ± 10 (9)
OBS02	GL06049	50° 37' 58.55" N 3° 18' 50.35" W	10	1.2	180–250	0.03 ± 0.01	0.80 ± 0.02	2.67 ± 0.14	0.94 ± 0.09	0.43 ± 0.02	2.57 ± 0.11	3.11 ± 0.13	0.61 ± 0.03	-	1.93 ± 0.15	0.17 ± 0.02	2.53 ± 0.15	57.8	220	189.1 ± 19.9	75 ± 9 (8)
CHAR05	GL06057	50° 50' 19.57" N 2° 55' 25.51"W	80	6.7	125–180	0.16 ± 0.04	0.18 ± 0.01	1.32 ± 0.08	0.82 ± 0.06	0.20 ± 0.01	0.87 ± 0.04	5.30 ± 0.21	1.30 ± 0.05	-	0.75 ± 0.07	0.08 ± 0.01	1.02 ± 0.07	2.3	240	375.3 ± 24.6	367 ± 35 (29)
CHAR06	GL06058	50° 50' 19.57" N 2° 55' 25.51"W	80	7.0	125–180	0.15 ± 0.04	0.23 ± 0.01	1.55 ± 0.10	0.67 ± 0.07	0.21 ± 0.01	1.09 ± 0.05	3.90 ± 0.16	1.00 ± 0.04	-	0.84 ± 0.08	0.07 ± 0.01	1.12 ± 0.08	5.7	280	318.3 ± 33.3	284 ± 36 (32)

Table 2: Analytical acceptability of sample suite age estimates and caveats for consideration

Generic considerations	Field Code	Lab Code	Sample specific considerations
None	DON01	GL05058	Minor feldspar contamination (see 4.1.1); Dose Recovery underestimated (see 4.1.2); overdispersion of regenerative-dose data (see 4.1.4). Accept tentatively
	DON02	GL05059	Accept
	DON03	GL05060	Minor feldspar contamination (see 4.1.1); Dose Recovery underestimated (see 4.1.2); overdispersion of regenerative-dose data (see 4.1.4). Accept tentatively
	DON04	GL05061	Minor feldspar contamination (see 4.1.1); overdispersion of regenerative-dose data (see 4.1.4). Accept tentatively
	DON05	GL05062	Minor feldspar contamination (see 4.1.1). Accept
	PHAY01	GL05063	Overdispersion of regenerative-dose data, accept tentatively (see 4.1.4)
	PHAY02	GL05064	Dose Recovery underestimated (see 3.1.2); overdispersion of regenerative-dose data (see 4.1.4). Accept tentatively
	KILM01	GL06001	Minor feldspar contamination (see 4.1.1). Accept
	KILM03	GL06002	Minor feldspar contamination (see 4.1.1). Accept
	KILM05	GL06003	Minor feldspar contamination (see 4.1.1); Dose Recovery overestimated (see 4.1.2); overdispersion of regenerative-dose data (see 4.1.4); probably, yet relatively minor partial bleaching (see 4.2.1). Accept tentatively
	KILM06	GL06004	Minor feldspar contamination (see 4.1.1); overdispersion of regenerative-dose data (see 4.1.4). Accept tentatively
	CHAR01	GL06010	Minor feldspar contamination (see 4.1.1). Accept
	CHAR02	GL06011	Minor feldspar contamination (see 4.1.1). Accept
	CHAR03	GL06012	Substantial feldspar contamination (see 4.1.1); Dose Recovery underestimated (see 4.1.2); probable, yet relatively minor partial bleaching (see 4.2.1). Accept tentatively as minimum age estimate
	CHAR04	GL06013	Minor feldspar contamination (see 4.1.1). Accept
	YELL01	GL06032	Overdispersion of regenerative-dose data (see 4.1.4). Accept tentatively
	YELL02	GL06033	Minor feldspar contamination (see 4.1.1); Limited sample mass. Accept tentatively
	YELL03	GL06034	Limited sample mass; U disequilibrium (see 5.0). Accept as minimum age estimate
	YELL04	GL06035	Limited sample mass; overdispersion of regenerative-dose data (see 4.1.4). Accept tentatively
	OML01	GL06045	Minor feldspar contamination (see 4.1.1); Dose Recovery overestimated (see 4.1.2). Accept tentatively
	OML02	GL06046	Minor feldspar contamination (see 4.1.1); overdispersion of regenerative-dose data (see 4.1.4). Accept tentatively
	OML03	GL06047	Substantial feldspar contamination (see 4.1.1); Dose Recovery underestimated (see 4.1.2). Accept tentatively
	OBS01	GL06048	Substantial feldspar contamination (see 4.1.1); overdispersion of regenerative-dose data (see 4.1.4). Accept tentatively
	OBS02	GL06049	Substantial feldspar contamination (see 4.1.1); Dose Recovery overestimated (see 4.1.2). Accept tentatively
	CHAR05	GL06057	Minor feldspar contamination (see 4.1.1). Accept
	CHAR06	GL06058	Minor feldspar contamination (see 4.1.1); overdispersion of regenerative-dose data (see 4.1.4). Accept tentatively

APPENDIX 1: MEASUREMENTS OF SAMPLE GL05058

Fig. 1 Signal Calibration

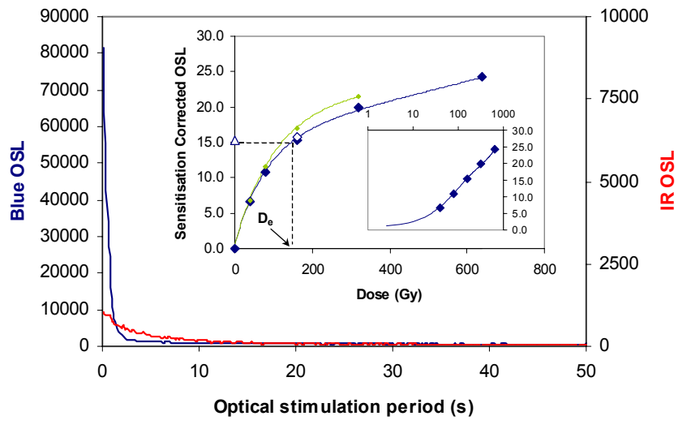

Signal Calibration Natural blue and laboratory-induced infrared (IR) OSL signals. Detectable IR signal decays are diagnostic of feldspar contamination. Inset, the natural blue OSL signal (open triangle) of each aliquot is calibrated against known laboratory doses to yield equivalent dose (D_e) values. Where D_e values are >40 Gy, a **pulsed irradiation** response is shown; pulsed irradiation D_e values are used in age calculations if significantly different from continuous irradiation-based D_e. Where D_e values are >100Gy, a log-linear plot of dose response is shown; D_e can be confidently interpolated if signal response increases with dose.

Irradiation-Preheat Cycling The acquisition of D_e values is necessarily predicated upon thermal treatment of aliquots succeeding environmental and laboratory irradiation. Repeated irradiation and thermal treatment results in aliquot sensitisation, rendering calibration of the natural signal inaccurate. This sensitisation can be monitored and corrected for. The accuracy of correction can be preheat dependent; irradiation-preheat cycling quantifies this dependence for laboratory-induced signals, examining the reproducibility of corrected OSL resultant of repeat laboratory doses.

D_e Preheat Dependence Quantifies the combined effects of thermal transfer and sensitisation on the natural signal. Insignificant adjustment in D_e may reflect limited influence of these effects

Dose Recovery Attempts to replicate the above diagnostic, yet provide improved resolution of thermal effects through removal of variability induced by heterogeneous dose absorption in the environment and using a precise lab dose to simulate natural dose. Based on this and preceding data an appropriate thermal treatment is selected to refine the final D_e value.

Inter-aliquot D_e distribution Provides a measure of inter-aliquot statistical concordance in D_e values derived from **natural** and **laboratory** irradiation. Discordant data (those points lying beyond ±2 standardised ln D_e) reflects heterogeneous dose absorption and/or inaccuracies in calibration.

Signal Analysis Statistically significant increase in **natural** D_e value with signal stimulation period is indicative of a partially-bleached signal, provided a significant increase in D_e results from **simulated partial bleaching** along with insignificant adjustment in D_e for simulated **zero** and **full bleach** conditions. Ages from such samples are considered maximum estimates.

Th & U Decay Activities Statistical concordance (equilibrium) in the activities of daughter radioisotopes in the Th and U decay series may signify the temporal stability of D_r emissions from these chains. Significant differences (disequilibrium) in activity indicate addition or removal of isotopes creating a time-dependent shift in D_r values and increased uncertainty in the accuracy of age estimates

Age Range The **mean age range** provides an estimate of sediment burial period based on mean D_e and D_r values with associated analytical uncertainties. The probability distribution indicates the inter-aliquot variability in age. The **maximum influence** of temporal variations in D_r forced by minima-maxima variation in moisture content and overburden thickness may prove instructive where there is uncertainty in these parameters, however the combined extremes represented should not be construed as preferred age estimates.

Fig. 2 Irradiation-Preheat Cycling

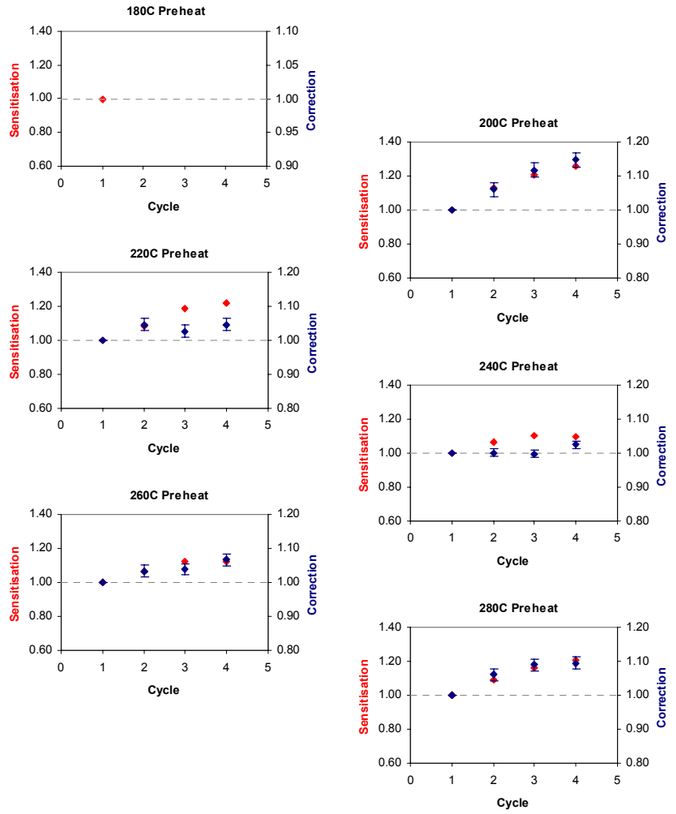

Fig. 3 D_e Preheat Dependence

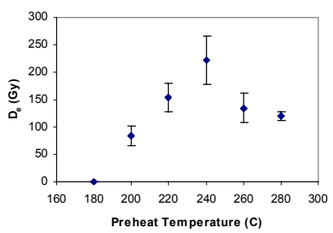

Fig. 4 Dose Recovery

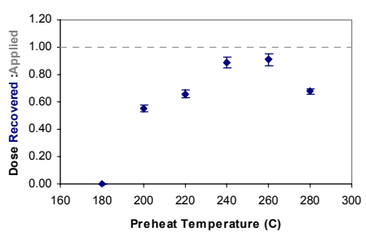

Fig. 5 Inter-aliquot D_e distribution

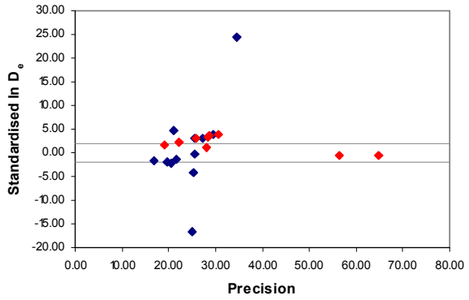

Fig. 6 Signal Analysis

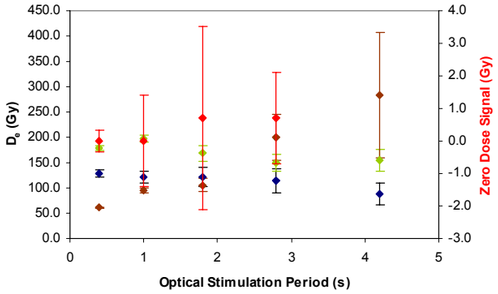

Fig. 7 Th & U Decay Activities

Insufficient Sample Mass

Fig. 8 Age Range

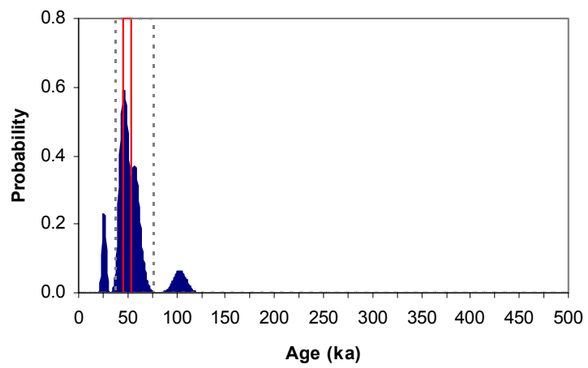

Sample: GL05058

APPENDIX 2: MEASUREMENTS OF SAMPLE GL05059

Fig. 1 Signal Calibration

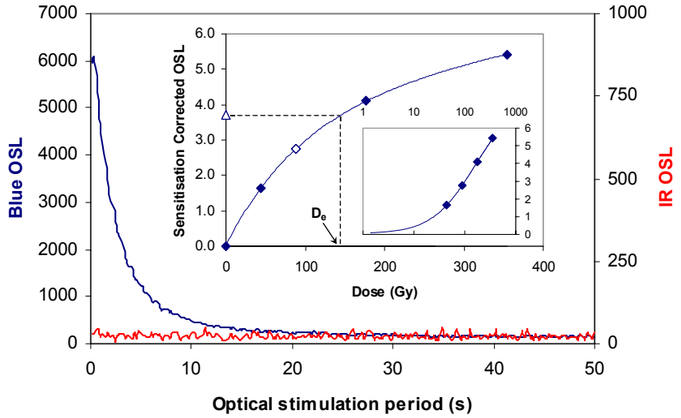

Signal Calibration Natural blue and laboratory-induced infrared (IR) OSL signals. Detectable IR signal decays are diagnostic of feldspar contamination. Inset, the natural blue OSL signal (open triangle) of each aliquot is calibrated against known laboratory doses to yield equivalent dose (D_e) values. Where D_e values are >40 Gy, a **pulsed irradiation** response is shown; pulsed irradiation D_e values are used in age calculations if significantly different from continuous irradiation-based D_e. Where D_e values are >100Gy, a log-linear plot of dose response is shown; D_e can be confidently interpolated if signal response increases with dose.

Irradiation-Preheat Cycling The acquisition of D_e values is necessarily predicated upon thermal treatment of aliquots succeeding environmental and laboratory irradiation. Repeated irradiation and thermal treatment results in aliquot sensitisation, rendering calibration of the natural signal inaccurate. This sensitisation can be monitored and corrected for. The accuracy of correction can be preheat dependent; irradiation-preheat cycling quantifies this dependence for laboratory-induced signals, examining the reproducibility of corrected OSL resultant of repeat laboratory doses.

D_e Preheat Dependence Quantifies the combined effects of thermal transfer and sensitisation on the natural signal. Insignificant adjustment in D_e may reflect limited influence of these effects

Dose Recovery Attempts to replicate the above diagnostic, yet provide improved resolution of thermal effects through removal of variability induced by heterogeneous dose absorption in the environment and using a precise lab dose to simulate natural dose. Based on this and preceding data an appropriate thermal treatment is selected to refine the final D_e value.

Inter-aliquot D_e distribution Provides a measure of inter-aliquot statistical concordance in D_e values derived from **natural** and **laboratory** irradiation. Discordant data (those points lying beyond **±2 standardised ln D_e**) reflects heterogeneous dose absorption and/or inaccuracies in calibration.

Signal Analysis Statistically significant increase in **natural** D_e value with signal stimulation period is indicative of a partially-bleached signal, provided a significant increase in D_e results from **simulated partial bleaching** along with insignificant adjustment in D_e for simulated **zero** and **full bleach** conditions. Ages from such samples are considered maximum estimates.

Th & U Decay Activities Statistical concordance (equilibrium) in the activities of daughter radioisotopes in the Th and U decay series may signify the temporal stability of D_r emissions from these chains. Significant differences (disequilibrium) in activity indicate addition or removal of isotopes creating a time-dependent shift in D_r values and increased uncertainty in the accuracy of age estimates

Age Range The **mean age range** provides an estimate of sediment burial period based on mean D_e and D_r values with associated analytical uncertainties. The probability distribution indicates the inter-aliquot variability in age. The **maximum influence** of temporal variations in D_r forced by minima-maxima variation in moisture content and overburden thickness may prove instructive where there is uncertainty in these parameters, however the combined extremes represented should not be construed as preferred age estimates.

Fig. 2 Irradiation-Preheat Cycling

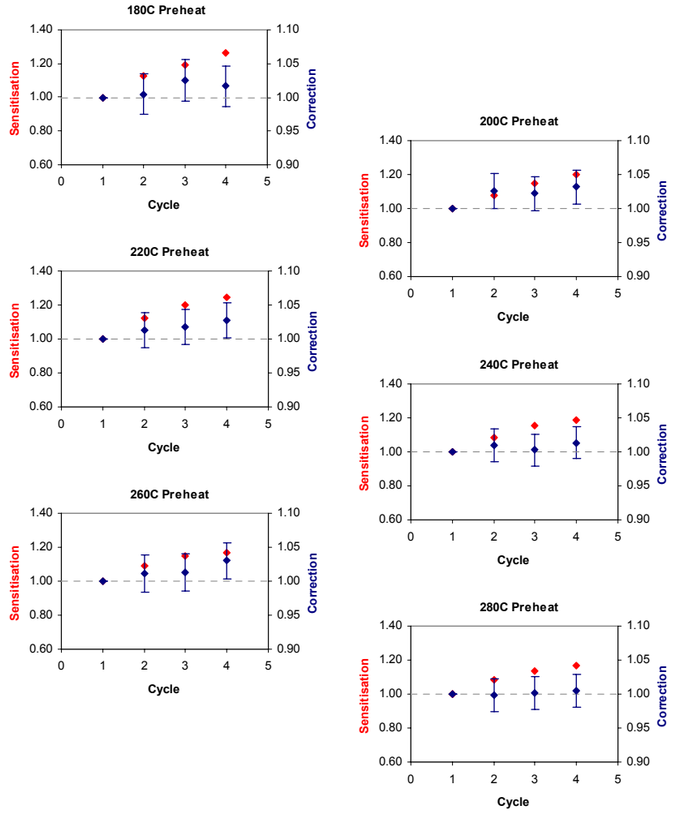

Fig. 3 D_e Preheat Dependence

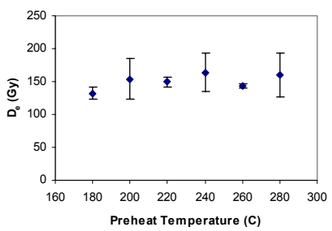

Fig. 4 Dose Recovery

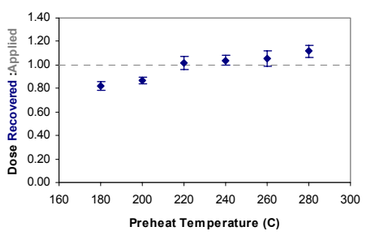

Sample: GL05059

Fig. 5 Inter-aliquot D_e distribution

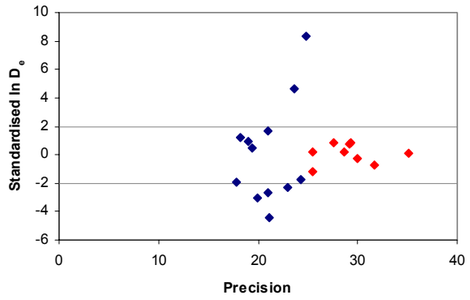

Fig. 6 Signal Analysis

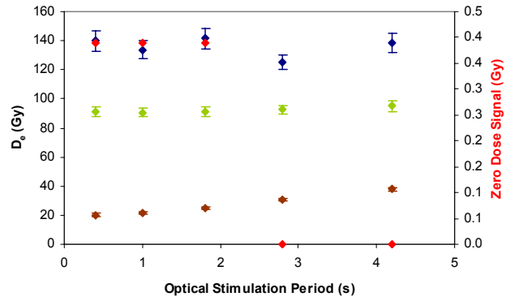

Fig. 7 Th & U Decay Activities

Insufficient Sample Mass

Fig. 8 Age Range

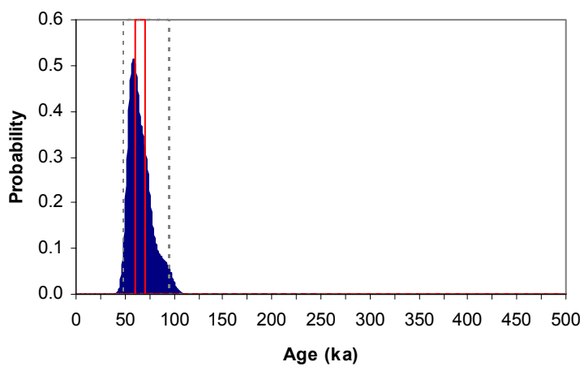

APPENDIX 3: MEASUREMENTS OF SAMPLE GL05060

Fig. 1 Signal Calibration

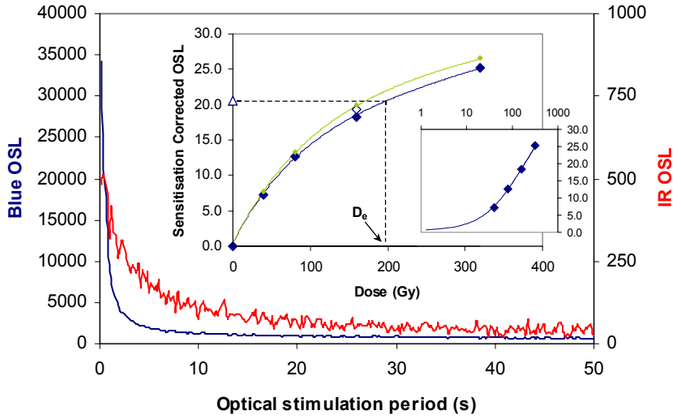

Signal Calibration Natural blue and laboratory-induced infrared (IR) OSL signals. Detectable IR signal decays are diagnostic of feldspar contamination. Inset, the natural blue OSL signal (open triangle) of each aliquot is calibrated against known laboratory doses to yield equivalent dose (D_e) values. Where D_e values are >40 Gy, a **pulsed irradiation** response is shown; pulsed irradiation D_e values are used in age calculations if significantly different from continuous irradiation-based D_e. Where D_e values are >100Gy, a log-linear plot of dose response is shown; D_e can be confidently interpolated if signal response increases with dose.

Irradiation-Preheat Cycling The acquisition of D_e values is necessarily predicated upon thermal treatment of aliquots succeeding environmental and laboratory irradiation. Repeated irradiation and thermal treatment results in aliquot sensitisation, rendering calibration of the natural signal inaccurate. This sensitisation can be monitored and corrected for. The accuracy of correction can be preheat dependent; irradiation-preheat cycling quantifies this dependence for laboratory-induced signals, examining the reproducibility of corrected OSL resultant of repeat laboratory doses.

D_e Preheat Dependence Quantifies the combined effects of thermal transfer and sensitisation on the natural signal. Insignificant adjustment in D_e may reflect limited influence of these effects

Dose Recovery Attempts to replicate the above diagnostic, yet provide improved resolution of thermal effects through removal of variability induced by heterogeneous dose absorption in the environment and using a precise lab dose to simulate natural dose. Based on this and preceding data an appropriate thermal treatment is selected to refine the final D_e value.

Inter-aliquot D_e distribution Provides a measure of inter-aliquot statistical concordance in D_e values derived from **natural** and **laboratory** irradiation. Discordant data (those points lying beyond **±2 standardised ln D_e**) reflects heterogeneous dose absorption and/or inaccuracies in calibration.

Signal Analysis Statistically significant increase in **natural** D_e value with signal stimulation period is indicative of a partially-bleached signal, provided a significant increase in D_e results from **simulated partial bleaching** along with insignificant adjustment in D_e for simulated **zero** and **full bleach** conditions. Ages from such samples are considered maximum estimates.

Th & U Decay Activities Statistical concordance (equilibrium) in the activities of daughter radioisotopes in the Th and U decay series may signify the temporal stability of D_r emissions from these chains. Significant differences (disequilibrium) in activity indicate addition or removal of isotopes creating a time-dependent shift in D_r values and increased uncertainty in the accuracy of age estimates

Age Range The **mean age range** provides an estimate of sediment burial period based on mean D_e and D_r values with associated analytical uncertainties. The probability distribution indicates the inter-aliquot variability in age. The **maximum influence** of temporal variations in D_r forced by minima-maxima variation in moisture content and overburden thickness may prove instructive where there is uncertainty in these parameters, however the combined extremes represented should not be construed as preferred age estimates.

Fig. 2 Irradiation-Preheat Cycling

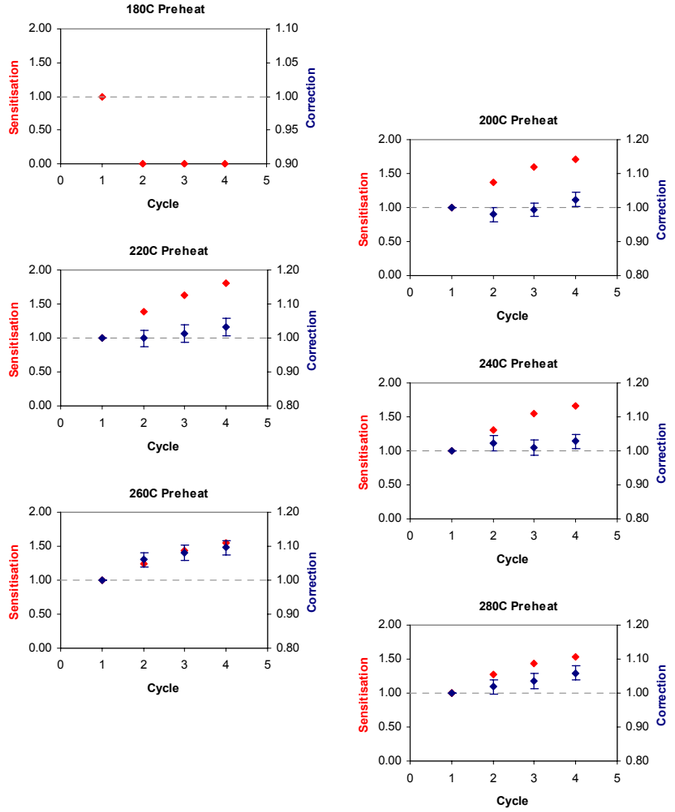

Fig. 3 D_e Preheat Dependence

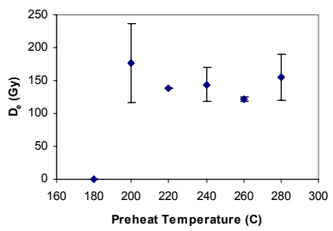

Fig. 4 Dose Recovery

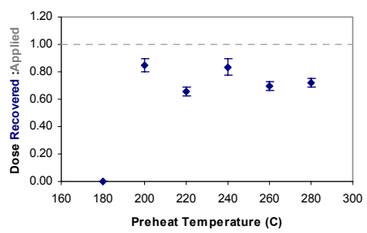

Sample: GL05060

Fig. 5 Inter-aliquot D_e distribution

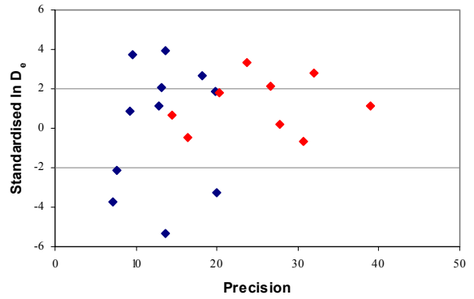

Fig. 6 Signal Analysis

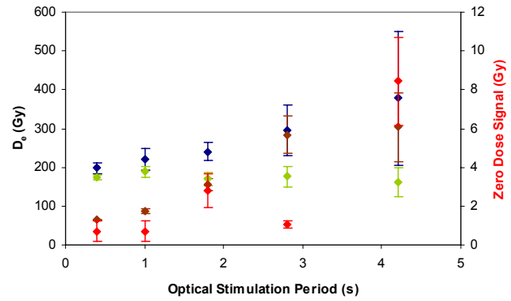

Fig. 7 Th & U Decay Activities

Insufficient Sample Mass

Fig. 8 Age Range

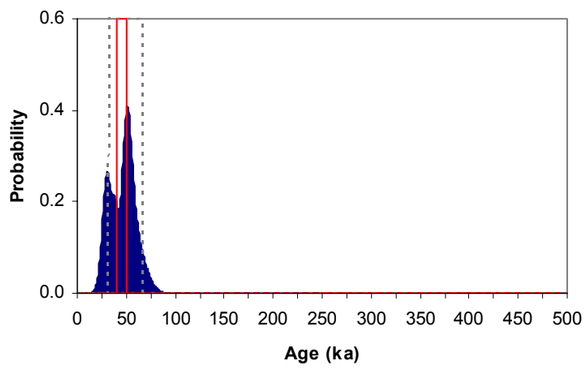

APPENDIX 4: MEASUREMENTS OF SAMPLE GL05061

Fig. 1 Signal Calibration

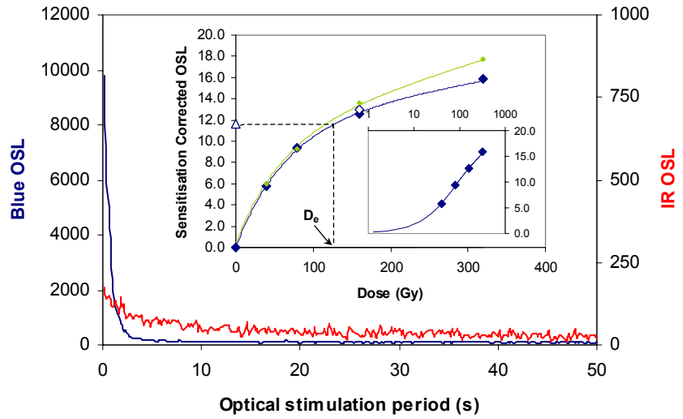

Signal Calibration Natural blue and laboratory-induced infrared (IR) OSL signals. Detectable IR signal decays are diagnostic of feldspar contamination. Inset, the natural blue OSL signal (open triangle) of each aliquot is calibrated against known laboratory doses to yield equivalent dose (D_e) values. Where D_e values are >40 Gy, a **pulsed irradiation** response is shown; pulsed irradiation D_e values are used in age calculations if significantly different from continuous irradiation-based D_e. Where D_e values are >100Gy, a log-linear plot of dose response is shown; D_e can be confidently interpolated if signal response increases with dose.

Irradiation-Preheat Cycling The acquisition of D_e values is necessarily predicated upon thermal treatment of aliquots succeeding environmental and laboratory irradiation. Repeated irradiation and thermal treatment results in aliquot sensitisation, rendering calibration of the natural signal inaccurate. This sensitisation can be monitored and corrected for. The accuracy of correction can be preheat dependent; irradiation-preheat cycling quantifies this dependence for laboratory-induced signals, examining the reproducibility of corrected OSL resultant of repeat laboratory doses.

D_e Preheat Dependence Quantifies the combined effects of thermal transfer and sensitisation on the natural signal. Insignificant adjustment in D_e may reflect limited influence of these effects

Dose Recovery Attempts to replicate the above diagnostic, yet provide improved resolution of thermal effects through removal of variability induced by heterogeneous dose absorption in the environment and using a precise lab dose to simulate natural dose. Based on this and preceding data an appropriate thermal treatment is selected to refine the final D_e value.

Inter-aliquot D_e distribution Provides a measure of inter-aliquot statistical concordance in D_e values derived from **natural** and **laboratory** irradiation. Discordant data (those points lying beyond ±2 standardised ln D_e) reflects heterogeneous dose absorption and/or inaccuracies in calibration.

Signal Analysis Statistically significant increase in **natural** D_e value with signal stimulation period is indicative of a partially-bleached signal, provided a significant increase in D_e results from **simulated partial bleaching** along with insignificant adjustment in D_e for simulated **zero** and **full bleach** conditions. Ages from such samples are considered maximum estimates.

Th & U Decay Activities Statistical concordance (equilibrium) in the activities of daughter radioisotopes in the Th and U decay series may signify the temporal stability of D_r emissions from these chains. Significant differences (disequilibrium) in activity indicate addition or removal of isotopes creating a time-dependent shift in D_r values and increased uncertainty in the accuracy of age estimates

Age Range The **mean age range** provides an estimate of sediment burial period based on mean D_e and D_r values with associated analytical uncertainties. The probability distribution indicates the inter-aliquot variability in age. The **maximum influence** of temporal variations in D_r forced by minima-maxima variation in moisture content and overburden thickness may prove instructive where there is uncertainty in these parameters, however the combined extremes represented should not be construed as preferred age estimates.

Fig. 2 Irradiation-Preheat Cycling

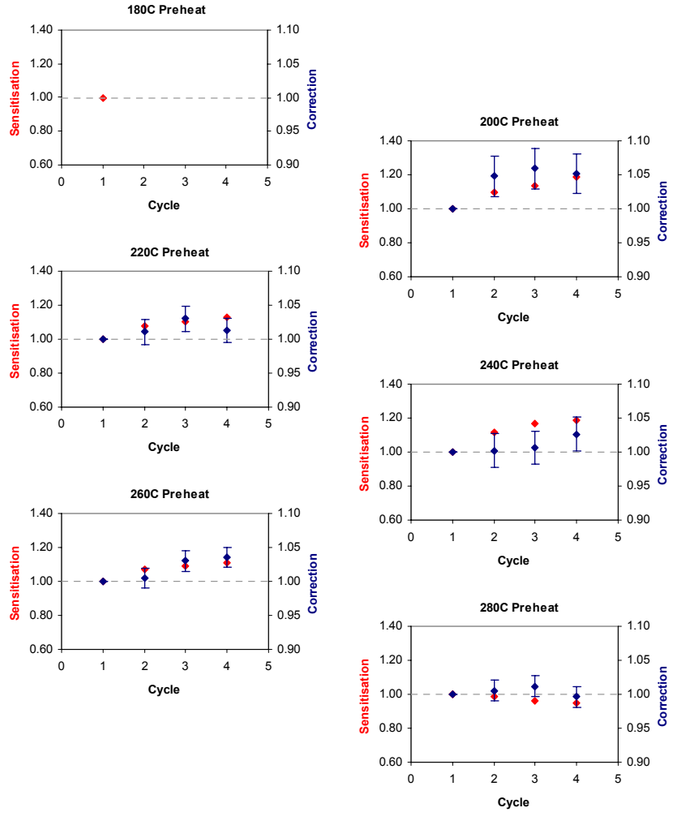

Fig. 3 D_e Preheat Dependence

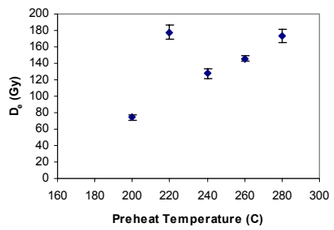

Fig. 4 Dose Recovery

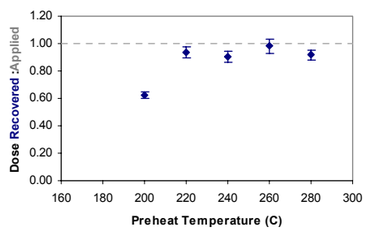

Sample: GL05061

Fig. 5 Inter-aliquot D_e distribution

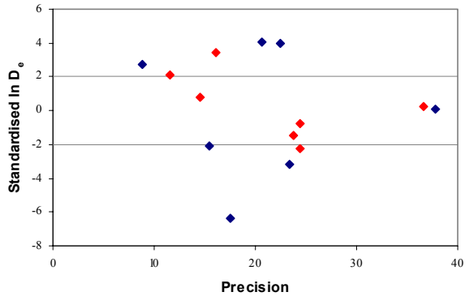

Fig. 6 Signal Analysis

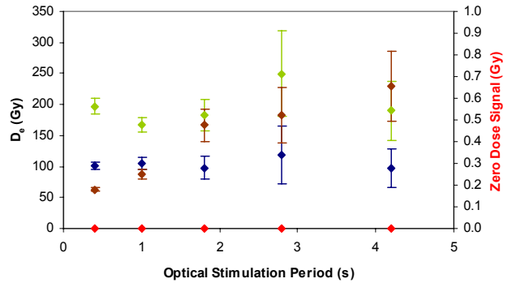

Fig. 7 Th & U Decay Activities

Activity (Bq.kg^{-1})

Insufficient Sample Mass

Fig. 8 Age Range

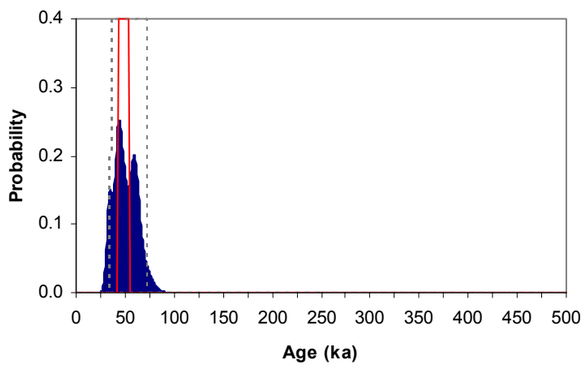

APPENDIX 5: MEASUREMENTS OF SAMPLE GL05062

Fig. 1 Signal Calibration

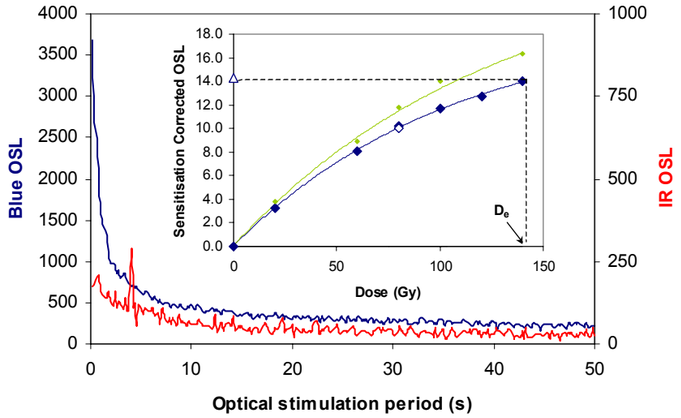

Signal Calibration Natural blue and laboratory-induced infrared (IR) OSL signals. Detectable IR signal decays are diagnostic of feldspar contamination. Inset, the natural blue OSL signal (open triangle) of each aliquot is calibrated against known laboratory doses to yield equivalent dose (D_e) values. Where D_e values are >40 Gy, a **pulsed irradiation** response is shown; pulsed irradiation D_e values are used in age calculations if significantly different from continuous irradiation-based D_e. Where D_e values are >100Gy, a log-linear plot of dose response is shown; D_e can be confidently interpolated if signal response increases with dose.

Irradiation-Preheat Cycling The acquisition of D_e values is necessarily predicated upon thermal treatment of aliquots succeeding environmental and laboratory irradiation. Repeated irradiation and thermal treatment results in aliquot sensitisation, rendering calibration of the natural signal inaccurate. This sensitisation can be monitored and corrected for. The accuracy of correction can be preheat dependent; irradiation-preheat cycling quantifies this dependence for laboratory-induced signals, examining the reproducibility of corrected OSL resultant of repeat laboratory doses.

D_e Preheat Dependence Quantifies the combined effects of thermal transfer and sensitisation on the natural signal. Insignificant adjustment in D_e may reflect limited influence of these effects

Dose Recovery Attempts to replicate the above diagnostic, yet provide improved resolution of thermal effects through removal of variability induced by heterogeneous dose absorption in the environment and using a precise lab dose to simulate natural dose. Based on this and preceding data an appropriate thermal treatment is selected to refine the final D_e value.

Inter-aliquot D_e distribution Provides a measure of inter-aliquot statistical concordance in D_e values derived from **natural** and **laboratory** irradiation. Discordant data (those points lying beyond **±2 standardised ln D_e**) reflects heterogeneous dose absorption and/or inaccuracies in calibration.

Signal Analysis Statistically significant increase in **natural** D_e value with signal stimulation period is indicative of a partially-bleached signal, provided a significant increase in D_e results from **simulated partial bleaching** along with insignificant adjustment in D_e for simulated **zero** and **full bleach** conditions. Ages from such samples are considered maximum estimates.

Th & U Decay Activities Statistical concordance (equilibrium) in the activities of daughter radioisotopes in the Th and U decay series may signify the temporal stability of D_r emissions from these chains. Significant differences (disequilibrium) in activity indicate addition or removal of isotopes creating a time-dependent shift in D_r values and increased uncertainty in the accuracy of age estimates

Age Range The **mean age range** provides an estimate of sediment burial period based on mean D_e and D_r values with associated analytical uncertainties. The probability distribution indicates the inter-aliquot variability in age. The **maximum influence** of temporal variations in D_r forced by minima-maxima variation in moisture content and overburden thickness may prove instructive where there is uncertainty in these parameters, however the combined extremes represented should not be construed as preferred age estimates.

Fig. 2 Irradiation-Preheat Cycling

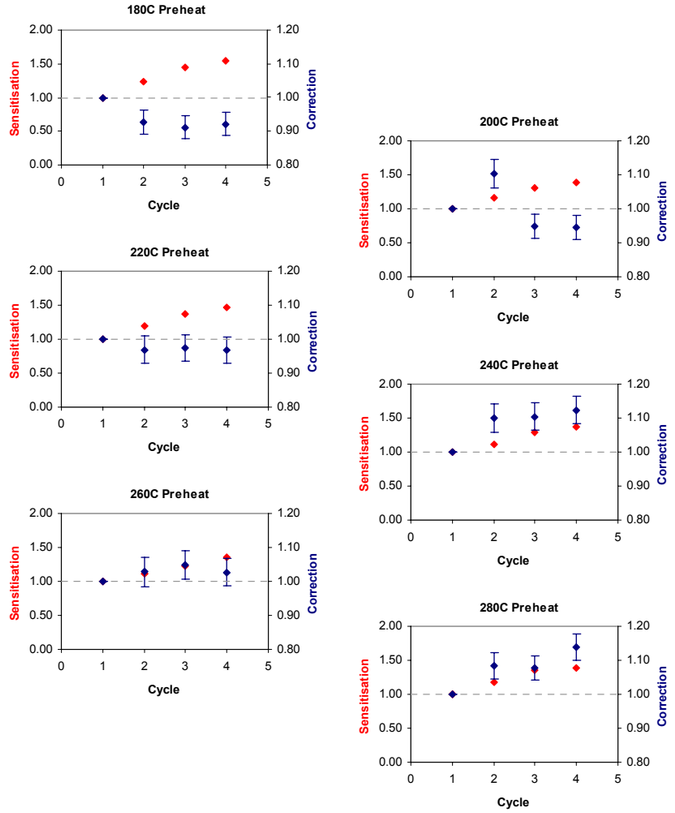

Fig. 3 D_e Preheat Dependence

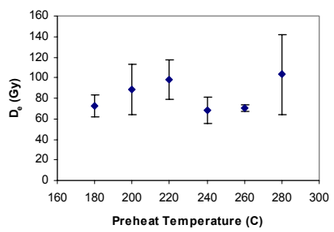

Fig. 4 Dose Recovery

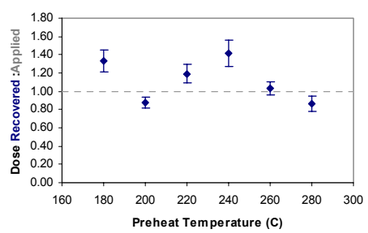

Sample: GL05062

Fig. 5 Inter-aliquot D_e distribution

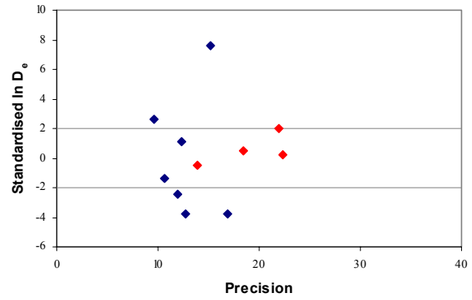

Fig. 6 Signal Analysis

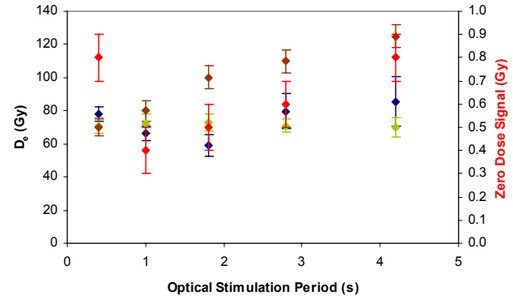

Fig. 7 Th & U Decay Activities

Insufficient Sample Mass

Fig. 8 Age Range

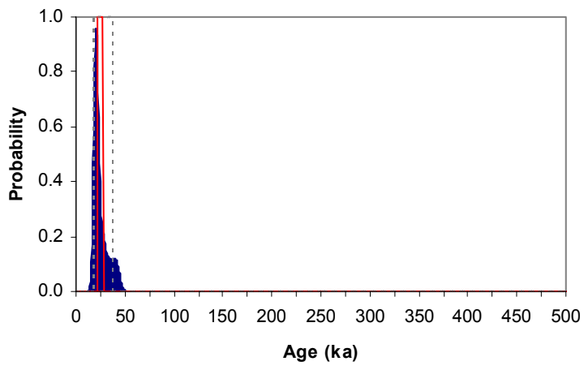

APPENDIX 6: MEASUREMENTS OF SAMPLE GL05063

Fig. 1 Signal Calibration

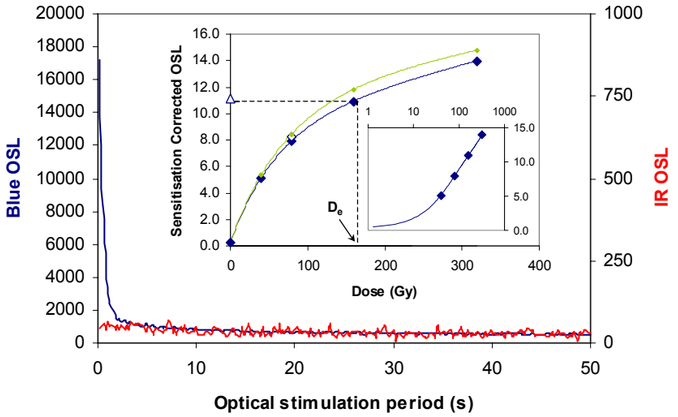

Signal Calibration Natural blue and laboratory-induced infrared (IR) OSL signals. Detectable IR signal decays are diagnostic of feldspar contamination. Inset, the natural blue OSL signal (open triangle) of each aliquot is calibrated against known laboratory doses to yield equivalent dose (D_e) values. Where D_e values are >40 Gy, a **pulsed irradiation** response is shown; pulsed irradiation D_e values are used in age calculations if significantly different from continuous irradiation-based D_e. Where D_e values are >100Gy, a log-linear plot of dose response is shown; D_e can be confidently interpolated if signal response increases with dose.

Irradiation-Preheat Cycling The acquisition of D_e values is necessarily predicated upon thermal treatment of aliquots succeeding environmental and laboratory irradiation. Repeated irradiation and thermal treatment results in aliquot sensitisation, rendering calibration of the natural signal inaccurate. This sensitisation can be monitored and corrected for. The accuracy of correction can be preheat dependent; irradiation-preheat cycling quantifies this dependence for laboratory-induced signals, examining the reproducibility of corrected OSL resultant of repeat laboratory doses.

D_e Preheat Dependence Quantifies the combined effects of thermal transfer and sensitisation on the natural signal. Insignificant adjustment in D_e may reflect limited influence of these effects

Dose Recovery Attempts to replicate the above diagnostic, yet provide improved resolution of thermal effects through removal of variability induced by heterogeneous dose absorption in the environment and using a precise lab dose to simulate natural dose. Based on this and preceding data an appropriate thermal treatment is selected to refine the final D_e value.

Inter-aliquot D_e distribution Provides a measure of inter-aliquot statistical concordance in D_e values derived from **natural** and **laboratory** irradiation. Discordant data (those points lying beyond **±2 standardised ln D_e**) reflects heterogeneous dose absorption and/or inaccuracies in calibration.

Signal Analysis Statistically significant increase in **natural** D_e value with signal stimulation period is indicative of a partially-bleached signal, provided a significant increase in D_e results from **simulated partial bleaching** along with insignificant adjustment in D_e for simulated **zero** and **full bleach** conditions. Ages from such samples are considered maximum estimates.

Th & U Decay Activities Statistical concordance (equilibrium) in the activities of daughter radioisotopes in the Th and U decay series may signify the temporal stability of D_r emissions from these chains. Significant differences (disequilibrium) in activity indicate addition or removal of isotopes creating a time-dependent shift in D_r values and increased uncertainty in the accuracy of age estimates

Age Range The **mean age range** provides an estimate of sediment burial period based on mean D_e and D_r values with associated analytical uncertainties. The probability distribution indicates the inter-aliquot variability in age. The **maximum influence** of temporal variations in D_r forced by minima-maxima variation in moisture content and overburden thickness may prove instructive where there is uncertainty in these parameters, however the combined extremes represented should not be construed as preferred age estimates.

Fig. 2 Irradiation-Preheat Cycling

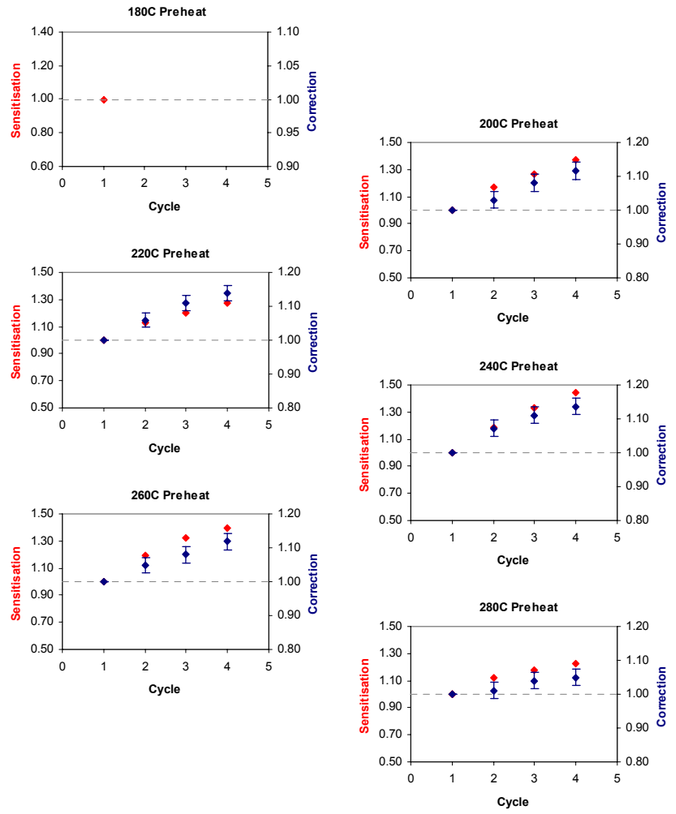

Fig. 3 D_e Preheat Dependence

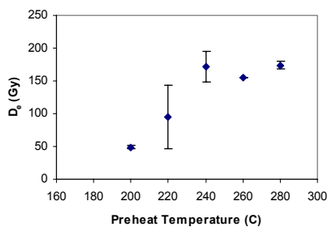

Fig. 4 Dose Recovery

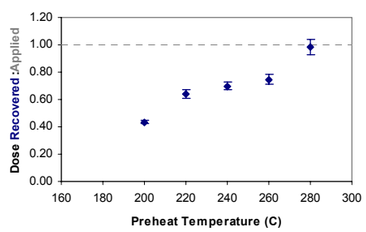

Sample: GL05063

Fig. 5 Inter-aliquot D_e distribution

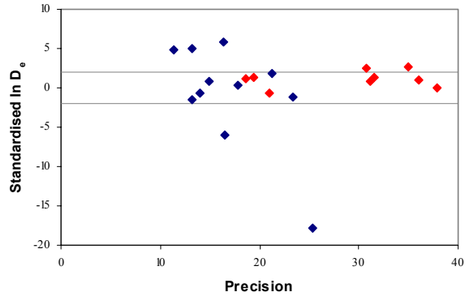

Fig. 6 Signal Analysis

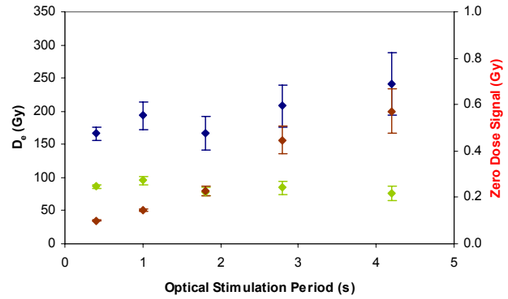

Fig. 7 Th & U Decay Activities

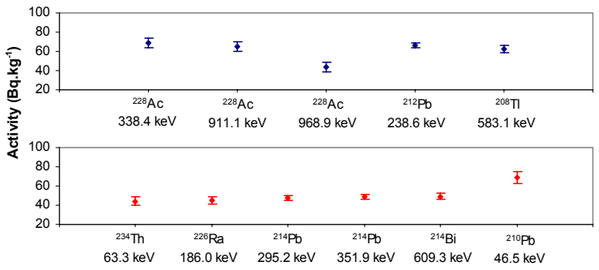

Fig. 8 Age Range

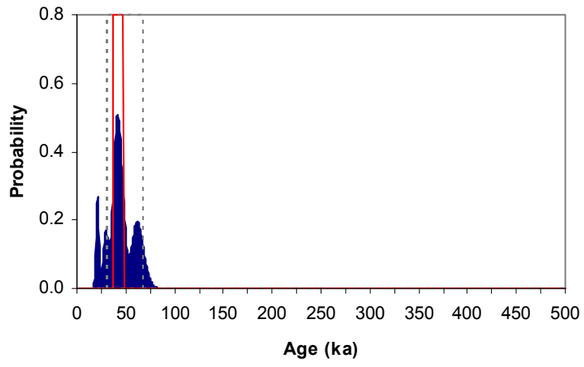

APPENDIX 7: MEASUREMENTS OF SAMPLE GL06064

Fig. 1 Signal Calibration

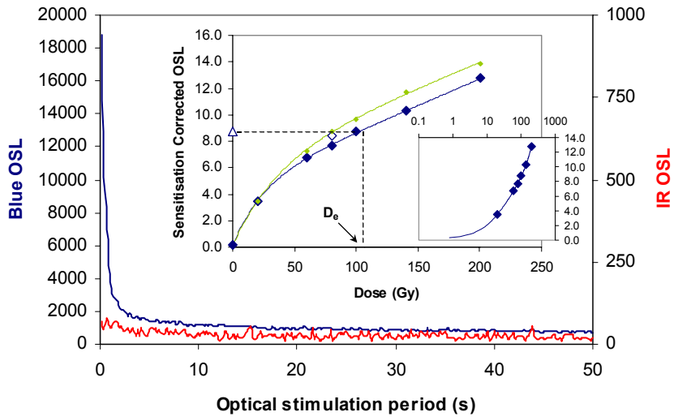

Signal Calibration Natural blue and laboratory-induced infrared (IR) OSL signals. Detectable IR signal decays are diagnostic of feldspar contamination. Inset, the natural blue OSL signal (open triangle) of each aliquot is calibrated against known laboratory doses to yield equivalent dose (D_e) values. Where D_e values are >40 Gy, a **pulsed irradiation** response is shown; pulsed irradiation D_e values are used in age calculations if significantly different from continuous irradiation-based D_e. Where D_e values are >100Gy, a log-linear plot of dose response is shown; D_e can be confidently interpolated if signal response increases with dose.

Irradiation-Preheat Cycling The acquisition of D_e values is necessarily predicated upon thermal treatment of aliquots succeeding environmental and laboratory irradiation. Repeated irradiation and thermal treatment results in aliquot sensitisation, rendering calibration of the natural signal inaccurate. This sensitisation can be monitored and corrected for. The accuracy of correction can be preheat dependent; irradiation-preheat cycling quantifies this dependence for laboratory-induced signals, examining the reproducibility of corrected OSL resultant of repeat laboratory doses.

D_e Preheat Dependence Quantifies the combined effects of thermal transfer and sensitisation on the natural signal. Insignificant adjustment in D_e may reflect limited influence of these effects

Dose Recovery Attempts to replicate the above diagnostic, yet provide improved resolution of thermal effects through removal of variability induced by heterogeneous dose absorption in the environment and using a precise lab dose to simulate natural dose. Based on this and preceding data an appropriate thermal treatment is selected to refine the final D_e value.

Inter-aliquot D_e distribution Provides a measure of inter-aliquot statistical concordance in D_e values derived from **natural** and **laboratory** irradiation. Discordant data (those points lying beyond **±2 standardised ln D_e**) reflects heterogeneous dose absorption and/or inaccuracies in calibration.

Signal Analysis Statistically significant increase in **natural** D_e value with signal stimulation period is indicative of a partially-bleached signal, provided a significant increase in D_e results from **simulated partial bleaching** along with insignificant adjustment in D_e for simulated **zero** and **full bleach** conditions. Ages from such samples are considered maximum estimates.

Th & U Decay Activities Statistical concordance (equilibrium) in the activities of daughter radioisotopes in the Th and U decay series may signify the temporal stability of D_r emissions from these chains. Significant differences (disequilibrium) in activity indicate addition or removal of isotopes creating a time-dependent shift in D_r values and increased uncertainty in the accuracy of age estimates

Age Range The **mean age range** provides an estimate of sediment burial period based on mean D_e and D_r values with associated analytical uncertainties. The probability distribution indicates the inter-aliquot variability in age. The **maximum influence** of temporal variations in D_r forced by minima-maxima variation in moisture content and overburden thickness may prove instructive where there is uncertainty in these parameters, however the combined extremes represented should not be construed as preferred age estimates.

Fig. 2 Irradiation-Preheat Cycling

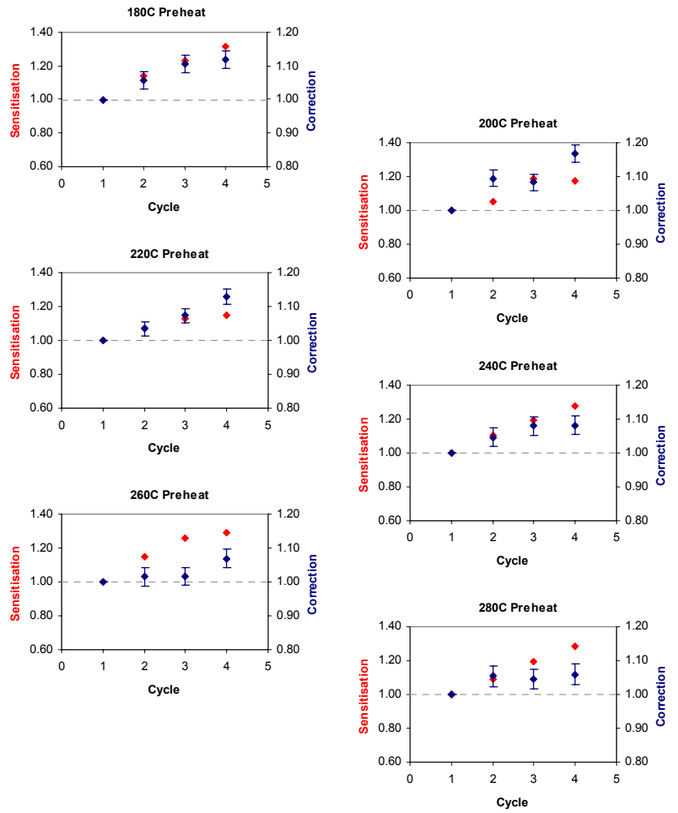

Fig. 3 D_e Preheat Dependence

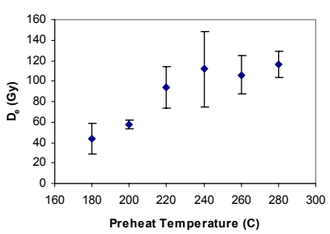

Fig. 4 Dose Recovery

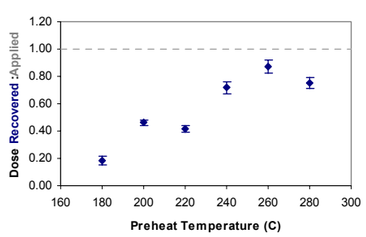

Sample: GL05064

Fig. 5 Inter-aliquot D_e distribution

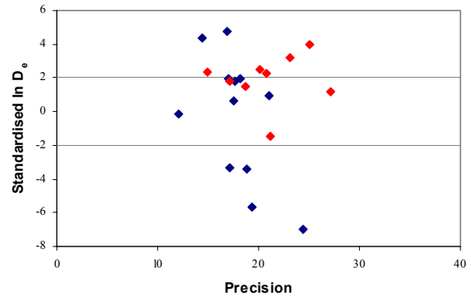

Fig. 6 Signal Analysis

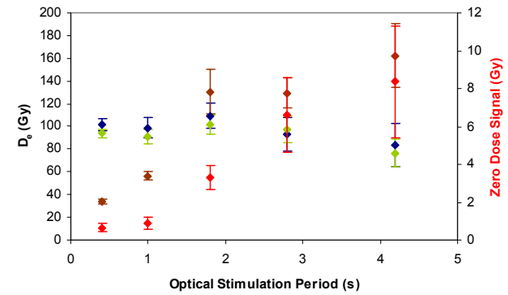

Fig. 7 Th & U Decay Activities

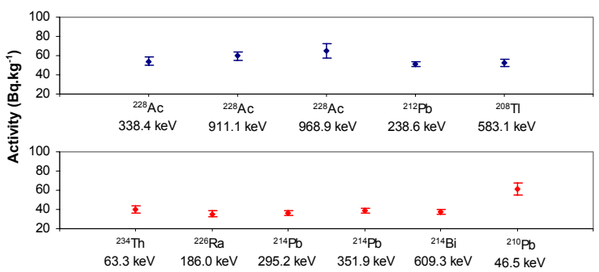

Fig. 8 Age Range

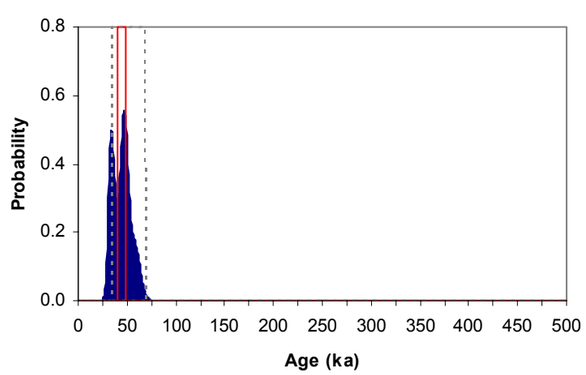

APPENDIX 8: MEASUREMENTS OF SAMPLE GL06001

Fig. 1 Signal Calibration

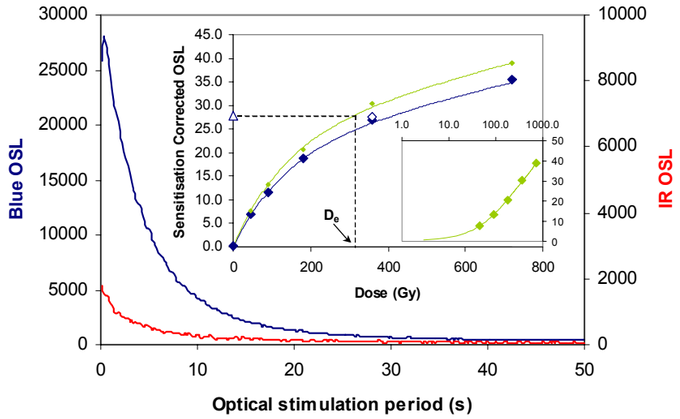

Signal Calibration Natural blue and laboratory-induced infrared (IR) OSL signals. Detectable IR signal decays are diagnostic of feldspar contamination. Inset, the natural blue OSL signal (open triangle) of each aliquot is calibrated against known laboratory doses to yield equivalent dose (D_e) values. Where D_e values are >40 Gy, a **pulsed irradiation** response is shown; pulsed irradiation D_e values are used in age calculations if significantly different from continuous irradiation-based D_e. Where D_e values are >100Gy, a log-linear plot of dose response is shown; D_e can be confidently interpolated if signal response increases with dose.

Irradiation-Preheat Cycling The acquisition of D_e values is necessarily predicated upon thermal treatment of aliquots succeeding environmental and laboratory irradiation. Repeated irradiation and thermal treatment results in aliquot sensitisation, rendering calibration of the natural signal inaccurate. This sensitisation can be monitored and corrected for. The accuracy of correction can be preheat dependent; irradiation-preheat cycling quantifies this dependence for laboratory-induced signals, examining the reproducibility of corrected OSL resultant of repeat laboratory doses.

D_e Preheat Dependence Quantifies the combined effects of thermal transfer and sensitisation on the natural signal. Insignificant adjustment in D_e may reflect limited influence of these effects

Dose Recovery Attempts to replicate the above diagnostic, yet provide improved resolution of thermal effects through removal of variability induced by heterogeneous dose absorption in the environment and using a precise lab dose to simulate natural dose. Based on this and preceding data an appropriate thermal treatment is selected to refine the final D_e value.

Inter-aliquot D_e distribution Provides a measure of inter-aliquot statistical concordance in D_e values derived from **natural** and **laboratory** irradiation. Discordant data (those points lying beyond **±2 standardised ln D_e**) reflects heterogeneous dose absorption and/or inaccuracies in calibration.

Signal Analysis Statistically significant increase in **natural** D_e value with signal stimulation period is indicative of a partially-bleached signal, provided a significant increase in D_e results from **simulated partial bleaching** along with insignificant adjustment in D_e for simulated **zero** and **full bleach** conditions. Ages from such samples are considered maximum estimates.

Th & U Decay Activities Statistical concordance (equilibrium) in the activities of daughter radioisotopes in the Th and U decay series may signify the temporal stability of D_r emissions from these chains. Significant differences (disequilibrium) in activity indicate addition or removal of isotopes creating a time-dependent shift in D_r values and increased uncertainty in the accuracy of age estimates

Age Range The **mean age range** provides an estimate of sediment burial period based on mean D_e and D_r values with associated analytical uncertainties. The probability distribution indicates the inter-aliquot variability in age. The **maximum influence** of temporal variations in D_r forced by minima-maxima variation in moisture content and overburden thickness may prove instructive where there is uncertainty in these parameters, however the combined extremes represented should not be construed as preferred age estimates.

Fig. 2 Irradiation-Preheat Cycling

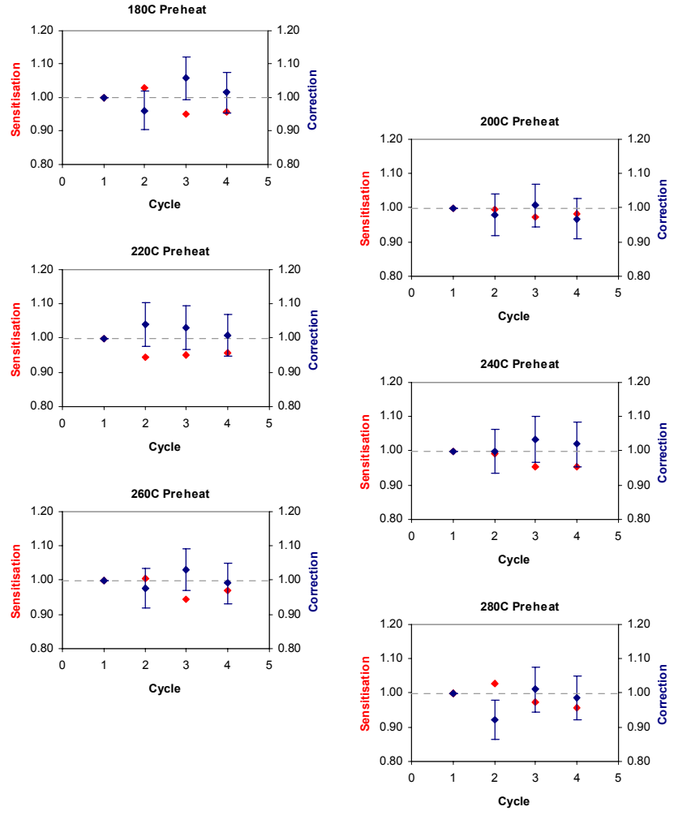

Fig. 3 D_e Preheat Dependence

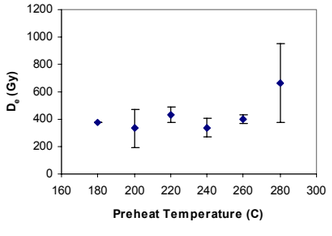

Fig. 4 Dose Recovery

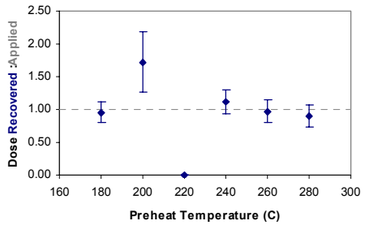

Fig. 5 Inter-aliquot D_e distribution

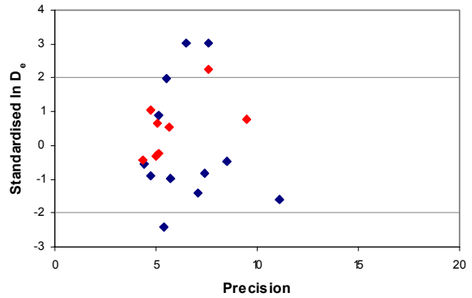

Fig. 6 Signal Analysis

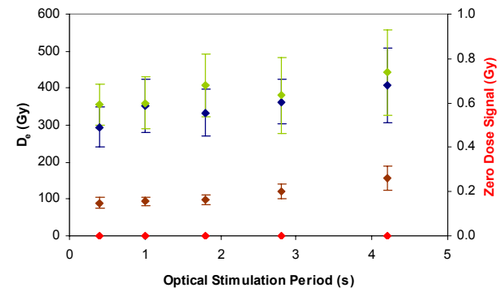

Fig. 7 Th & U Decay Activities

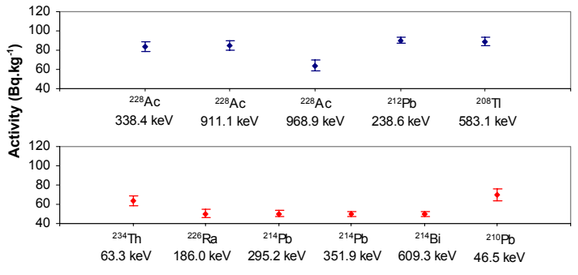

Fig. 8 Age Range

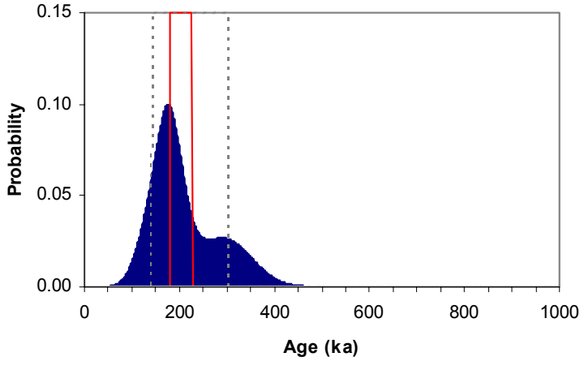

Sample: GL06001

APPENDIX 9: MEASUREMENTS OF SAMPLE GL06002

Fig. 1 Signal Calibration

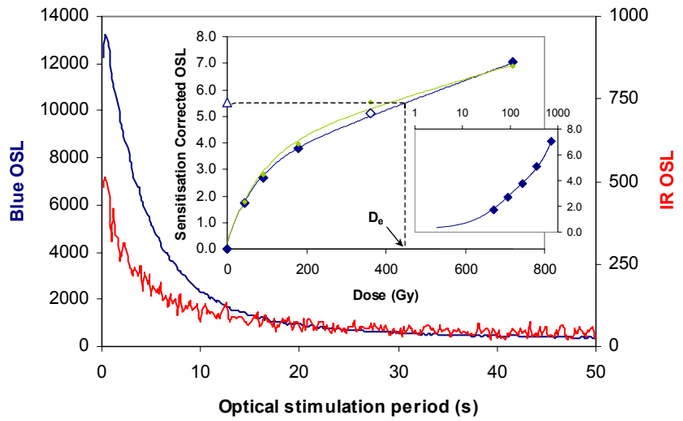

Signal Calibration Natural blue and laboratory-induced infrared (IR) OSL signals. Detectable IR signal decays are diagnostic of feldspar contamination. Inset, the natural blue OSL signal (open triangle) of each aliquot is calibrated against known laboratory doses to yield equivalent dose (D_e) values. Where D_e values are >40 Gy, a **pulsed irradiation** response is shown; pulsed irradiation D_e values are used in age calculations if significantly different from continuous irradiation-based D_e. Where D_e values are >100Gy, a log-linear plot of dose response is shown; D_e can be confidently interpolated if signal response increases with dose.

Irradiation-Preheat Cycling The acquisition of D_e values is necessarily predicated upon thermal treatment of aliquots succeeding environmental and laboratory irradiation. Repeated irradiation and thermal treatment results in aliquot sensitisation, rendering calibration of the natural signal inaccurate. This sensitisation can be monitored and corrected for. The accuracy of correction can be preheat dependent; irradiation-preheat cycling quantifies this dependence for laboratory-induced signals, examining the reproducibility of corrected OSL resultant of repeat laboratory doses.

D_e Preheat Dependence Quantifies the combined effects of thermal transfer and sensitisation on the natural signal. Insignificant adjustment in D_e may reflect limited influence of these effects

Dose Recovery Attempts to replicate the above diagnostic, yet provide improved resolution of thermal effects through removal of variability induced by heterogeneous dose absorption in the environment and using a precise lab dose to simulate natural dose. Based on this and preceding data an appropriate thermal treatment is selected to refine the final D_e value.

Inter-aliquot D_e distribution Provides a measure of inter-aliquot statistical concordance in D_e values derived from **natural** and **laboratory** irradiation. Discordant data (those points lying beyond **±2 standardised ln D_e**) reflects heterogeneous dose absorption and/or inaccuracies in calibration.

Signal Analysis Statistically significant increase in **natural** D_e value with signal stimulation period is indicative of a partially-bleached signal, provided a significant increase in D_e results from **simulated partial bleaching** along with insignificant adjustment in D_e for simulated **zero** and **full bleach** conditions. Ages from such samples are considered maximum estimates.

Th & U Decay Activities Statistical concordance (equilibrium) in the activities of daughter radioisotopes in the Th and U decay series may signify the temporal stability of D_r emissions from these chains. Significant differences (disequilibrium) in activity indicate addition or removal of isotopes creating a time-dependent shift in D_r values and increased uncertainty in the accuracy of age estimates

Age Range The **mean age range** provides an estimate of sediment burial period based on mean D_e and D_r values with associated analytical uncertainties. The probability distribution indicates the inter-aliquot variability in age. The **maximum influence** of temporal variations in D_r forced by minima-maxima variation in moisture content and overburden thickness may prove instructive where there is uncertainty in these parameters, however the combined extremes represented should not be construed as preferred age estimates.

Fig. 2 Irradiation-Preheat Cycling

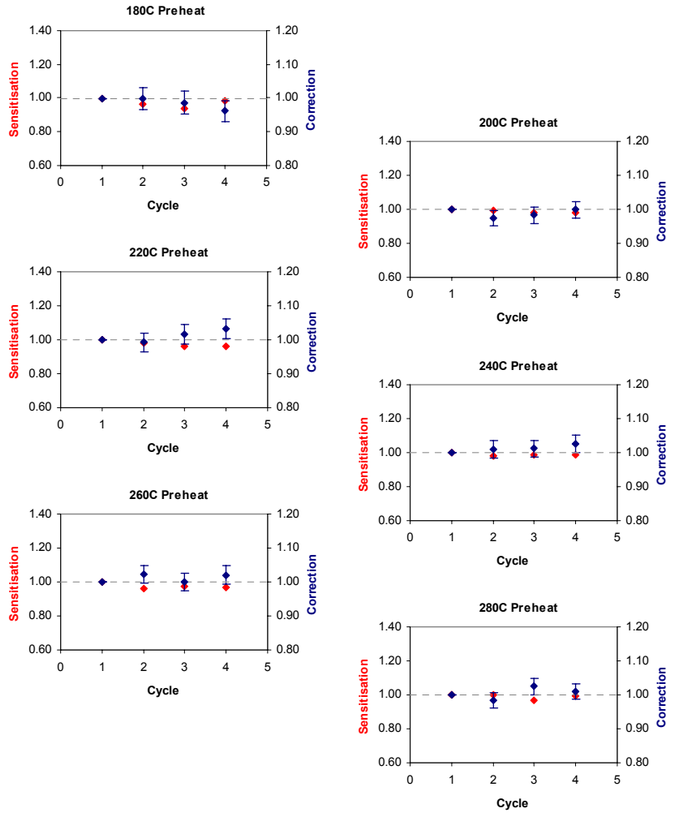

Fig. 3 D_e Preheat Dependence

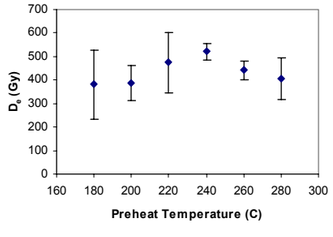

Fig. 4 Dose Recovery

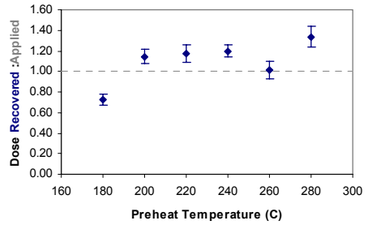

Sample: GL06002

Fig. 5 Inter-aliquot D_e distribution

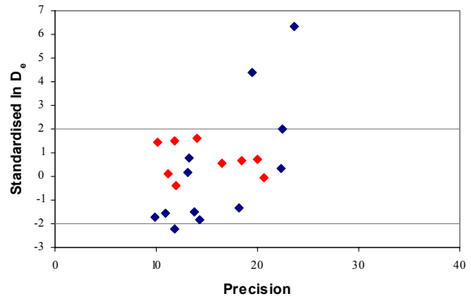

Fig. 6 Signal Analysis

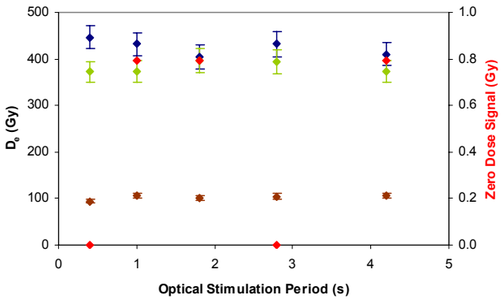

Fig. 7 Th & U Decay Activities

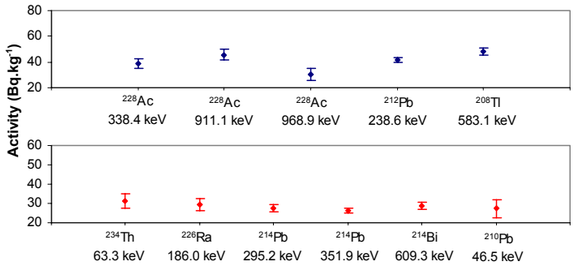

Fig. 8 Age Range

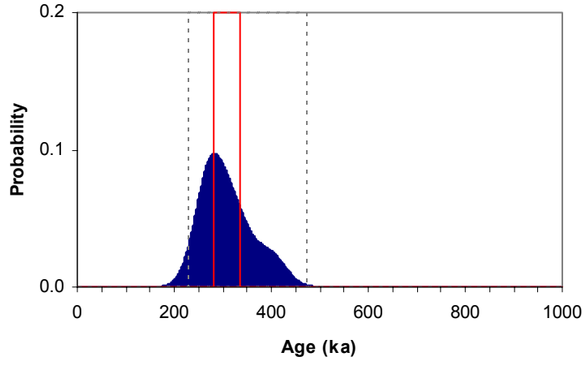

APPENDIX 10: MEASUREMENTS OF SAMPLE GL06003

Fig. 1 Signal Calibration

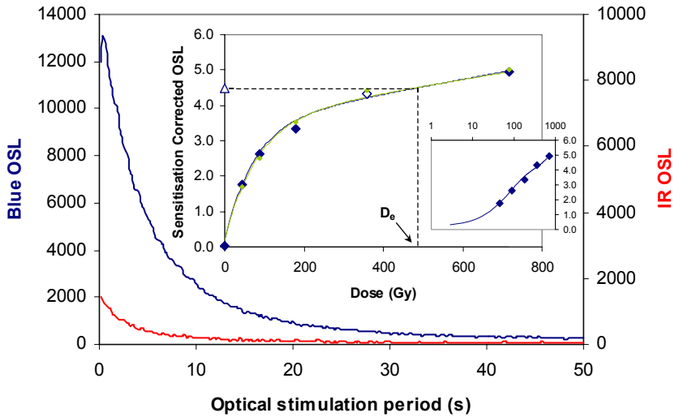

Signal Calibration Natural blue and laboratory-induced infrared (IR) OSL signals. Detectable IR signal decays are diagnostic of feldspar contamination. Inset, the natural blue OSL signal (open triangle) of each aliquot is calibrated against known laboratory doses to yield equivalent dose (D_e) values. Where D_e values are >40 Gy, a **pulsed irradiation** response is shown; pulsed irradiation D_e values are used in age calculations if significantly different from continuous irradiation-based D_e. Where D_e values are >100Gy, a log-linear plot of dose response is shown; D_e can be confidently interpolated if signal response increases with dose.

Irradiation-Preheat Cycling The acquisition of D_e values is necessarily predicated upon thermal treatment of aliquots succeeding environmental and laboratory irradiation. Repeated irradiation and thermal treatment results in aliquot sensitisation, rendering calibration of the natural signal inaccurate. This sensitisation can be monitored and corrected for. The accuracy of correction can be preheat dependent; irradiation-preheat cycling quantifies this dependence for laboratory-induced signals, examining the reproducibility of corrected OSL resultant of repeat laboratory doses.

D_e Preheat Dependence Quantifies the combined effects of thermal transfer and sensitisation on the natural signal. Insignificant adjustment in D_e may reflect limited influence of these effects

Dose Recovery Attempts to replicate the above diagnostic, yet provide improved resolution of thermal effects through removal of variability induced by heterogeneous dose absorption in the environment and using a precise lab dose to simulate natural dose. Based on this and preceding data an appropriate thermal treatment is selected to refine the final D_e value.

Inter-aliquot D_e distribution Provides a measure of inter-aliquot statistical concordance in D_e values derived from **natural** and **laboratory** irradiation. Discordant data (those points lying beyond ±2 standardised ln D_e) reflects heterogeneous dose absorption and/or inaccuracies in calibration.

Signal Analysis Statistically significant increase in **natural** D_e value with signal stimulation period is indicative of a partially-bleached signal, provided a significant increase in D_e results from **simulated partial bleaching** along with insignificant adjustment in D_e for simulated **zero** and **full bleach** conditions. Ages from such samples are considered maximum estimates.

Th & U Decay Activities Statistical concordance (equilibrium) in the activities of daughter radioisotopes in the Th and U decay series may signify the temporal stability of D_r emissions from these chains. Significant differences (disequilibrium) in activity indicate addition or removal of isotopes creating a time-dependent shift in D_r values and increased uncertainty in the accuracy of age estimates

Age Range The **mean age range** provides an estimate of sediment burial period based on mean D_e and D_r values with associated analytical uncertainties. The probability distribution indicates the inter-aliquot variability in age. The **maximum influence** of temporal variations in D_r forced by minima-maxima variation in moisture content and overburden thickness may prove instructive where there is uncertainty in these parameters, however the combined extremes represented should not be construed as preferred age estimates.

Fig. 2 Irradiation-Preheat Cycling

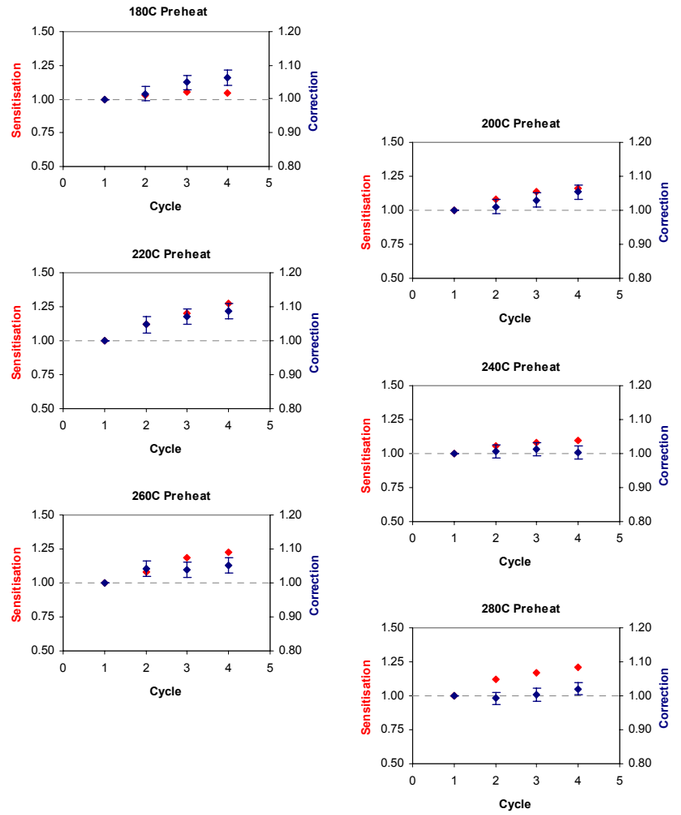

Fig. 3 D_e Preheat Dependence

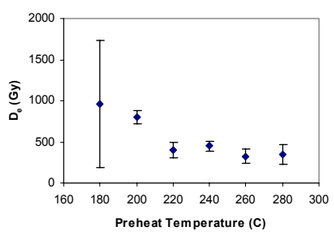

Fig. 4 Dose Recovery

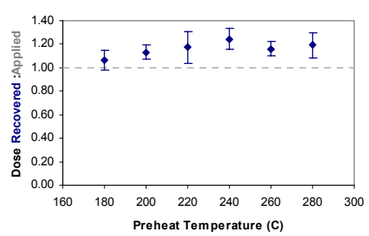

Sample: GL06003

Fig. 5 Inter-aliquot D_e distribution

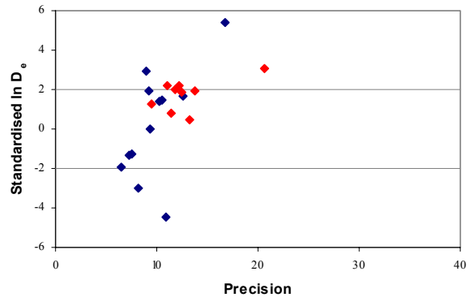

Fig. 6 Signal Analysis

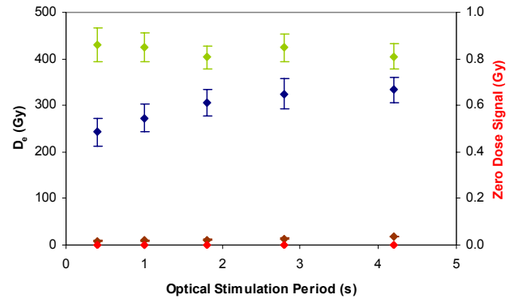

Fig. 7 Th & U Decay Activities

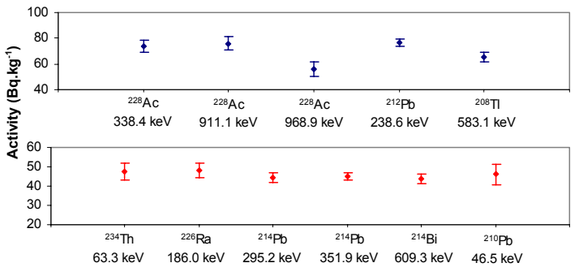

Fig. 8 Age Range

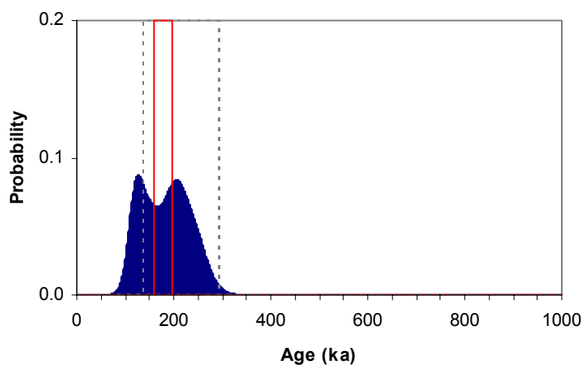

APPENDIX 11: MEASUREMENTS OF SAMPLE GL06004

Fig. 1 Signal Calibration

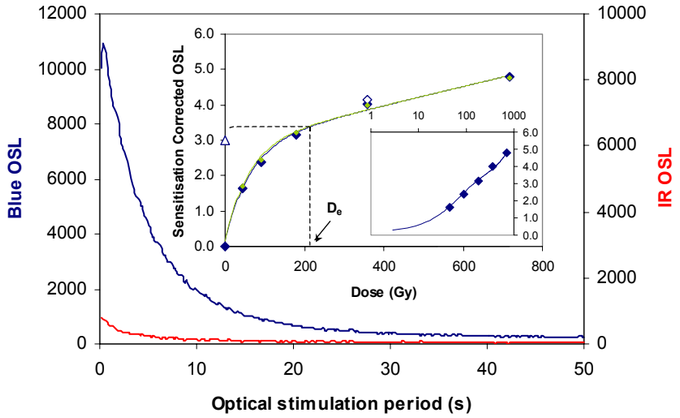

Signal Calibration Natural blue and laboratory-induced infrared (IR) OSL signals. Detectable IR signal decays are diagnostic of feldspar contamination. Inset, the natural blue OSL signal (open triangle) of each aliquot is calibrated against known laboratory doses to yield equivalent dose (D_e) values. Where D_e values are >40 Gy, a **pulsed irradiation** response is shown; pulsed irradiation D_e values are used in age calculations if significantly different from continuous irradiation-based D_e. Where D_e values are >100Gy, a log-linear plot of dose response is shown; D_e can be confidently interpolated if signal response increases with dose.

Irradiation-Preheat Cycling The acquisition of D_e values is necessarily predicated upon thermal treatment of aliquots succeeding environmental and laboratory irradiation. Repeated irradiation and thermal treatment results in aliquot sensitisation, rendering calibration of the natural signal inaccurate. This sensitisation can be monitored and corrected for. The accuracy of correction can be preheat dependent; irradiation-preheat cycling quantifies this dependence for laboratory-induced signals, examining the reproducibility of corrected OSL resultant of repeat laboratory doses.

D_e Preheat Dependence Quantifies the combined effects of thermal transfer and sensitisation on the natural signal. Insignificant adjustment in D_e may reflect limited influence of these effects

Dose Recovery Attempts to replicate the above diagnostic, yet provide improved resolution of thermal effects through removal of variability induced by heterogeneous dose absorption in the environment and using a precise lab dose to simulate natural dose. Based on this and preceding data an appropriate thermal treatment is selected to refine the final D_e value.

Inter-aliquot D_e distribution Provides a measure of inter-aliquot statistical concordance in D_e values derived from **natural** and **laboratory** irradiation. Discordant data (those points lying beyond ±2 standardised ln D_e) reflects heterogeneous dose absorption and/or inaccuracies in calibration.

Signal Analysis Statistically significant increase in **natural** D_e value with signal stimulation period is indicative of a partially-bleached signal, provided a significant increase in D_e results from **simulated partial bleaching** along with insignificant adjustment in D_e for simulated **zero** and **full bleach** conditions. Ages from such samples are considered maximum estimates.

Th & U Decay Activities Statistical concordance (equilibrium) in the activities of daughter radioisotopes in the Th and U decay series may signify the temporal stability of D_r emissions from these chains. Significant differences (disequilibrium) in activity indicate addition or removal of isotopes creating a time-dependent shift in D_r values and increased uncertainty in the accuracy of age estimates

Age Range The **mean age range** provides an estimate of sediment burial period based on mean D_e and D_r values with associated analytical uncertainties. The probability distribution indicates the inter-aliquot variability in age. The **maximum influence** of temporal variations in D_r forced by minima-maxima variation in moisture content and overburden thickness may prove instructive where there is uncertainty in these parameters, however the combined extremes represented should not be construed as preferred age estimates.

Fig. 2 Irradiation-Preheat Cycling

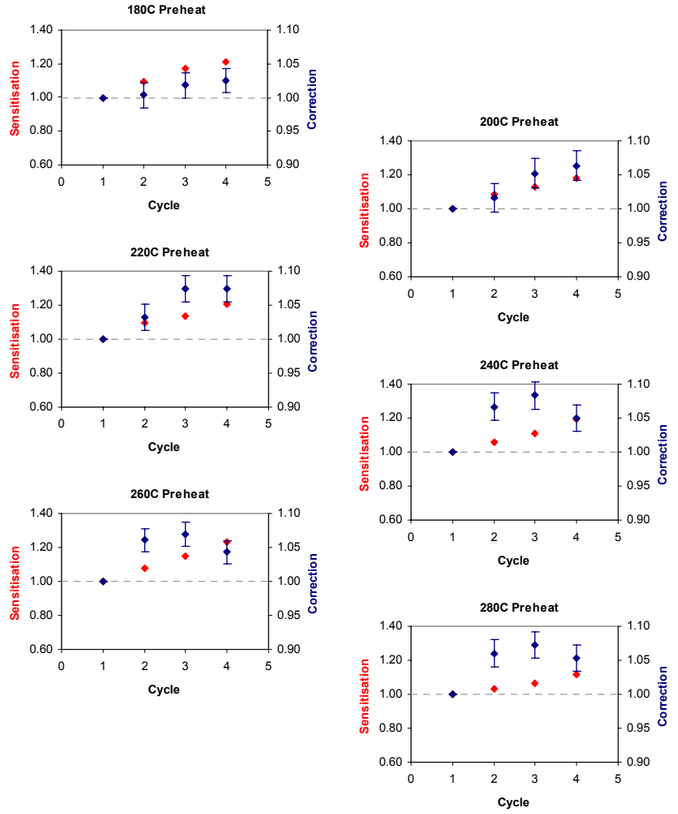

Fig. 3 D_e Preheat Dependence

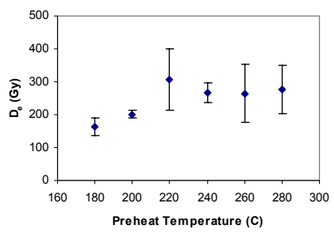

Fig. 4 Dose Recovery

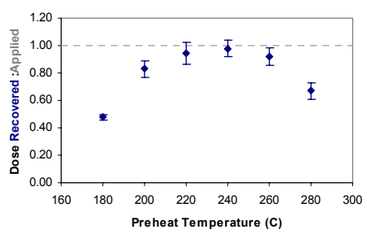

Sample: GL06004

Fig. 5 Inter-aliquot D_e distribution

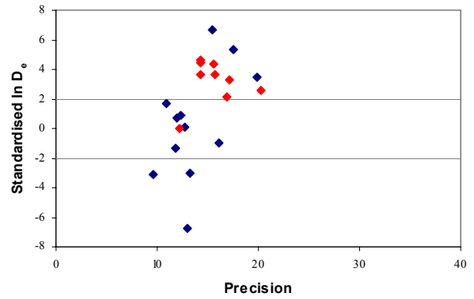

Fig. 6 Signal Analysis

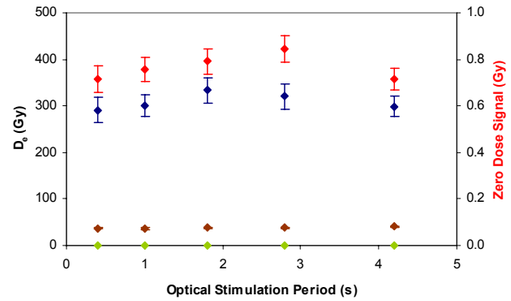

Fig. 7 Th & U Decay Activities

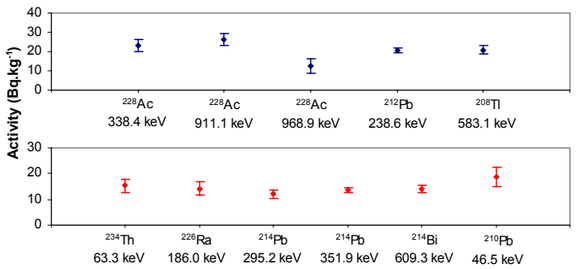

Fig. 8 Age Range

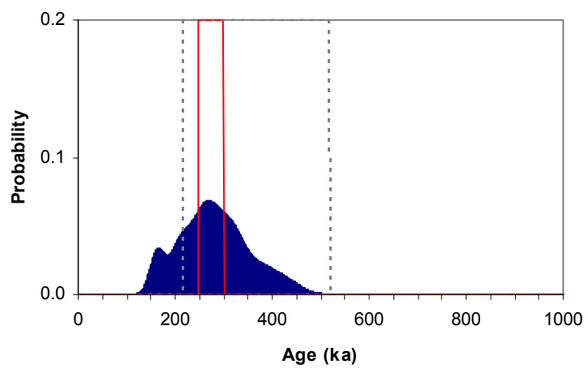

APPENDIX 12: MEASUREMENTS OF SAMPLE GL06010

Fig. 1 Signal Calibration

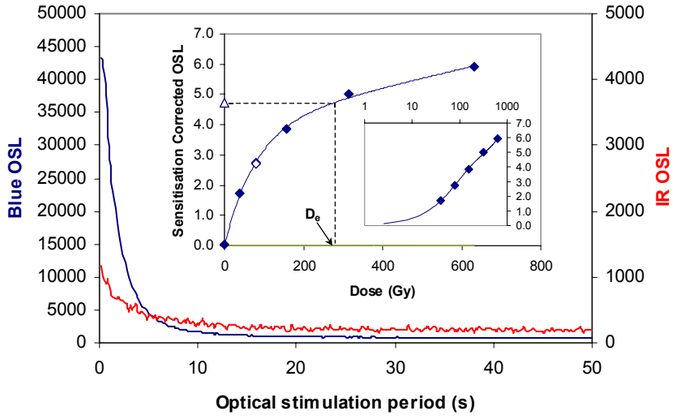

Signal Calibration Natural blue and laboratory-induced infrared (IR) OSL signals. Detectable IR signal decays are diagnostic of feldspar contamination. Inset, the natural blue OSL signal (open triangle) of each aliquot is calibrated against known laboratory doses to yield equivalent dose (D_e) values. Where D_e values are >40 Gy, a **pulsed irradiation** response is shown; pulsed irradiation D_e values are used in age calculations if significantly different from continuous irradiation-based D_e. Where D_e values are >100Gy, a log-linear plot of dose response is shown; D_e can be confidently interpolated if signal response increases with dose.

Irradiation-Preheat Cycling The acquisition of D_e values is necessarily predicated upon thermal treatment of aliquots succeeding environmental and laboratory irradiation. Repeated irradiation and thermal treatment results in aliquot sensitisation, rendering calibration of the natural signal inaccurate. This sensitisation can be monitored and corrected for. The accuracy of correction can be preheat dependent; irradiation-preheat cycling quantifies this dependence for laboratory-induced signals, examining the reproducibility of corrected OSL resultant of repeat laboratory doses.

D_e Preheat Dependence Quantifies the combined effects of thermal transfer and sensitisation on the natural signal. Insignificant adjustment in D_e may reflect limited influence of these effects

Dose Recovery Attempts to replicate the above diagnostic, yet provide improved resolution of thermal effects through removal of variability induced by heterogeneous dose absorption in the environment and using a precise lab dose to simulate natural dose. Based on this and preceding data an appropriate thermal treatment is selected to refine the final D_e value.

Inter-aliquot D_e distribution Provides a measure of inter-aliquot statistical concordance in D_e values derived from **natural** and **laboratory** irradiation. Discordant data (those points lying beyond **±2 standardised ln D_e**) reflects heterogeneous dose absorption and/or inaccuracies in calibration.

Signal Analysis Statistically significant increase in **natural** D_e value with signal stimulation period is indicative of a partially-bleached signal, provided a significant increase in D_e results from **simulated partial bleaching** along with insignificant adjustment in D_e for simulated **zero** and **full bleach** conditions. Ages from such samples are considered maximum estimates.

Th & U Decay Activities Statistical concordance (equilibrium) in the activities of daughter radioisotopes in the Th and U decay series may signify the temporal stability of D_r emissions from these chains. Significant differences (disequilibrium) in activity indicate addition or removal of isotopes creating a time-dependent shift in D_r values and increased uncertainty in the accuracy of age estimates

Age Range The **mean age range** provides an estimate of sediment burial period based on mean D_e and D_r values with associated analytical uncertainties. The probability distribution indicates the inter-aliquot variability in age. The **maximum influence** of temporal variations in D_r forced by minima-maxima variation in moisture content and overburden thickness may prove instructive where there is uncertainty in these parameters, however the combined extremes represented should not be construed as preferred age estimates.

Fig. 2 Irradiation-Preheat Cycling

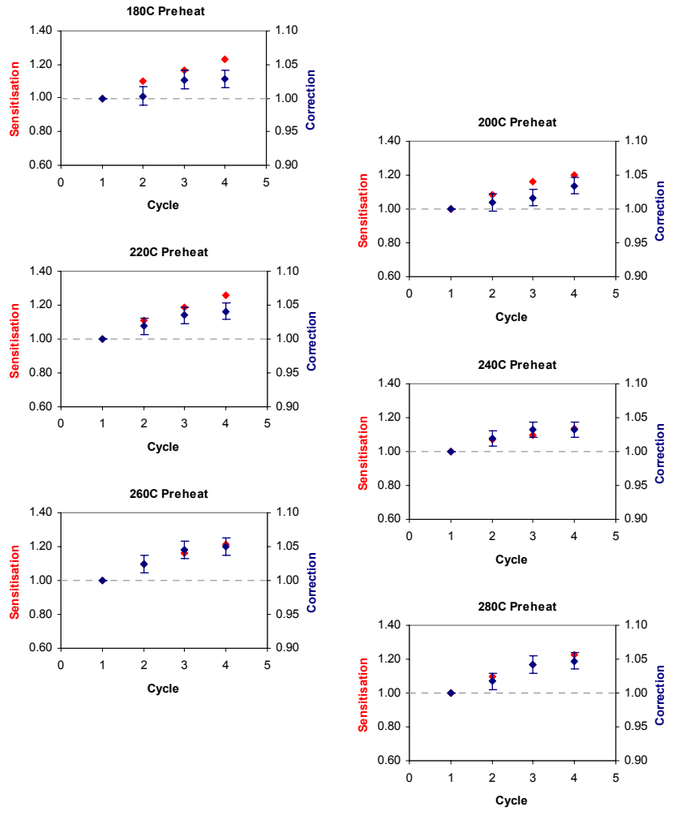

Fig. 3 D_e Preheat Dependence

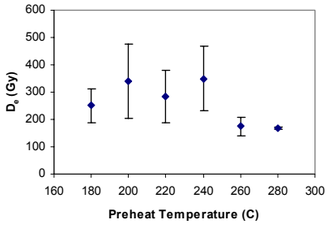

Fig. 4 Dose Recovery

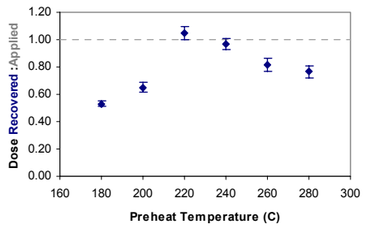

Sample: GL06010

Fig. 5 Inter-aliquot D_e distribution

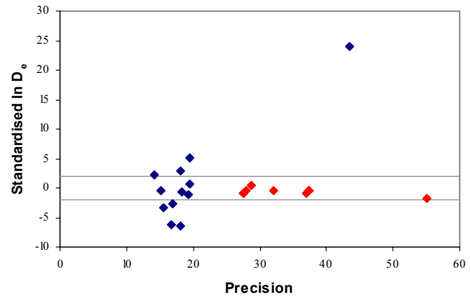

Fig. 6 Signal Analysis

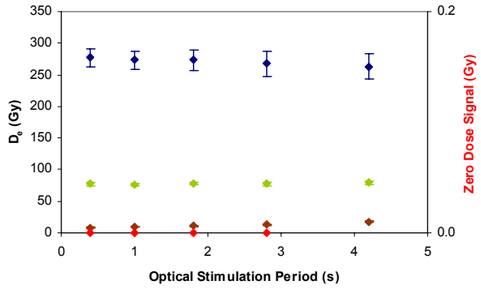

Fig. 7 Th & U Decay Activities

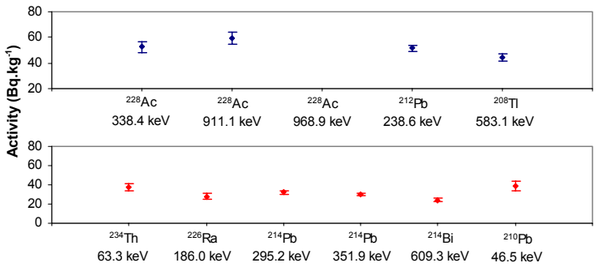

Fig. 8 Age Range

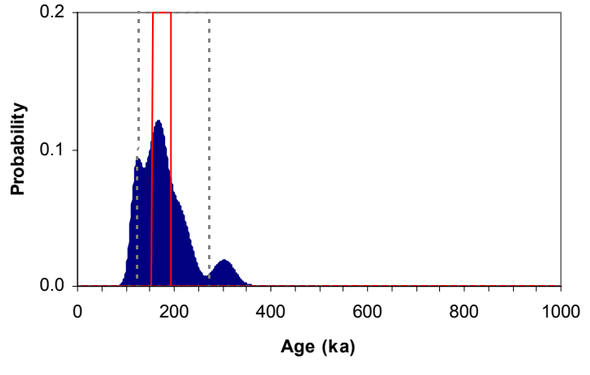

APPENDIX 13: MEASUREMENTS OF SAMPLE GL06011

Fig. 1 Signal Calibration

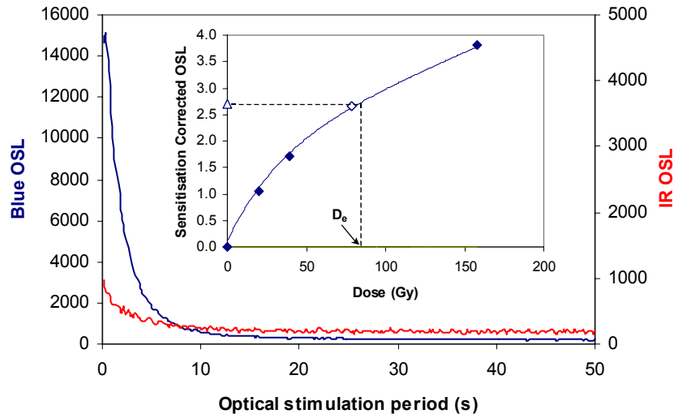

Signal Calibration Natural blue and laboratory-induced infrared (IR) OSL signals. Detectable IR signal decays are diagnostic of feldspar contamination. Inset, the natural blue OSL signal (open triangle) of each aliquot is calibrated against known laboratory doses to yield equivalent dose (D_e) values. Where D_e values are >40 Gy, a **pulsed irradiation** response is shown; pulsed irradiation D_e values are used in age calculations if significantly different from continuous irradiation-based D_e. Where D_e values are >100Gy, a log-linear plot of dose response is shown; D_e can be confidently interpolated if signal response increases with dose.

Irradiation-Preheat Cycling The acquisition of D_e values is necessarily predicated upon thermal treatment of aliquots succeeding environmental and laboratory irradiation. Repeated irradiation and thermal treatment results in aliquot sensitisation, rendering calibration of the natural signal inaccurate. This sensitisation can be monitored and corrected for. The accuracy of correction can be preheat dependent; irradiation-preheat cycling quantifies this dependence for laboratory-induced signals, examining the reproducibility of corrected OSL resultant of repeat laboratory doses.

D_e Preheat Dependence Quantifies the combined effects of thermal transfer and sensitisation on the natural signal. Insignificant adjustment in D_e may reflect limited influence of these effects

Dose Recovery Attempts to replicate the above diagnostic, yet provide improved resolution of thermal effects through removal of variability induced by heterogeneous dose absorption in the environment and using a precise lab dose to simulate natural dose. Based on this and preceding data an appropriate thermal treatment is selected to refine the final D_e value.

Inter-aliquot D_e distribution Provides a measure of inter-aliquot statistical concordance in D_e values derived from **natural** and **laboratory** irradiation. Discordant data (those points lying beyond ±2 standardised ln D_e) reflects heterogeneous dose absorption and/or inaccuracies in calibration.

Signal Analysis Statistically significant increase in **natural** D_e value with signal stimulation period is indicative of a partially-bleached signal, provided a significant increase in D_e results from **simulated partial bleaching** along with insignificant adjustment in D_e for simulated **zero** and **full bleach** conditions. Ages from such samples are considered maximum estimates.

Th & U Decay Activities Statistical concordance (equilibrium) in the activities of daughter radioisotopes in the Th and U decay series may signify the temporal stability of D_r emissions from these chains. Significant differences (disequilibrium) in activity indicate addition or removal of isotopes creating a time-dependent shift in D_r values and increased uncertainty in the accuracy of age estimates

Age Range The **mean age range** provides an estimate of sediment burial period based on mean D_e and D_r values with associated analytical uncertainties. The probability distribution indicates the inter-aliquot variability in age. The **maximum influence** of temporal variations in D_r forced by minima-maxima variation in moisture content and overburden thickness may prove instructive where there is uncertainty in these parameters, however the combined extremes represented should not be construed as preferred age estimates.

Fig. 2 Irradiation-Preheat Cycling

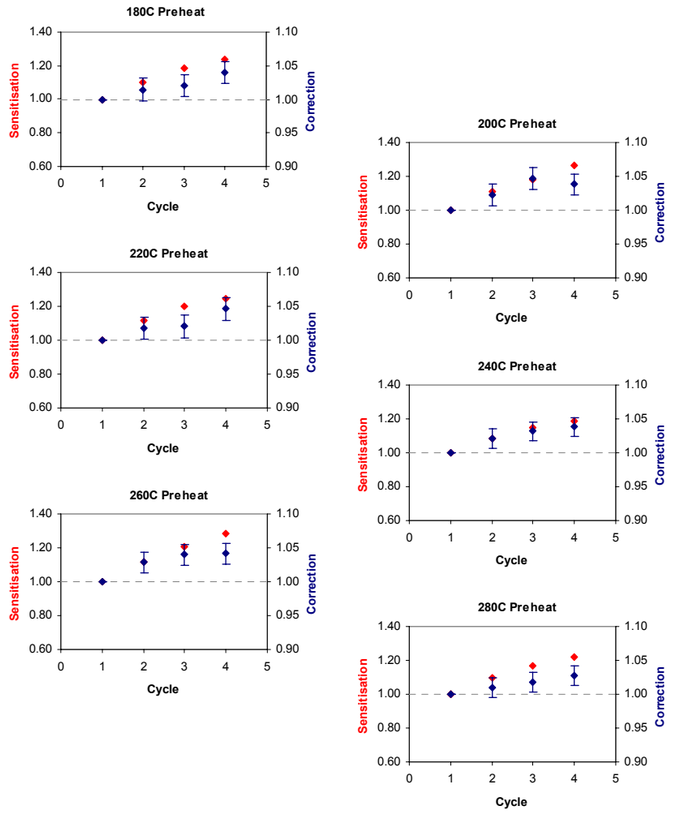

Fig. 3 D_e Preheat Dependence

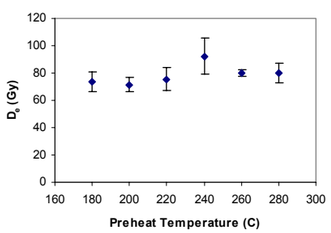

Fig. 4 Dose Recovery

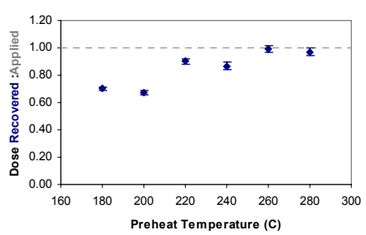

Sample: GL06011

Fig. 5 Inter-aliquot D_e distribution

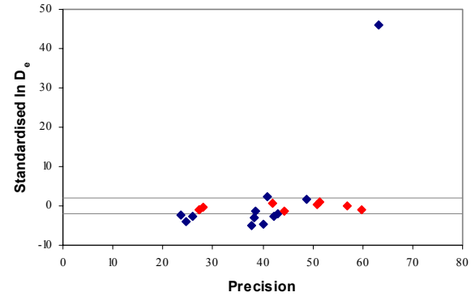

Fig. 6 Signal Analysis

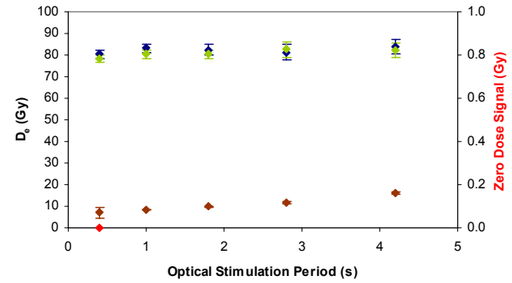

Fig. 7 Th & U Decay Activities

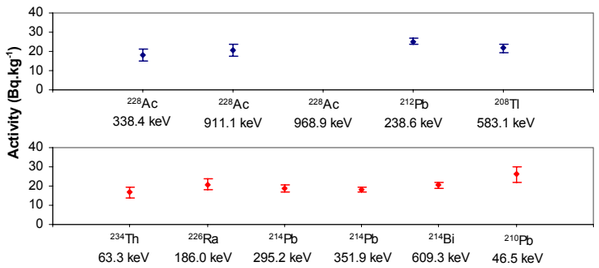

Fig. 8 Age Range

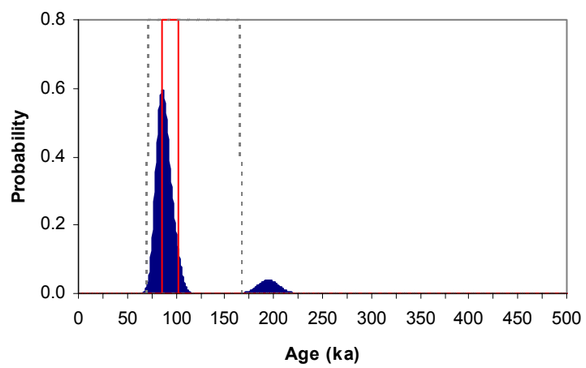

APPENDIX 14: MEASUREMENTS OF SAMPLE GL06012

Fig. 1 Signal Calibration

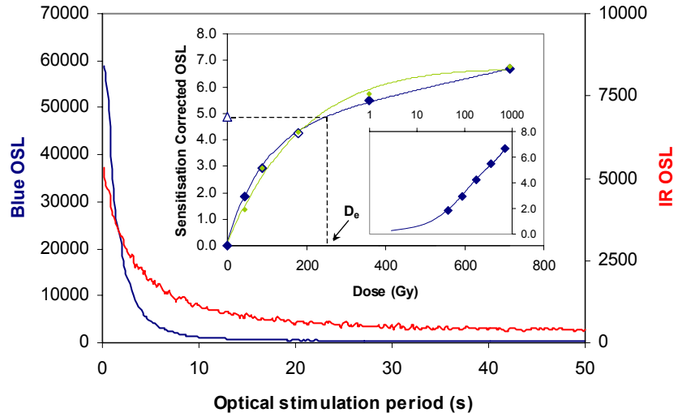

Signal Calibration Natural blue and laboratory-induced infrared (IR) OSL signals. Detectable IR signal decays are diagnostic of feldspar contamination. Inset, the natural blue OSL signal (open triangle) of each aliquot is calibrated against known laboratory doses to yield equivalent dose (D_e) values. Where D_e values are >40 Gy, a **pulsed irradiation** response is shown; pulsed irradiation D_e values are used in age calculations if significantly different from continuous irradiation-based D_e. Where D_e values are >100Gy, a log-linear plot of dose response is shown; D_e can be confidently interpolated if signal response increases with dose.

Irradiation-Preheat Cycling The acquisition of D_e values is necessarily predicated upon thermal treatment of aliquots succeeding environmental and laboratory irradiation. Repeated irradiation and thermal treatment results in aliquot sensitisation, rendering calibration of the natural signal inaccurate. This sensitisation can be monitored and corrected for. The accuracy of correction can be preheat dependent; irradiation-preheat cycling quantifies this dependence for laboratory-induced signals, examining the reproducibility of corrected OSL resultant of repeat laboratory doses.

D_e Preheat Dependence Quantifies the combined effects of thermal transfer and sensitisation on the natural signal. Insignificant adjustment in D_e may reflect limited influence of these effects

Dose Recovery Attempts to replicate the above diagnostic, yet provide improved resolution of thermal effects through removal of variability induced by heterogeneous dose absorption in the environment and using a precise lab dose to simulate natural dose. Based on this and preceding data an appropriate thermal treatment is selected to refine the final D_e value.

Inter-aliquot D_e distribution Provides a measure of inter-aliquot statistical concordance in D_e values derived from **natural** and **laboratory** irradiation. Discordant data (those points lying beyond ±2 standardised ln D_e) reflects heterogeneous dose absorption and/or inaccuracies in calibration.

Signal Analysis Statistically significant increase in **natural** D_e value with signal stimulation period is indicative of a partially-bleached signal, provided a significant increase in D_e results from **simulated partial bleaching** along with insignificant adjustment in D_e for simulated **zero** and **full bleach** conditions. Ages from such samples are considered maximum estimates.

Th & U Decay Activities Statistical concordance (equilibrium) in the activities of daughter radioisotopes in the Th and U decay series may signify the temporal stability of D_r emissions from these chains. Significant differences (disequilibrium) in activity indicate addition or removal of isotopes creating a time-dependent shift in D_r values and increased uncertainty in the accuracy of age estimates

Age Range The **mean age range** provides an estimate of sediment burial period based on mean D_e and D_r values with associated analytical uncertainties. The probability distribution indicates the inter-aliquot variability in age. The **maximum influence** of temporal variations in D_r forced by minima-maxima variation in moisture content and overburden thickness may prove instructive where there is uncertainty in these parameters, however the combined extremes represented should not be construed as preferred age estimates.

Fig. 2 Irradiation-Preheat Cycling

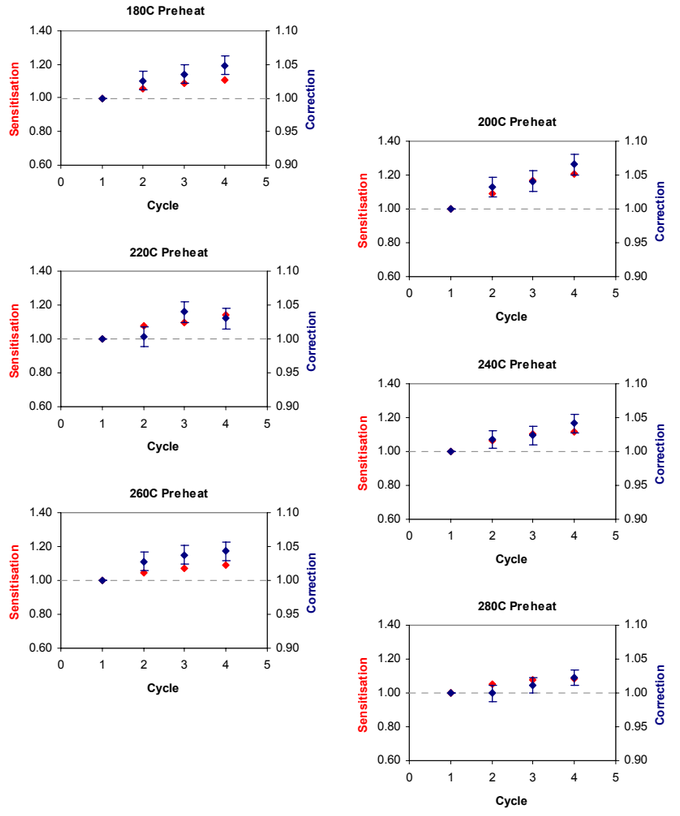

Fig. 3 D_e Preheat Dependence

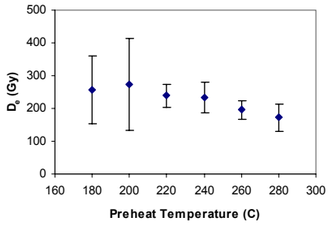

Fig. 4 Dose Recovery

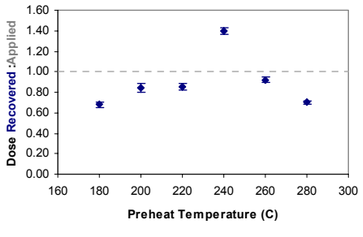

Sample: GL06012

Fig. 5 Inter-aliquot D_e distribution

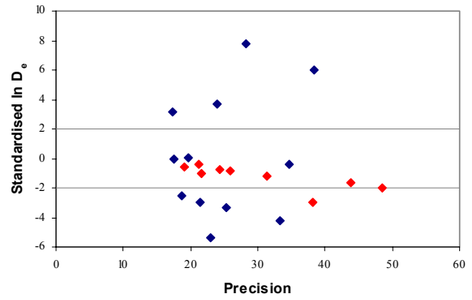

Fig. 6 Signal Analysis

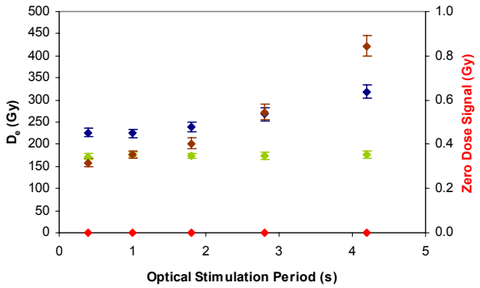

Fig. 7 Th & U Decay Activities

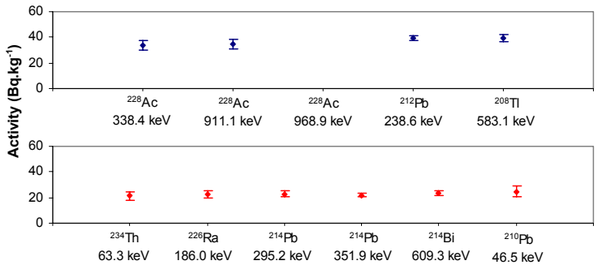

Fig. 8 Age Range

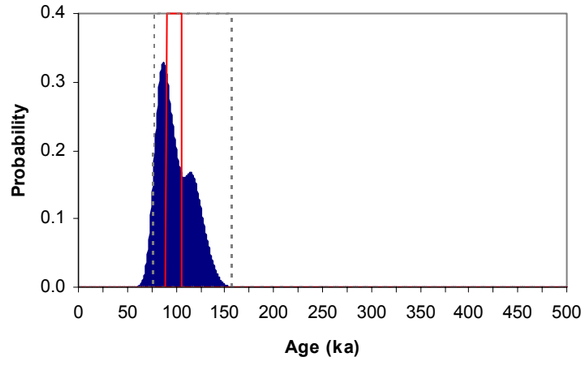

APPENDIX 15: MEASUREMENTS OF SAMPLE GL06013

Fig. 1 Signal Calibration

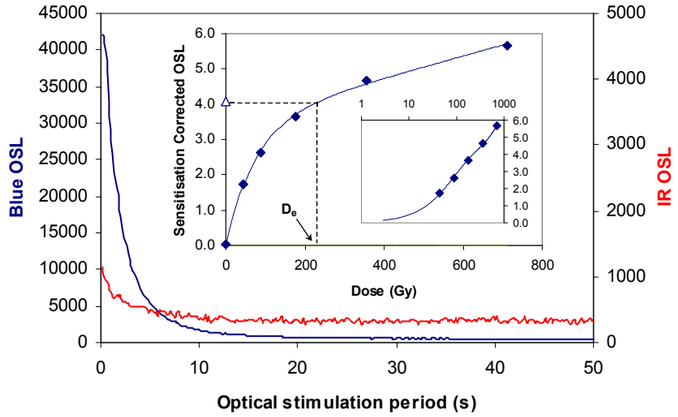

Signal Calibration Natural blue and laboratory-induced infrared (IR) OSL signals. Detectable IR signal decays are diagnostic of feldspar contamination. Inset, the natural blue OSL signal (open triangle) of each aliquot is calibrated against known laboratory doses to yield equivalent dose (D_e) values. Where D_e values are >40 Gy, a **pulsed irradiation** response is shown; pulsed irradiation D_e values are used in age calculations if significantly different from continuous irradiation-based D_e. Where D_e values are >100Gy, a log-linear plot of dose response is shown; D_e can be confidently interpolated if signal response increases with dose.

Irradiation-Preheat Cycling The acquisition of D_e values is necessarily predicated upon thermal treatment of aliquots succeeding environmental and laboratory irradiation. Repeated irradiation and thermal treatment results in aliquot sensitisation, rendering calibration of the natural signal inaccurate. This sensitisation can be monitored and corrected for. The accuracy of correction can be preheat dependent; irradiation-preheat cycling quantifies this dependence for laboratory-induced signals, examining the reproducibility of corrected OSL resultant of repeat laboratory doses.

D_e Preheat Dependence Quantifies the combined effects of thermal transfer and sensitisation on the natural signal. Insignificant adjustment in D_e may reflect limited influence of these effects

Dose Recovery Attempts to replicate the above diagnostic, yet provide improved resolution of thermal effects through removal of variability induced by heterogeneous dose absorption in the environment and using a precise lab dose to simulate natural dose. Based on this and preceding data an appropriate thermal treatment is selected to refine the final D_e value.

Inter-aliquot D_e distribution Provides a measure of inter-aliquot statistical concordance in D_e values derived from **natural** and **laboratory** irradiation. Discordant data (those points lying beyond **±2 standardised ln D_e**) reflects heterogeneous dose absorption and/or inaccuracies in calibration.

Signal Analysis Statistically significant increase in **natural** D_e value with signal stimulation period is indicative of a partially-bleached signal, provided a significant increase in D_e results from **simulated partial bleaching** along with insignificant adjustment in D_e for simulated **zero** and **full bleach** conditions. Ages from such samples are considered maximum estimates.

Th & U Decay Activities Statistical concordance (equilibrium) in the activities of daughter radioisotopes in the Th and U decay series may signify the temporal stability of D_r emissions from these chains. Significant differences (disequilibrium) in activity indicate addition or removal of isotopes creating a time-dependent shift in D_r values and increased uncertainty in the accuracy of age estimates

Age Range The **mean age range** provides an estimate of sediment burial period based on mean D_e and D_r values with associated analytical uncertainties. The probability distribution indicates the inter-aliquot variability in age. The **maximum influence** of temporal variations in D_r forced by minima-maxima variation in moisture content and overburden thickness may prove instructive where there is uncertainty in these parameters, however the combined extremes represented should not be construed as preferred age estimates.

Fig. 2 Irradiation-Preheat Cycling

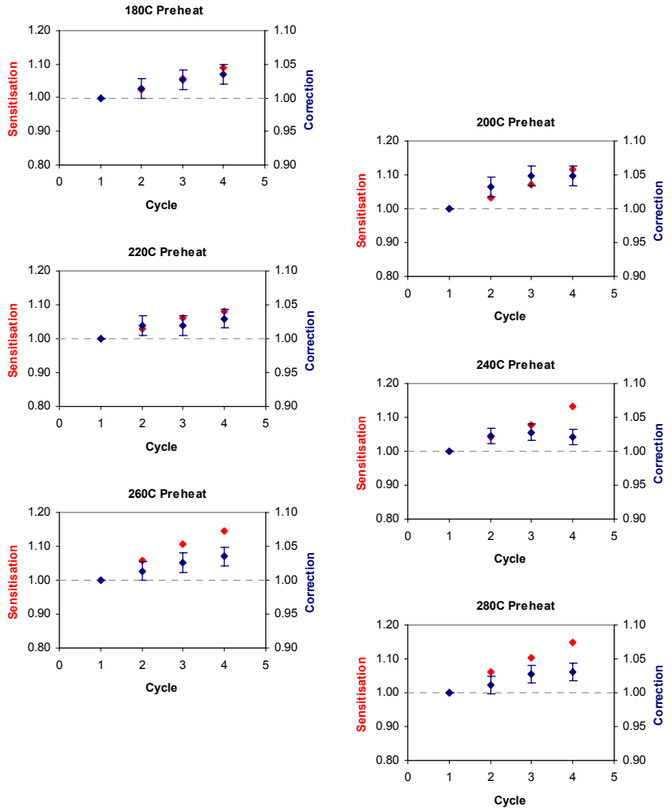

Fig. 3 D_e Preheat Dependence

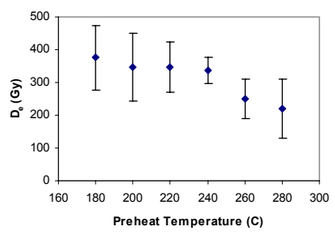

Fig. 4 Dose Recovery

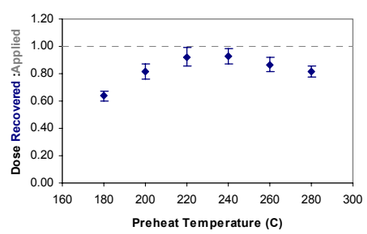

Sample: GL06013

Fig. 5 Inter-aliquot D_e distribution

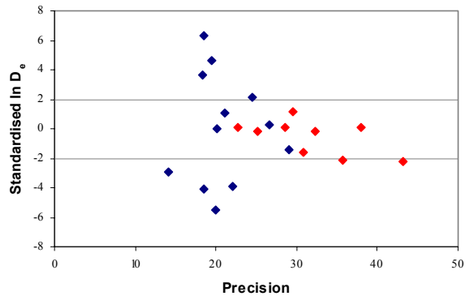

Fig. 6 Signal Analysis

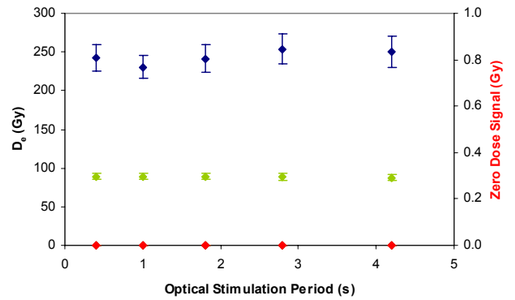

Fig. 7 Th & U Decay Activities

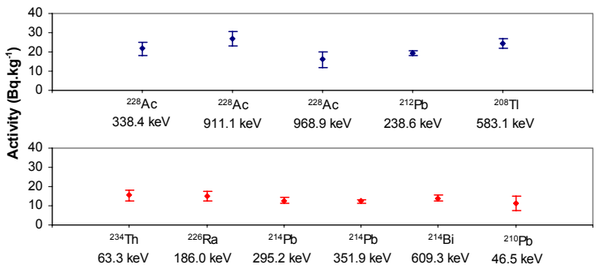

Fig. 8 Age Range

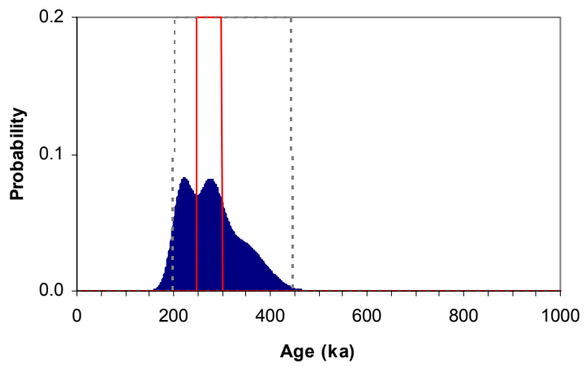

APPENDIX 16: MEASUREMENTS OF SAMPLE GL06032

Fig. 1 Signal Calibration

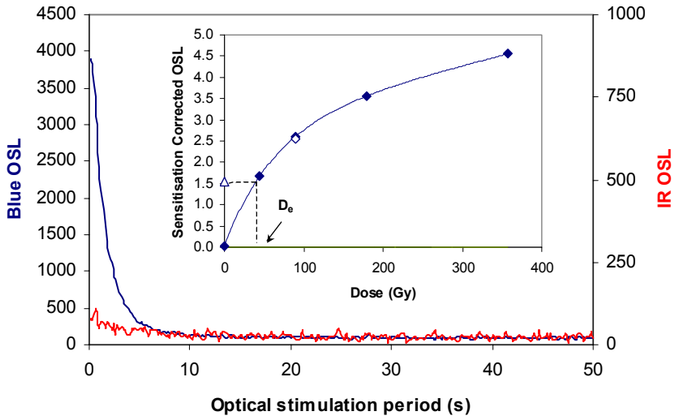

Signal Calibration Natural blue and laboratory-induced infrared (IR) OSL signals. Detectable IR signal decays are diagnostic of feldspar contamination. Inset, the natural blue OSL signal (open triangle) of each aliquot is calibrated against known laboratory doses to yield equivalent dose (D_e) values. Where D_e values are >40 Gy, a **pulsed irradiation** response is shown; pulsed irradiation D_e values are used in age calculations if significantly different from continuous irradiation-based D_e. Where D_e values are >100Gy, a log-linear plot of dose response is shown; D_e can be confidently interpolated if signal response increases with dose.

Irradiation-Preheat Cycling The acquisition of D_e values is necessarily predicated upon thermal treatment of aliquots succeeding environmental and laboratory irradiation. Repeated irradiation and thermal treatment results in aliquot sensitisation, rendering calibration of the natural signal inaccurate. This sensitisation can be monitored and corrected for. The accuracy of correction can be preheat dependent; irradiation-preheat cycling quantifies this dependence for laboratory-induced signals, examining the reproducibility of corrected OSL resultant of repeat laboratory doses.

D_e Preheat Dependence Quantifies the combined effects of thermal transfer and sensitisation on the natural signal. Insignificant adjustment in D_e may reflect limited influence of these effects

Dose Recovery Attempts to replicate the above diagnostic, yet provide improved resolution of thermal effects through removal of variability induced by heterogeneous dose absorption in the environment and using a precise lab dose to simulate natural dose. Based on this and preceding data an appropriate thermal treatment is selected to refine the final D_e value.

Inter-aliquot D_e distribution Provides a measure of inter-aliquot statistical concordance in D_e values derived from **natural** and **laboratory** irradiation. Discordant data (those points lying beyond **±2 standardised ln D_e**) reflects heterogeneous dose absorption and/or inaccuracies in calibration.

Signal Analysis Statistically significant increase in **natural** D_e value with signal stimulation period is indicative of a partially-bleached signal, provided a significant increase in D_e results from **simulated partial bleaching** along with insignificant adjustment in D_e for simulated **zero** and **full bleach** conditions. Ages from such samples are considered maximum estimates.

Th & U Decay Activities Statistical concordance (equilibrium) in the activities of daughter radioisotopes in the Th and U decay series may signify the temporal stability of D_r emissions from these chains. Significant differences (disequilibrium) in activity indicate addition or removal of isotopes creating a time-dependent shift in D_r values and increased uncertainty in the accuracy of age estimates

Age Range The **mean age range** provides an estimate of sediment burial period based on mean D_e and D_r values with associated analytical uncertainties. The probability distribution indicates the inter-aliquot variability in age. The **maximum influence** of temporal variations in D_r forced by minima-maxima variation in moisture content and overburden thickness may prove instructive where there is uncertainty in these parameters, however the combined extremes represented should not be construed as preferred age estimates.

Fig. 2 Irradiation-Preheat Cycling

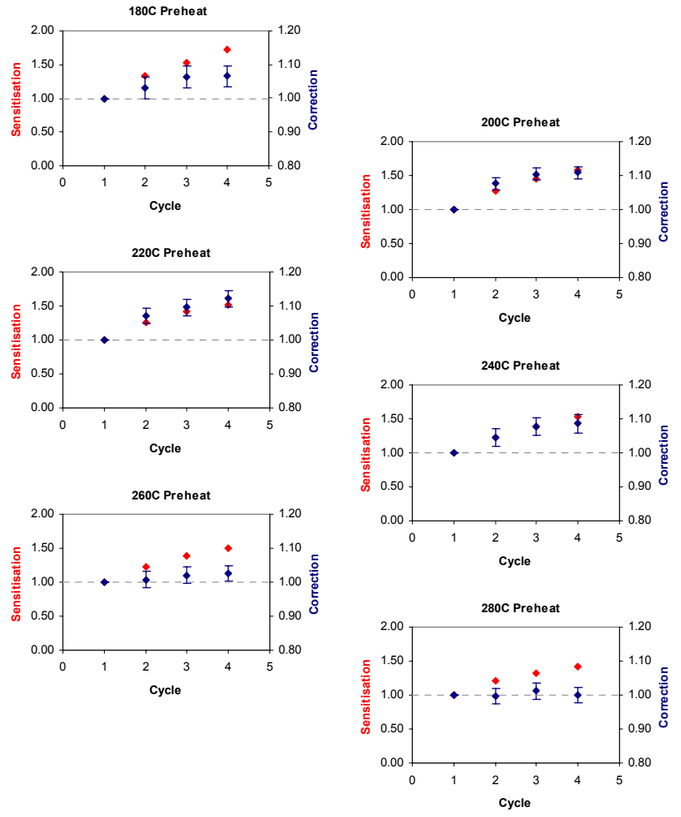

Fig. 3 D_e Preheat Dependence

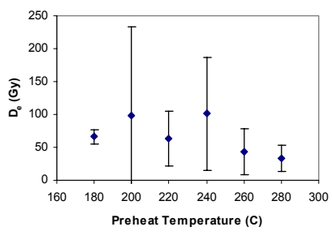

Fig. 4 Dose Recovery

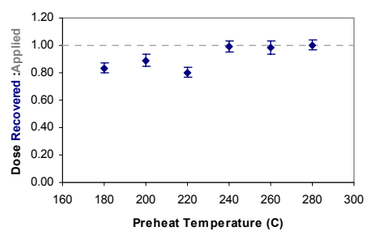

Sample: GL06032

Fig. 5 Inter-aliquot D_e distribution

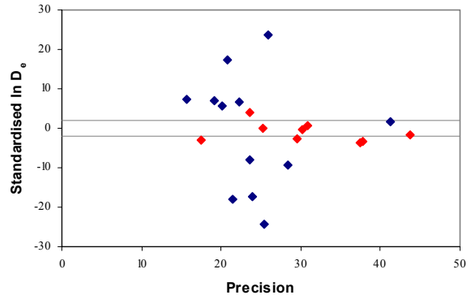

Fig. 6 Signal Analysis

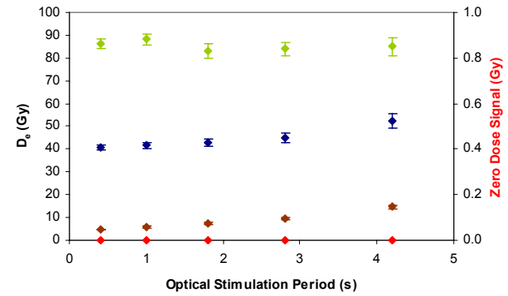

Fig. 7 Th & U Decay Activities

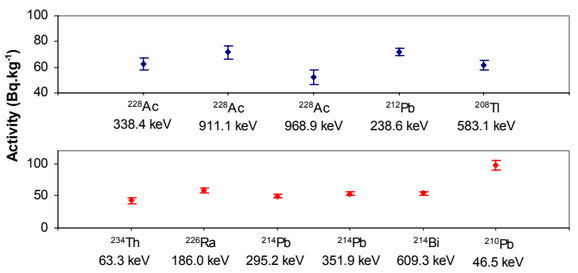

Fig. 8 Age Range

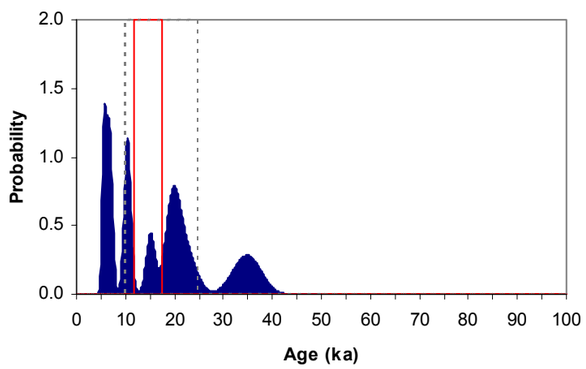

APPENDIX 17: MEASUREMENTS OF SAMPLE GL06033

Fig. 1 Signal Calibration

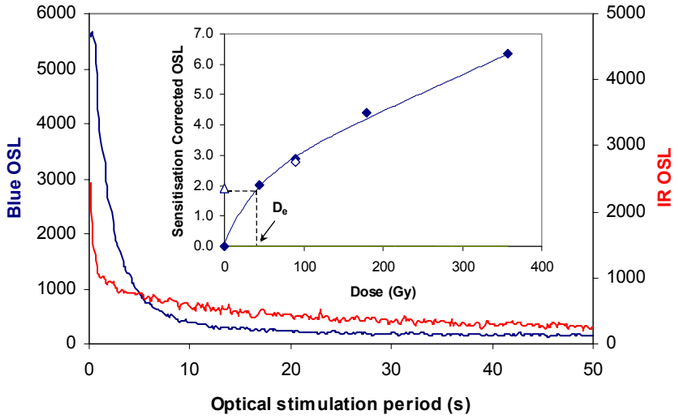

Signal Calibration Natural blue and laboratory-induced infrared (IR) OSL signals. Detectable IR signal decays are diagnostic of feldspar contamination. Inset, the natural blue OSL signal (open triangle) of each aliquot is calibrated against known laboratory doses to yield equivalent dose (D_e) values. Where D_e values are >40 Gy, a **pulsed irradiation** response is shown; pulsed irradiation D_e values are used in age calculations if significantly different from continuous irradiation-based D_e. Where D_e values are >100Gy, a log-linear plot of dose response is shown; D_e can be confidently interpolated if signal response increases with dose.

Irradiation-Preheat Cycling The acquisition of D_e values is necessarily predicated upon thermal treatment of aliquots succeeding environmental and laboratory irradiation. Repeated irradiation and thermal treatment results in aliquot sensitisation, rendering calibration of the natural signal inaccurate. This sensitisation can be monitored and corrected for. The accuracy of correction can be preheat dependent; irradiation-preheat cycling quantifies this dependence for laboratory-induced signals, examining the reproducibility of corrected OSL resultant of repeat laboratory doses.

D_e Preheat Dependence Quantifies the combined effects of thermal transfer and sensitisation on the natural signal. Insignificant adjustment in D_e may reflect limited influence of these effects

Dose Recovery Attempts to replicate the above diagnostic, yet provide improved resolution of thermal effects through removal of variability induced by heterogeneous dose absorption in the environment and using a precise lab dose to simulate natural dose. Based on this and preceding data an appropriate thermal treatment is selected to refine the final D_e value.

Inter-aliquot D_e distribution Provides a measure of inter-aliquot statistical concordance in D_e values derived from **natural** and **laboratory** irradiation. Discordant data (those points lying beyond **±2 standardised ln D_e**) reflects heterogeneous dose absorption and/or inaccuracies in calibration.

Signal Analysis Statistically significant increase in **natural** D_e value with signal stimulation period is indicative of a partially-bleached signal, provided a significant increase in D_e results from **simulated partial bleaching** along with insignificant adjustment in D_e for simulated **zero** and **full bleach** conditions. Ages from such samples are considered maximum estimates.

Th & U Decay Activities Statistical concordance (equilibrium) in the activities of daughter radioisotopes in the Th and U decay series may signify the temporal stability of D_r emissions from these chains. Significant differences (disequilibrium) in activity indicate addition or removal of isotopes creating a time-dependent shift in D_r values and increased uncertainty in the accuracy of age estimates

Age Range The **mean age range** provides an estimate of sediment burial period based on mean D_e and D_r values with associated analytical uncertainties. The probability distribution indicates the inter-aliquot variability in age. The **maximum influence** of temporal variations in D_r forced by minima-maxima variation in moisture content and overburden thickness may prove instructive where there is uncertainty in these parameters, however the combined extremes represented should not be construed as preferred age estimates.

Fig. 2 Irradiation-Preheat Cycling

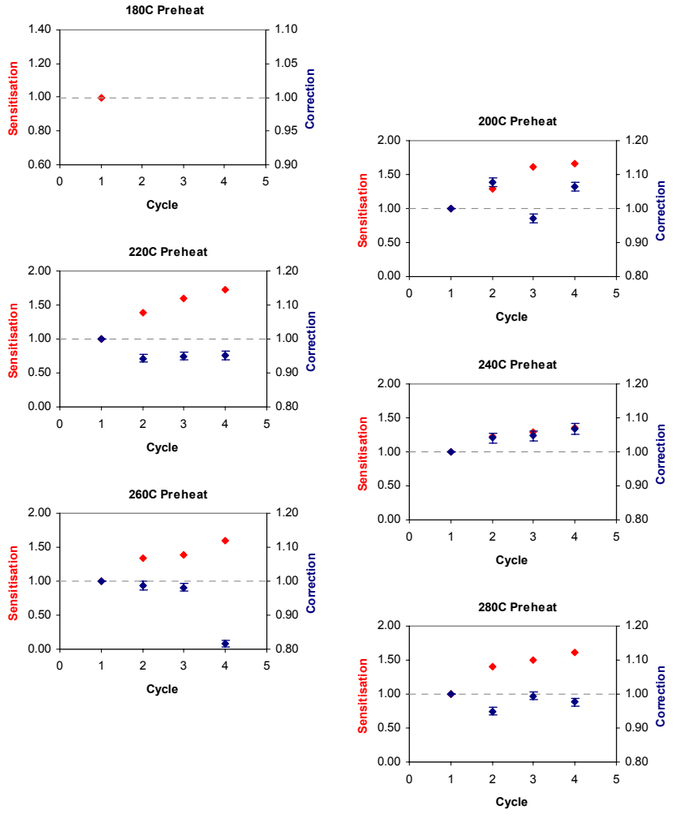

Fig. 3 D_e Preheat Dependence

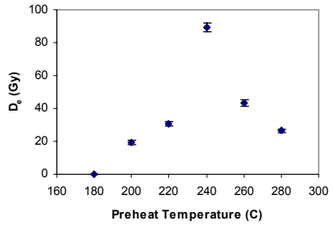

Fig. 4 Dose Recovery

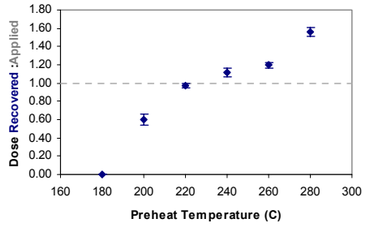

Sample: GL06033

Fig. 5 Inter-aliquot D_e distribution

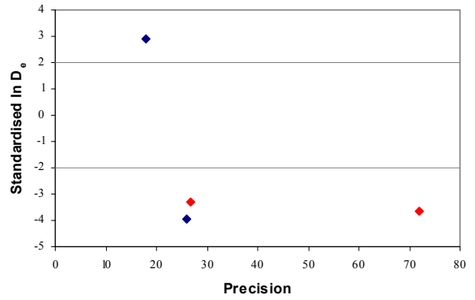

Fig. 6 Signal Analysis

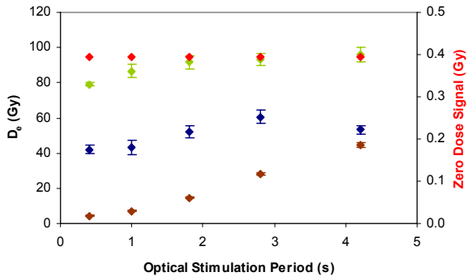

Fig. 7 Th & U Decay Activities

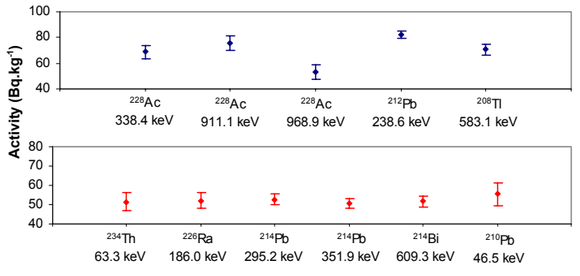

Fig. 8 Age Range

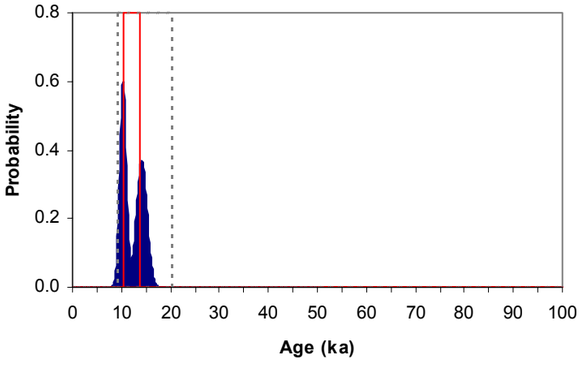

APPENDIX 18: MEASUREMENTS OF SAMPLE GL06034

Fig. 1 Signal Calibration

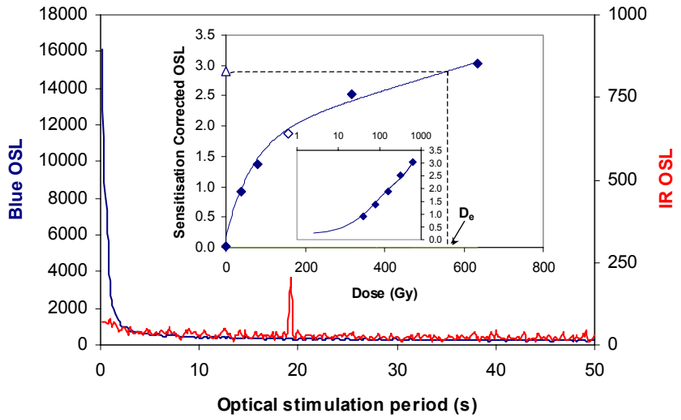

Signal Calibration Natural blue and laboratory-induced infrared (IR) OSL signals. Detectable IR signal decays are diagnostic of feldspar contamination. Inset, the natural blue OSL signal (open triangle) of each aliquot is calibrated against known laboratory doses to yield equivalent dose (D_e) values. Where D_e values are >40 Gy, a **pulsed irradiation** response is shown; pulsed irradiation D_e values are used in age calculations if significantly different from continuous irradiation-based D_e. Where D_e values are >100Gy, a log-linear plot of dose response is shown; D_e can be confidently interpolated if signal response increases with dose.

Irradiation-Preheat Cycling The acquisition of D_e values is necessarily predicated upon thermal treatment of aliquots succeeding environmental and laboratory irradiation. Repeated irradiation and thermal treatment results in aliquot sensitisation, rendering calibration of the natural signal inaccurate. This sensitisation can be monitored and corrected for. The accuracy of correction can be preheat dependent; irradiation-preheat cycling quantifies this dependence for laboratory-induced signals, examining the reproducibility of corrected OSL resultant of repeat laboratory doses.

D_e Preheat Dependence Quantifies the combined effects of thermal transfer and sensitisation on the natural signal. Insignificant adjustment in D_e may reflect limited influence of these effects

Dose Recovery Attempts to replicate the above diagnostic, yet provide improved resolution of thermal effects through removal of variability induced by heterogeneous dose absorption in the environment and using a precise lab dose to simulate natural dose. Based on this and preceding data an appropriate thermal treatment is selected to refine the final D_e value.

Inter-aliquot D_e distribution Provides a measure of inter-aliquot statistical concordance in D_e values derived from **natural** and **laboratory** irradiation. Discordant data (those points lying beyond **±2 standardised ln D_e**) reflects heterogeneous dose absorption and/or inaccuracies in calibration.

Signal Analysis Statistically significant increase in **natural** D_e value with signal stimulation period is indicative of a partially-bleached signal, provided a significant increase in D_e results from **simulated partial bleaching** along with insignificant adjustment in D_e for simulated **zero** and **full bleach** conditions. Ages from such samples are considered maximum estimates.

Th & U Decay Activities Statistical concordance (equilibrium) in the activities of daughter radioisotopes in the Th and U decay series may signify the temporal stability of D_r emissions from these chains. Significant differences (disequilibrium) in activity indicate addition or removal of isotopes creating a time-dependent shift in D_r values and increased uncertainty in the accuracy of age estimates

Age Range The **mean age range** provides an estimate of sediment burial period based on mean D_e and D_r values with associated analytical uncertainties. The probability distribution indicates the inter-aliquot variability in age. The **maximum influence** of temporal variations in D_r forced by minima-maxima variation in moisture content and overburden thickness may prove instructive where there is uncertainty in these parameters, however the combined extremes represented should not be construed as preferred age estimates.

Fig. 2 Irradiation-Preheat Cycling

Insufficient Sample Mass

Fig. 3 D_e Preheat Dependence

Insufficient Sample Mass

Fig. 4 Dose Recovery

Insufficient Sample Mass

Sample: GL06034

Fig. 5 Inter-aliquot D_e distribution

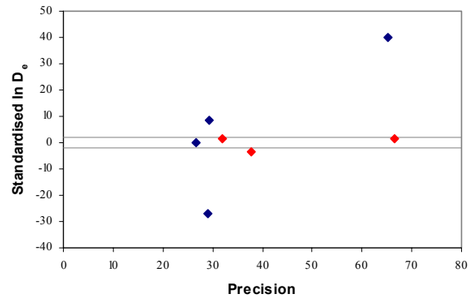

Fig. 6 Signal Analysis

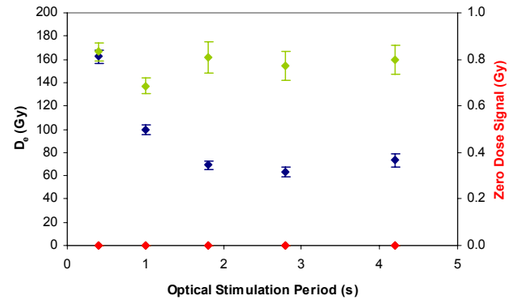

Fig. 7 Th & U Decay Activities

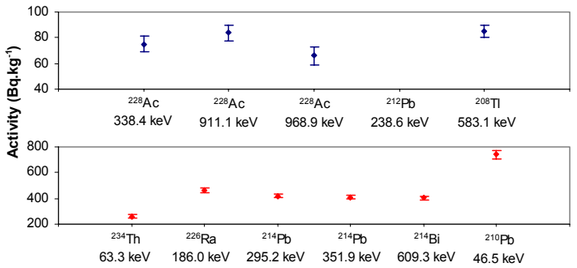

Fig. 8 Age Range

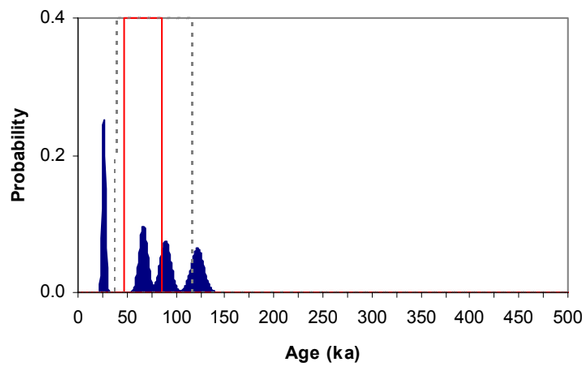

APPENDIX 19: MEASUREMENTS OF SAMPLE GL06035

Fig. 1 Signal Calibration

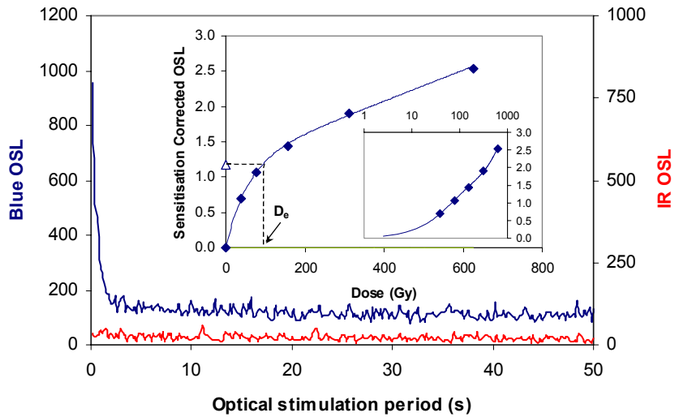

Signal Calibration Natural blue and laboratory-induced infrared (IR) OSL signals. Detectable IR signal decays are diagnostic of feldspar contamination. Inset, the natural blue OSL signal (open triangle) of each aliquot is calibrated against known laboratory doses to yield equivalent dose (D_e) values. Where D_e values are >40 Gy, a **pulsed irradiation** response is shown; pulsed irradiation D_e values are used in age calculations if significantly different from continuous irradiation-based D_e. Where D_e values are >100Gy, a log-linear plot of dose response is shown; D_e can be confidently interpolated if signal response increases with dose.

Irradiation-Preheat Cycling The acquisition of D_e values is necessarily predicated upon thermal treatment of aliquots succeeding environmental and laboratory irradiation. Repeated irradiation and thermal treatment results in aliquot sensitisation, rendering calibration of the natural signal inaccurate. This sensitisation can be monitored and corrected for. The accuracy of correction can be preheat dependent; irradiation-preheat cycling quantifies this dependence for laboratory-induced signals, examining the reproducibility of corrected OSL resultant of repeat laboratory doses.

D_e Preheat Dependence Quantifies the combined effects of thermal transfer and sensitisation on the natural signal. Insignificant adjustment in D_e may reflect limited influence of these effects

Dose Recovery Attempts to replicate the above diagnostic, yet provide improved resolution of thermal effects through removal of variability induced by heterogeneous dose absorption in the environment and using a precise lab dose to simulate natural dose. Based on this and preceding data an appropriate thermal treatment is selected to refine the final D_e value.

Inter-aliquot D_e distribution Provides a measure of inter-aliquot statistical concordance in D_e values derived from **natural** and **laboratory** irradiation. Discordant data (those points lying beyond **±2 standardised ln D_e**) reflects heterogeneous dose absorption and/or inaccuracies in calibration.

Signal Analysis Statistically significant increase in **natural** D_e value with signal stimulation period is indicative of a partially-bleached signal, provided a significant increase in D_e results from **simulated partial bleaching** along with insignificant adjustment in D_e for simulated **zero** and **full bleach** conditions. Ages from such samples are considered maximum estimates.

Th & U Decay Activities Statistical concordance (equilibrium) in the activities of daughter radioisotopes in the Th and U decay series may signify the temporal stability of D_r emissions from these chains. Significant differences (disequilibrium) in activity indicate addition or removal of isotopes creating a time-dependent shift in D_r values and increased uncertainty in the accuracy of age estimates

Age Range The **mean age range** provides an estimate of sediment burial period based on mean D_e and D_r values with associated analytical uncertainties. The probability distribution indicates the inter-aliquot variability in age. The **maximum influence** of temporal variations in D_r forced by minima-maxima variation in moisture content and overburden thickness may prove instructive where there is uncertainty in these parameters, however the combined extremes represented should not be construed as preferred age estimates.

Fig. 2 Irradiation-Preheat Cycling

Insufficient Sample Mass

Fig. 3 D_e Preheat Dependence

Insufficient Sample Mass

Fig. 4 Dose Recovery

Insufficient Sample Mass

Sample: GL06035

Fig. 5 Inter-aliquot D_e distribution

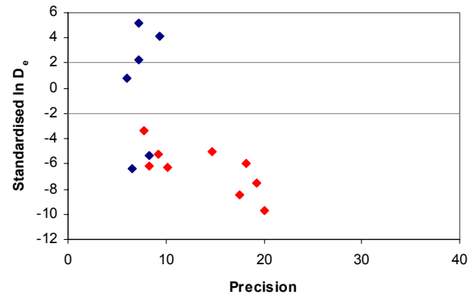

Fig. 6 Signal Analysis

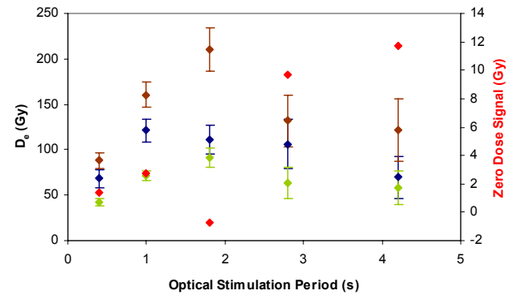

Fig. 7 Th & U Decay Activities

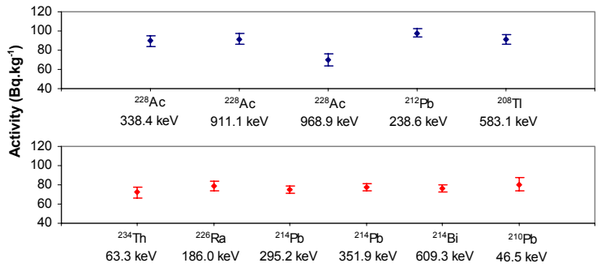

Fig. 8 Age Range

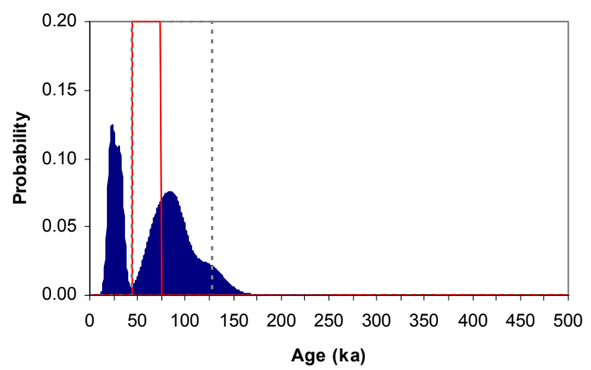

APPENDIX 20: MEASUREMENTS OF SAMPLE GL06045

Fig. 1 Signal Calibration

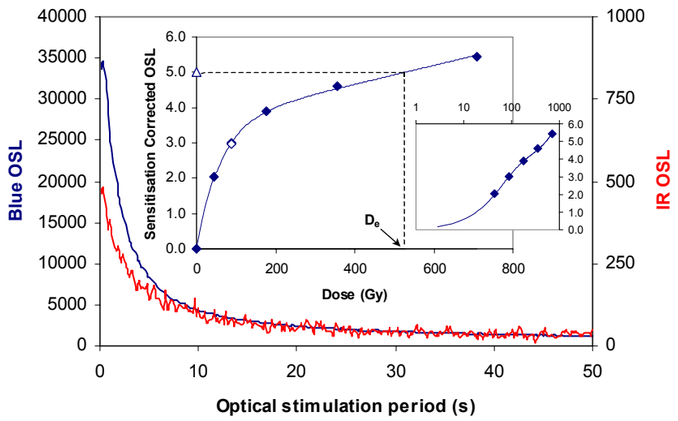

Signal Calibration Natural blue and laboratory-induced infrared (IR) OSL signals. Detectable IR signal decays are diagnostic of feldspar contamination. Inset, the natural blue OSL signal (open triangle) of each aliquot is calibrated against known laboratory doses to yield equivalent dose (D_e) values. Where D_e values are >40 Gy, a **pulsed irradiation** response is shown; pulsed irradiation D_e values are used in age calculations if significantly different from continuous irradiation-based D_e. Where D_e values are >100Gy, a log-linear plot of dose response is shown; D_e can be confidently interpolated if signal response increases with dose.

Irradiation-Preheat Cycling The acquisition of D_e values is necessarily predicated upon thermal treatment of aliquots succeeding environmental and laboratory irradiation. Repeated irradiation and thermal treatment results in aliquot sensitisation, rendering calibration of the natural signal inaccurate. This sensitisation can be monitored and corrected for. The accuracy of correction can be preheat dependent; irradiation-preheat cycling quantifies this dependence for laboratory-induced signals, examining the reproducibility of corrected OSL resultant of repeat laboratory doses.

D_e Preheat Dependence Quantifies the combined effects of thermal transfer and sensitisation on the natural signal. Insignificant adjustment in D_e may reflect limited influence of these effects

Dose Recovery Attempts to replicate the above diagnostic, yet provide improved resolution of thermal effects through removal of variability induced by heterogeneous dose absorption in the environment and using a precise lab dose to simulate natural dose. Based on this and preceding data an appropriate thermal treatment is selected to refine the final D_e value.

Inter-aliquot D_e distribution Provides a measure of inter-aliquot statistical concordance in D_e values derived from **natural** and **laboratory** irradiation. Discordant data (those points lying beyond **±2 standardised ln D_e**) reflects heterogeneous dose absorption and/or inaccuracies in calibration.

Signal Analysis Statistically significant increase in **natural** D_e value with signal stimulation period is indicative of a partially-bleached signal, provided a significant increase in D_e results from **simulated partial bleaching** along with insignificant adjustment in D_e for simulated **zero** and **full bleach** conditions. Ages from such samples are considered maximum estimates.

Th & U Decay Activities Statistical concordance (equilibrium) in the activities of daughter radioisotopes in the Th and U decay series may signify the temporal stability of D_r emissions from these chains. Significant differences (disequilibrium) in activity indicate addition or removal of isotopes creating a time-dependent shift in D_r values and increased uncertainty in the accuracy of age estimates

Age Range The **mean age range** provides an estimate of sediment burial period based on mean D_e and D_r values with associated analytical uncertainties. The probability distribution indicates the inter-aliquot variability in age. The **maximum influence** of temporal variations in D_r forced by minima-maxima variation in moisture content and overburden thickness may prove instructive where there is uncertainty in these parameters, however the combined extremes represented should not be construed as preferred age estimates.

Fig. 2 Irradiation-Preheat Cycling

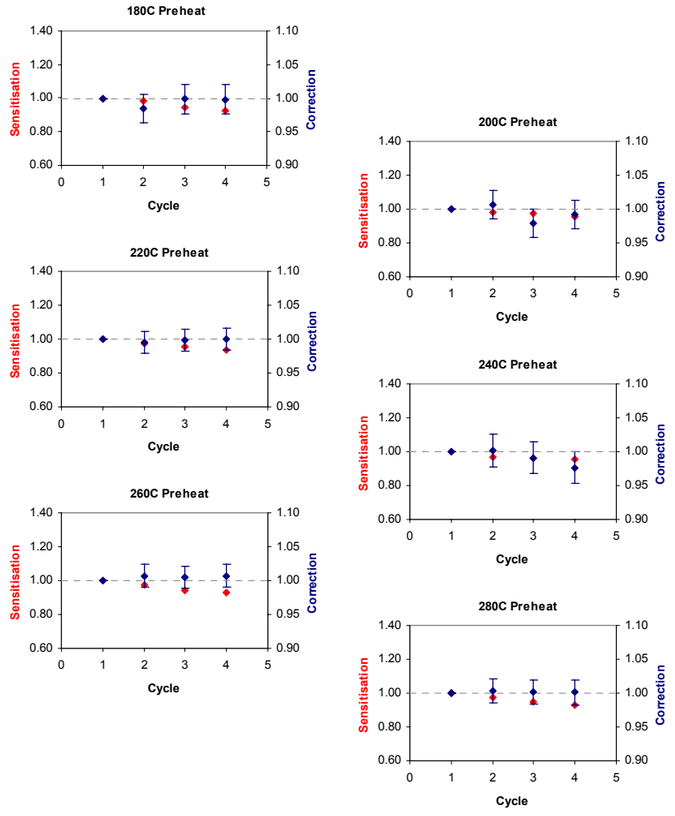

Fig. 3 D_e Preheat Dependence

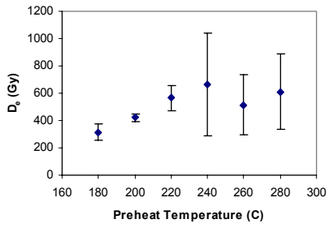

Fig. 4 Dose Recovery

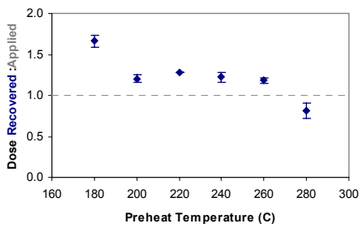

Sample: GL06045

Fig. 5 Inter-aliquot D_e distribution

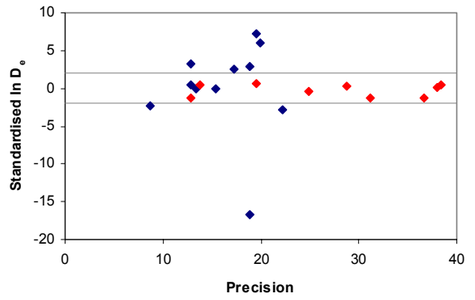

Fig. 6 Signal Analysis

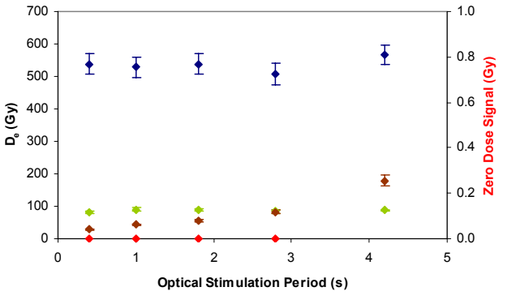

Fig. 7 Th & U Decay Activities

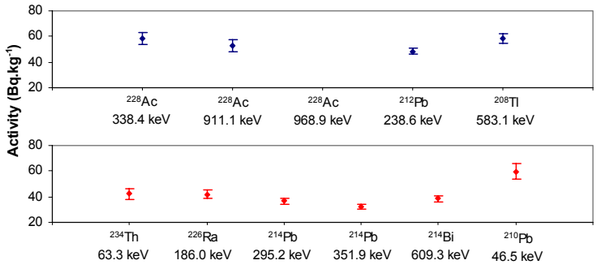

Fig. 8 Age Range

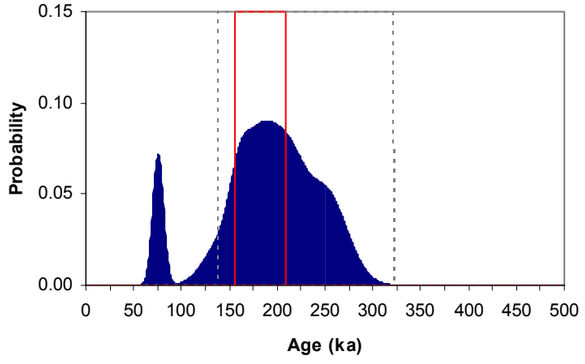

APPENDIX 21: MEASUREMENTS OF SAMPLE GL06046

Fig. 1 Signal Calibration

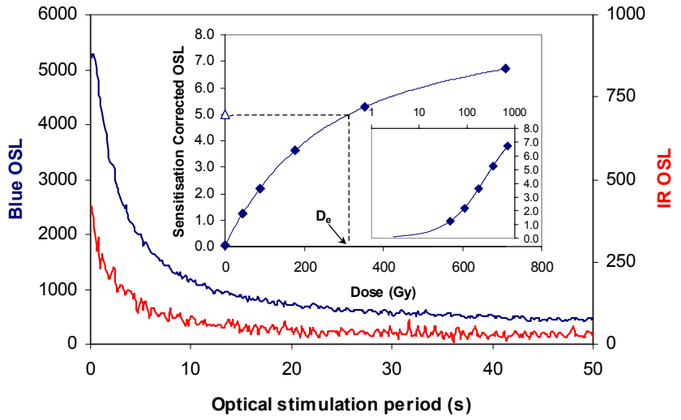

Signal Calibration Natural blue and laboratory-induced infrared (IR) OSL signals. Detectable IR signal decays are diagnostic of feldspar contamination. Inset, the natural blue OSL signal (open triangle) of each aliquot is calibrated against known laboratory doses to yield equivalent dose (D_e) values. Where D_e values are >40 Gy, a **pulsed irradiation** response is shown; pulsed irradiation D_e values are used in age calculations if significantly different from continuous irradiation-based D_e. Where D_e values are >100Gy, a log-linear plot of dose response is shown; D_e can be confidently interpolated if signal response increases with dose.

Irradiation-Preheat Cycling The acquisition of D_e values is necessarily predicated upon thermal treatment of aliquots succeeding environmental and laboratory irradiation. Repeated irradiation and thermal treatment results in aliquot sensitisation, rendering calibration of the natural signal inaccurate. This sensitisation can be monitored and corrected for. The accuracy of correction can be preheat dependent; irradiation-preheat cycling quantifies this dependence for laboratory-induced signals, examining the reproducibility of corrected OSL resultant of repeat laboratory doses.

D_e Preheat Dependence Quantifies the combined effects of thermal transfer and sensitisation on the natural signal. Insignificant adjustment in D_e may reflect limited influence of these effects

Dose Recovery Attempts to replicate the above diagnostic, yet provide improved resolution of thermal effects through removal of variability induced by heterogeneous dose absorption in the environment and using a precise lab dose to simulate natural dose. Based on this and preceding data an appropriate thermal treatment is selected to refine the final D_e value.

Inter-aliquot D_e distribution Provides a measure of inter-aliquot statistical concordance in D_e values derived from **natural** and **laboratory** irradiation. Discordant data (those points lying beyond **±2 standardised ln D_e**) reflects heterogeneous dose absorption and/or inaccuracies in calibration.

Signal Analysis Statistically significant increase in **natural** D_e value with signal stimulation period is indicative of a partially-bleached signal, provided a significant increase in D_e results from **simulated partial bleaching** along with insignificant adjustment in D_e for simulated **zero** and **full bleach** conditions. Ages from such samples are considered maximum estimates.

Th & U Decay Activities Statistical concordance (equilibrium) in the activities of daughter radioisotopes in the Th and U decay series may signify the temporal stability of D_r emissions from these chains. Significant differences (disequilibrium) in activity indicate addition or removal of isotopes creating a time-dependent shift in D_r values and increased uncertainty in the accuracy of age estimates

Age Range The **mean age range** provides an estimate of sediment burial period based on mean D_e and D_r values with associated analytical uncertainties. The probability distribution indicates the inter-aliquot variability in age. The **maximum influence** of temporal variations in D_r forced by minima-maxima variation in moisture content and overburden thickness may prove instructive where there is uncertainty in these parameters, however the combined extremes represented should not be construed as preferred age estimates.

Fig. 2 Irradiation-Preheat Cycling

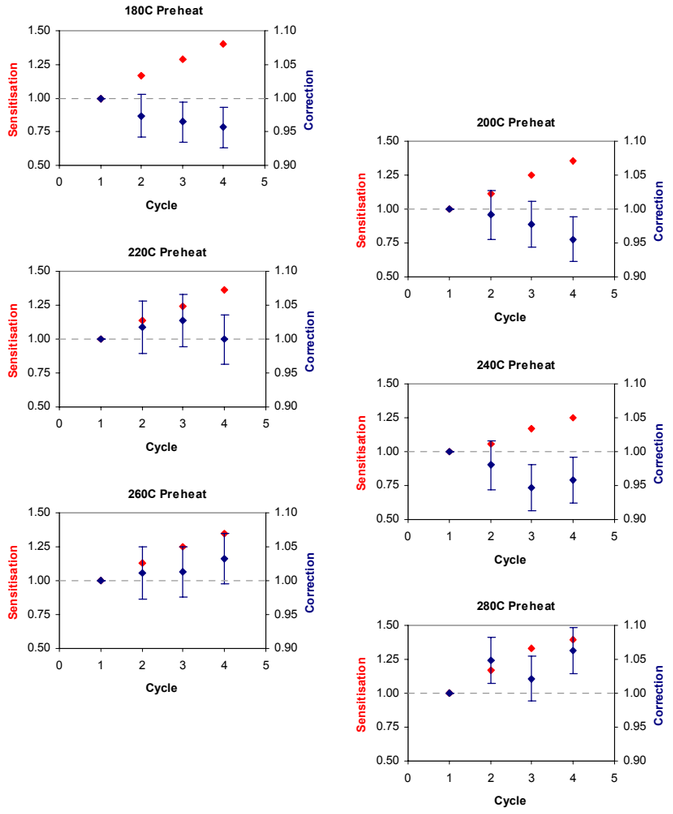

Fig. 3 D_e Preheat Dependence

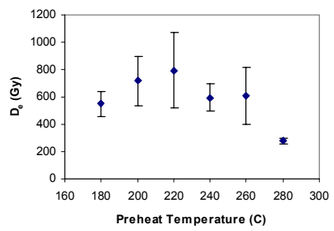

Fig. 4 Dose Recovery

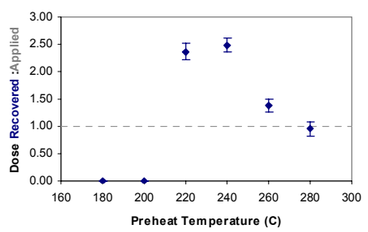

Sample: GL06046

Fig. 5 Inter-aliquot D_e distribution

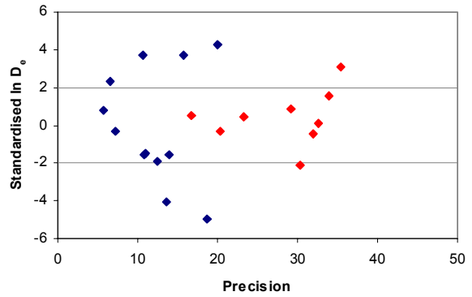

Fig. 6 Signal Analysis

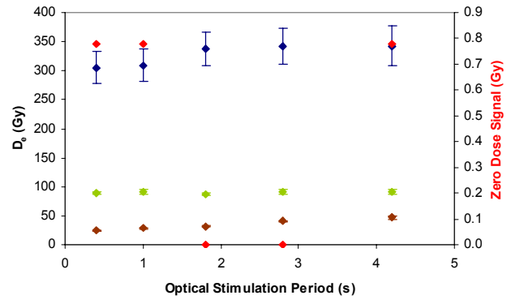

Fig. 7 Th & U Decay Activities

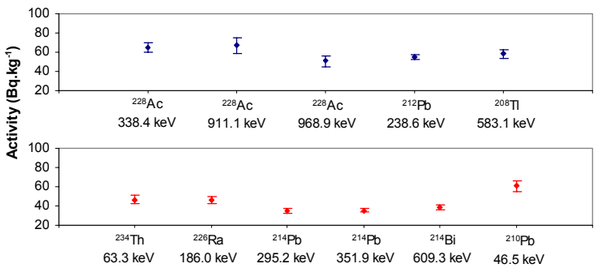

Fig. 8 Age Range

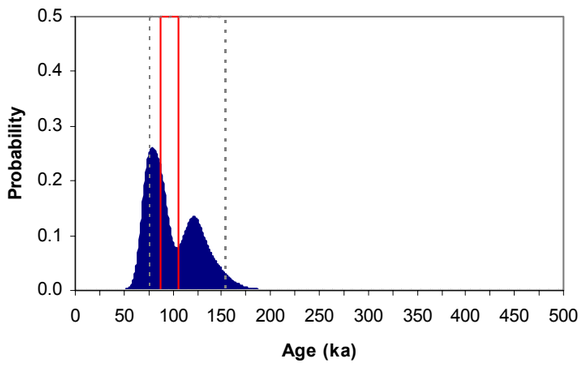

APPENDIX 22: MEASUREMENTS OF SAMPLE GL06047

Fig. 1 Signal Calibration

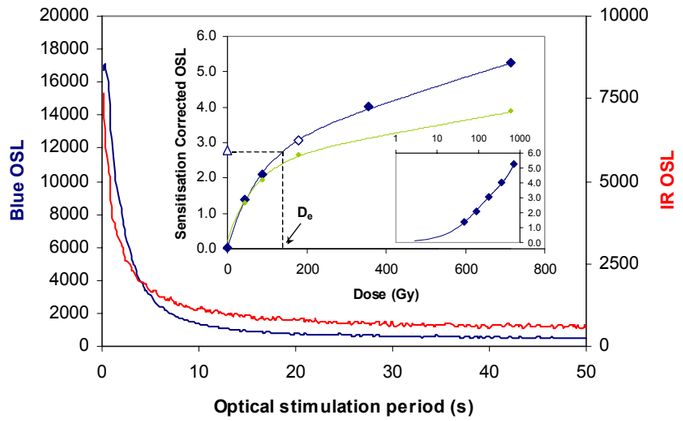

Signal Calibration Natural blue and laboratory-induced infrared (IR) OSL signals. Detectable IR signal decays are diagnostic of feldspar contamination. Inset, the natural blue OSL signal (open triangle) of each aliquot is calibrated against known laboratory doses to yield equivalent dose (D_e) values. Where D_e values are >40 Gy, a **pulsed irradiation** response is shown; pulsed irradiation D_e values are used in age calculations if significantly different from continuous irradiation-based D_e. Where D_e values are >100Gy, a log-linear plot of dose response is shown; D_e can be confidently interpolated if signal response increases with dose.

Irradiation-Preheat Cycling The acquisition of D_e values is necessarily predicated upon thermal treatment of aliquots succeeding environmental and laboratory irradiation. Repeated irradiation and thermal treatment results in aliquot sensitisation, rendering calibration of the natural signal inaccurate. This sensitisation can be monitored and corrected for. The accuracy of correction can be preheat dependent; irradiation-preheat cycling quantifies this dependence for laboratory-induced signals, examining the reproducibility of corrected OSL resultant of repeat laboratory doses.

D_e Preheat Dependence Quantifies the combined effects of thermal transfer and sensitisation on the natural signal. Insignificant adjustment in D_e may reflect limited influence of these effects

Dose Recovery Attempts to replicate the above diagnostic, yet provide improved resolution of thermal effects through removal of variability induced by heterogeneous dose absorption in the environment and using a precise lab dose to simulate natural dose. Based on this and preceding data an appropriate thermal treatment is selected to refine the final D_e value.

Inter-aliquot D_e distribution Provides a measure of inter-aliquot statistical concordance in D_e values derived from **natural** and **laboratory** irradiation. Discordant data (those points lying beyond **±2 standardised ln D_e**) reflects heterogeneous dose absorption and/or inaccuracies in calibration.

Signal Analysis Statistically significant increase in **natural** D_e value with signal stimulation period is indicative of a partially-bleached signal, provided a significant increase in D_e results from **simulated partial bleaching** along with insignificant adjustment in D_e for simulated **zero** and **full bleach** conditions. Ages from such samples are considered maximum estimates.

Th & U Decay Activities Statistical concordance (equilibrium) in the activities of daughter radioisotopes in the Th and U decay series may signify the temporal stability of D_r emissions from these chains. Significant differences (disequilibrium) in activity indicate addition or removal of isotopes creating a time-dependent shift in D_r values and increased uncertainty in the accuracy of age estimates

Age Range The **mean age range** provides an estimate of sediment burial period based on mean D_e and D_r values with associated analytical uncertainties. The probability distribution indicates the inter-aliquot variability in age. The **maximum influence** of temporal variations in D_r forced by minima-maxima variation in moisture content and overburden thickness may prove instructive where there is uncertainty in these parameters, however the combined extremes represented should not be construed as preferred age estimates.

Fig. 2 Irradiation-Preheat Cycling

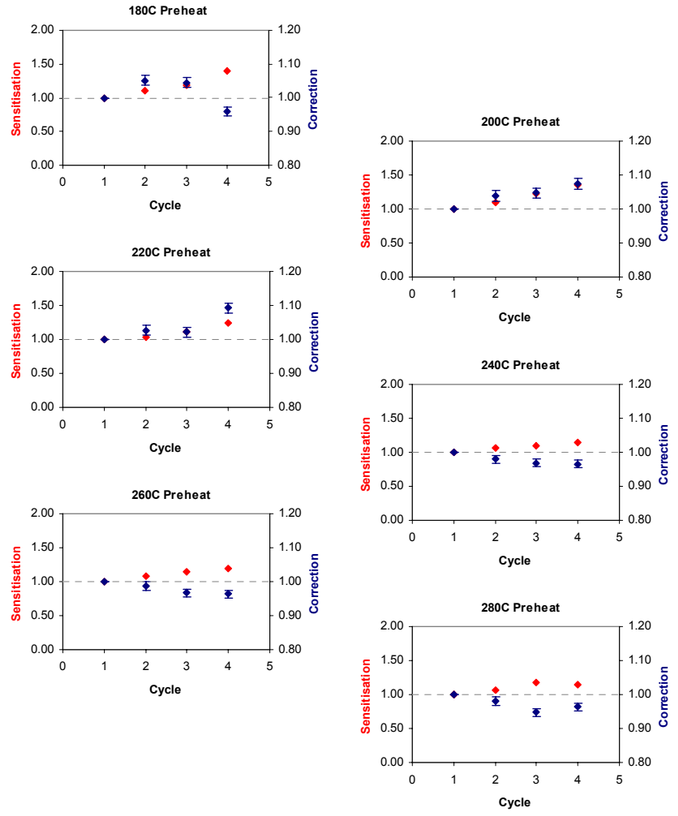

Fig. 3 D_e Preheat Dependence

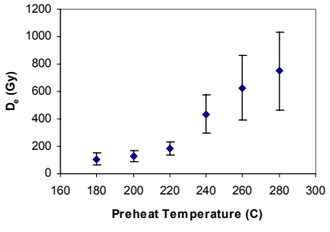

Fig. 4 Dose Recovery

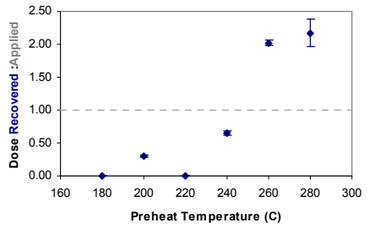

Fig. 5 Inter-aliquot D_e distribution

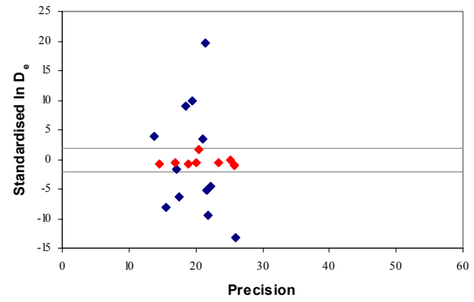

Fig. 6 Signal Analysis

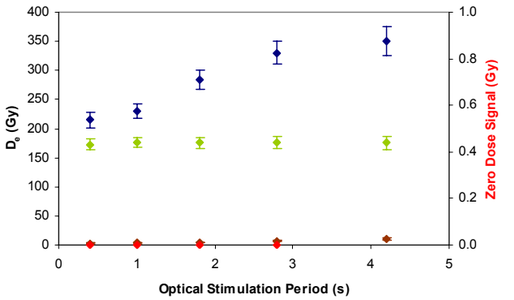

Fig. 7 Th & U Decay Activities

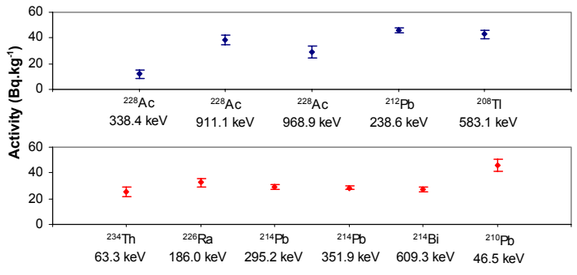

Fig. 8 Age Range

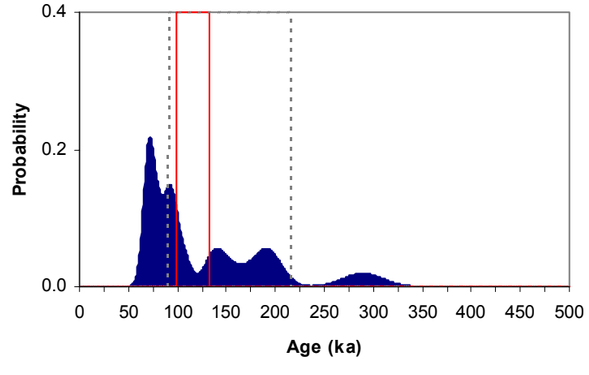

Sample: GL06047

APPENDIX 23: MEASUREMENTS OF SAMPLE GL06048

Fig. 1 Signal Calibration

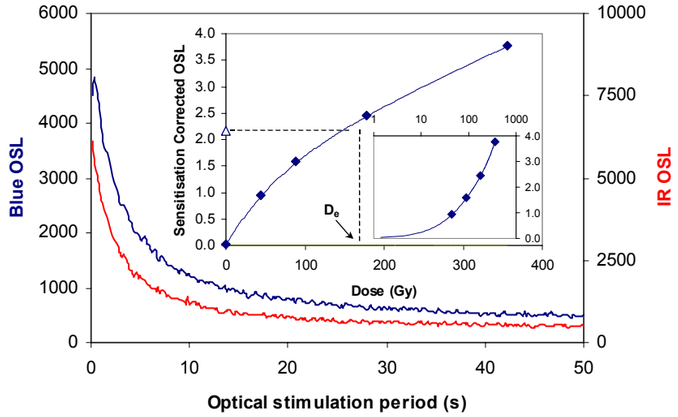

Signal Calibration Natural blue and laboratory-induced infrared (IR) OSL signals. Detectable IR signal decays are diagnostic of feldspar contamination. Inset, the natural blue OSL signal (open triangle) of each aliquot is calibrated against known laboratory doses to yield equivalent dose (D_e) values. Where D_e values are >40 Gy, a **pulsed irradiation** response is shown; pulsed irradiation D_e values are used in age calculations if significantly different from continuous irradiation-based D_e. Where D_e values are >100Gy, a log-linear plot of dose response is shown; D_e can be confidently interpolated if signal response increases with dose.

Irradiation-Preheat Cycling The acquisition of D_e values is necessarily predicated upon thermal treatment of aliquots succeeding environmental and laboratory irradiation. Repeated irradiation and thermal treatment results in aliquot sensitisation, rendering calibration of the natural signal inaccurate. This sensitisation can be monitored and corrected for. The accuracy of correction can be preheat dependent; irradiation-preheat cycling quantifies this dependence for laboratory-induced signals, examining the reproducibility of corrected OSL resultant of repeat laboratory doses.

D_e Preheat Dependence Quantifies the combined effects of thermal transfer and sensitisation on the natural signal. Insignificant adjustment in D_e may reflect limited influence of these effects

Dose Recovery Attempts to replicate the above diagnostic, yet provide improved resolution of thermal effects through removal of variability induced by heterogeneous dose absorption in the environment and using a precise lab dose to simulate natural dose. Based on this and preceding data an appropriate thermal treatment is selected to refine the final D_e value.

Inter-aliquot D_e distribution Provides a measure of inter-aliquot statistical concordance in D_e values derived from **natural** and **laboratory** irradiation. Discordant data (those points lying beyond **±2 standardised ln D_e**) reflects heterogeneous dose absorption and/or inaccuracies in calibration.

Signal Analysis Statistically significant increase in **natural** D_e value with signal stimulation period is indicative of a partially-bleached signal, provided a significant increase in D_e results from **simulated partial bleaching** along with insignificant adjustment in D_e for simulated **zero** and **full bleach** conditions. Ages from such samples are considered maximum estimates.

Th & U Decay Activities Statistical concordance (equilibrium) in the activities of daughter radioisotopes in the Th and U decay series may signify the temporal stability of D_r emissions from these chains. Significant differences (disequilibrium) in activity indicate addition or removal of isotopes creating a time-dependent shift in D_r values and increased uncertainty in the accuracy of age estimates

Age Range The **mean age range** provides an estimate of sediment burial period based on mean D_e and D_r values with associated analytical uncertainties. The probability distribution indicates the inter-aliquot variability in age. The **maximum influence** of temporal variations in D_r forced by minima-maxima variation in moisture content and overburden thickness may prove instructive where there is uncertainty in these parameters, however the combined extremes represented should not be construed as preferred age estimates.

Fig. 2 Irradiation-Preheat Cycling

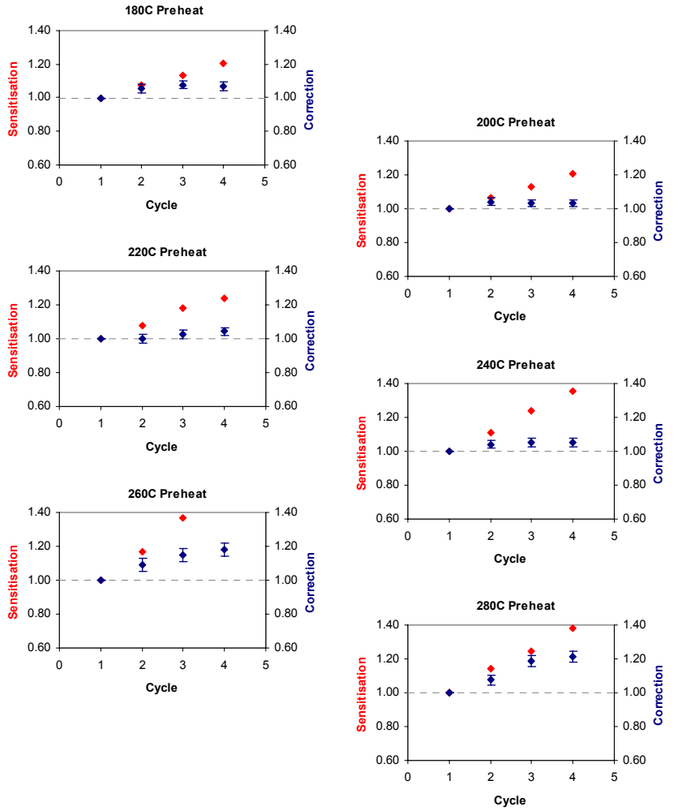

Fig. 3 D_e Preheat Dependence

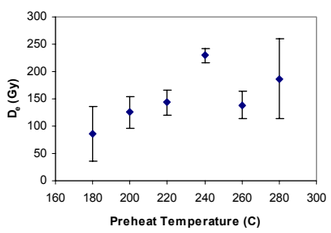

Fig. 4 Dose Recovery

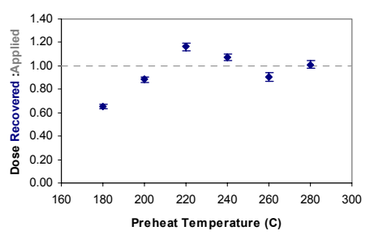

Fig. 5 Inter-aliquot D_e distribution

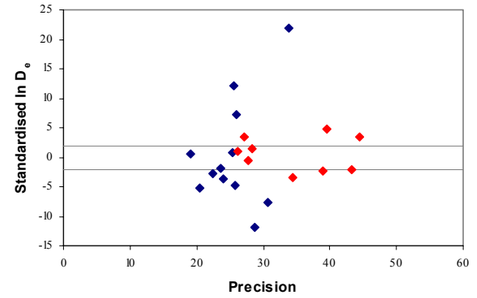

Fig. 6 Signal Analysis

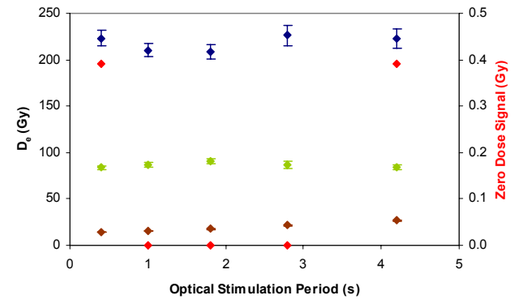

Fig. 7 Th & U Decay Activities

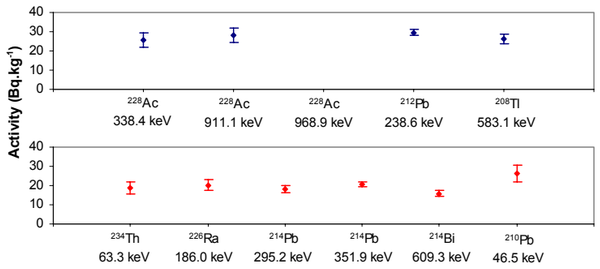

Fig. 8 Age Range

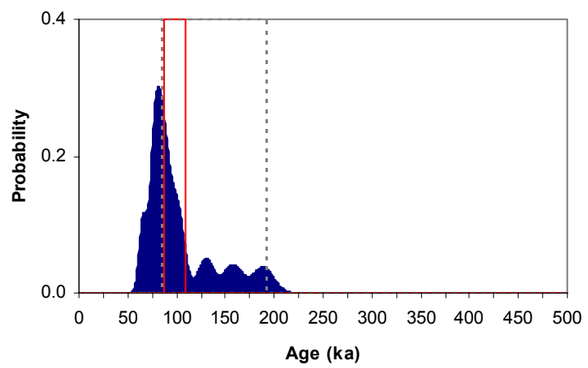

Sample: GL06048

APPENDIX 24: MEASUREMENTS OF SAMPLE GL06049

Fig. 1 Signal Calibration

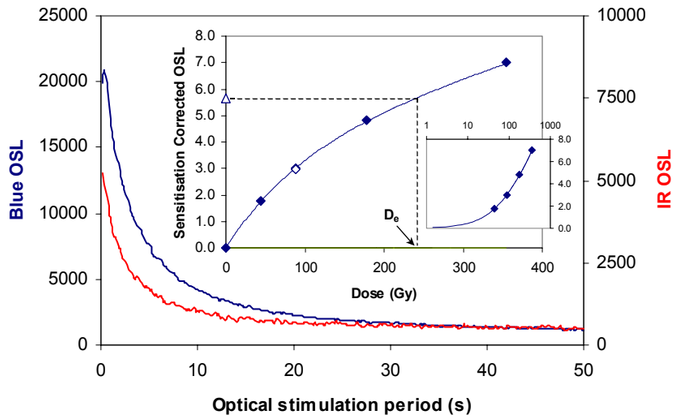

Signal Calibration Natural blue and laboratory-induced infrared (IR) OSL signals. Detectable IR signal decays are diagnostic of feldspar contamination. Inset, the natural blue OSL signal (open triangle) of each aliquot is calibrated against known laboratory doses to yield equivalent dose (D_e) values. Where D_e values are >40 Gy, a **pulsed irradiation** response is shown; pulsed irradiation D_e values are used in age calculations if significantly different from continuous irradiation-based D_e. Where D_e values are >100Gy, a log-linear plot of dose response is shown; D_e can be confidently interpolated if signal response increases with dose.

Irradiation-Preheat Cycling The acquisition of D_e values is necessarily predicated upon thermal treatment of aliquots succeeding environmental and laboratory irradiation. Repeated irradiation and thermal treatment results in aliquot sensitisation, rendering calibration of the natural signal inaccurate. This sensitisation can be monitored and corrected for. The accuracy of correction can be preheat dependent; irradiation-preheat cycling quantifies this dependence for laboratory-induced signals, examining the reproducibility of corrected OSL resultant of repeat laboratory doses.

D_e Preheat Dependence Quantifies the combined effects of thermal transfer and sensitisation on the natural signal. Insignificant adjustment in D_e may reflect limited influence of these effects

Dose Recovery Attempts to replicate the above diagnostic, yet provide improved resolution of thermal effects through removal of variability induced by heterogeneous dose absorption in the environment and using a precise lab dose to simulate natural dose. Based on this and preceding data an appropriate thermal treatment is selected to refine the final D_e value.

Inter-aliquot D_e distribution Provides a measure of inter-aliquot statistical concordance in D_e values derived from **natural** and **laboratory** irradiation. Discordant data (those points lying beyond **±2 standardised ln D_e**) reflects heterogeneous dose absorption and/or inaccuracies in calibration.

Signal Analysis Statistically significant increase in **natural** D_e value with signal stimulation period is indicative of a partially-bleached signal, provided a significant increase in D_e results from **simulated partial bleaching** along with insignificant adjustment in D_e for simulated **zero** and **full bleach** conditions. Ages from such samples are considered maximum estimates.

Th & U Decay Activities Statistical concordance (equilibrium) in the activities of daughter radioisotopes in the Th and U decay series may signify the temporal stability of D_r emissions from these chains. Significant differences (disequilibrium) in activity indicate addition or removal of isotopes creating a time-dependent shift in D_r values and increased uncertainty in the accuracy of age estimates

Age Range The **mean age range** provides an estimate of sediment burial period based on mean D_e and D_r values with associated analytical uncertainties. The probability distribution indicates the inter-aliquot variability in age. The **maximum influence** of temporal variations in D_r forced by minima-maxima variation in moisture content and overburden thickness may prove instructive where there is uncertainty in these parameters, however the combined extremes represented should not be construed as preferred age estimates.

Fig. 2 Irradiation-Preheat Cycling

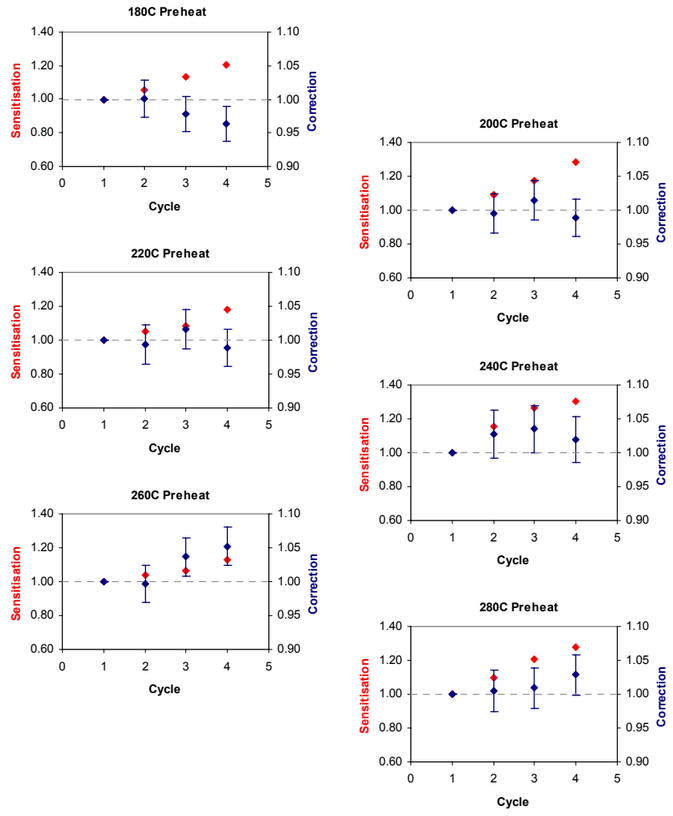

Fig. 3 D_e Preheat Dependence

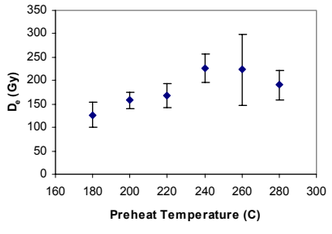

Fig. 4 Dose Recovery

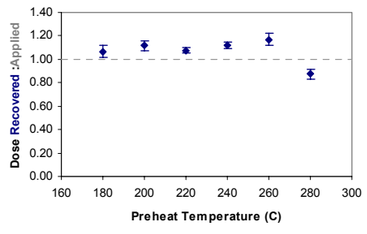

Sample: GL06049

Fig. 5 Inter-aliquot D_e distribution

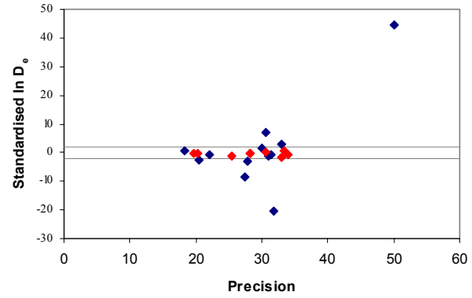

Fig. 6 Signal Analysis

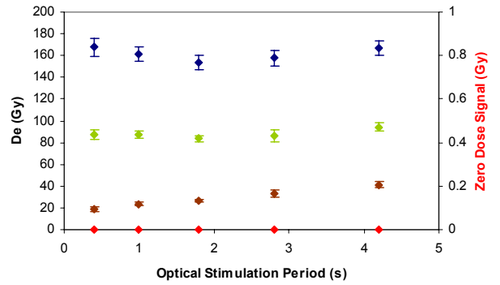

Fig. 7 Th & U Decay Activities

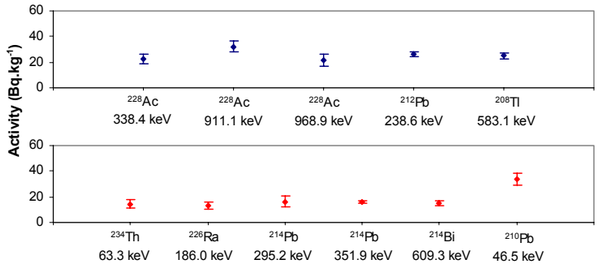

Fig. 8 Age Range

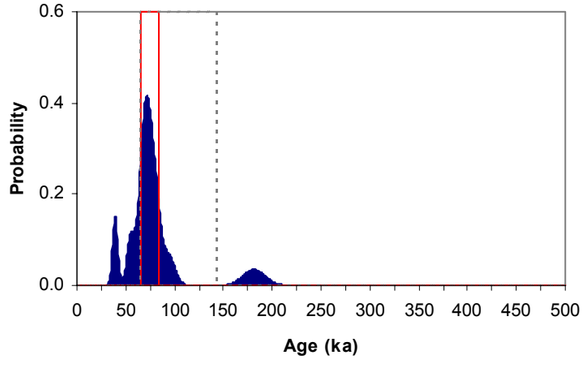

APPENDIX 25: MEASUREMENTS OF SAMPLE GL06057

Fig. 1 Signal Calibration

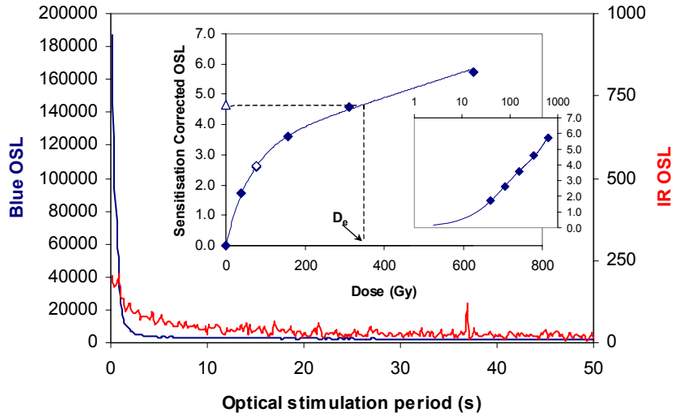

Signal Calibration Natural blue and laboratory-induced infrared (IR) OSL signals. Detectable IR signal decays are diagnostic of feldspar contamination. Inset, the natural blue OSL signal (open triangle) of each aliquot is calibrated against known laboratory doses to yield equivalent dose (D_e) values. Where D_e values are >40 Gy, a **pulsed irradiation** response is shown; pulsed irradiation D_e values are used in age calculations if significantly different from continuous irradiation-based D_e. Where D_e values are >100Gy, a log-linear plot of dose response is shown; D_e can be confidently interpolated if signal response increases with dose.

Irradiation-Preheat Cycling The acquisition of D_e values is necessarily predicated upon thermal treatment of aliquots succeeding environmental and laboratory irradiation. Repeated irradiation and thermal treatment results in aliquot sensitisation, rendering calibration of the natural signal inaccurate. This sensitisation can be monitored and corrected for. The accuracy of correction can be preheat dependent; irradiation-preheat cycling quantifies this dependence for laboratory-induced signals, examining the reproducibility of corrected OSL resultant of repeat laboratory doses.

D_e Preheat Dependence Quantifies the combined effects of thermal transfer and sensitisation on the natural signal. Insignificant adjustment in D_e may reflect limited influence of these effects

Dose Recovery Attempts to replicate the above diagnostic, yet provide improved resolution of thermal effects through removal of variability induced by heterogeneous dose absorption in the environment and using a precise lab dose to simulate natural dose. Based on this and preceding data an appropriate thermal treatment is selected to refine the final D_e value.

Inter-aliquot D_e distribution Provides a measure of inter-aliquot statistical concordance in D_e values derived from **natural** and **laboratory** irradiation. Discordant data (those points lying beyond **±2 standardised ln D_e**) reflects heterogeneous dose absorption and/or inaccuracies in calibration.

Signal Analysis Statistically significant increase in **natural** D_e value with signal stimulation period is indicative of a partially-bleached signal, provided a significant increase in D_e results from **simulated partial bleaching** along with insignificant adjustment in D_e for simulated **zero** and **full bleach** conditions. Ages from such samples are considered maximum estimates.

Th & U Decay Activities Statistical concordance (equilibrium) in the activities of daughter radioisotopes in the Th and U decay series may signify the temporal stability of D_r emissions from these chains. Significant differences (disequilibrium) in activity indicate addition or removal of isotopes creating a time-dependent shift in D_r values and increased uncertainty in the accuracy of age estimates

Age Range The **mean age range** provides an estimate of sediment burial period based on mean D_e and D_r values with associated analytical uncertainties. The probability distribution indicates the inter-aliquot variability in age. The **maximum influence** of temporal variations in D_r forced by minima-maxima variation in moisture content and overburden thickness may prove instructive where there is uncertainty in these parameters, however the combined extremes represented should not be construed as preferred age estimates.

Fig. 2 Irradiation-Preheat Cycling

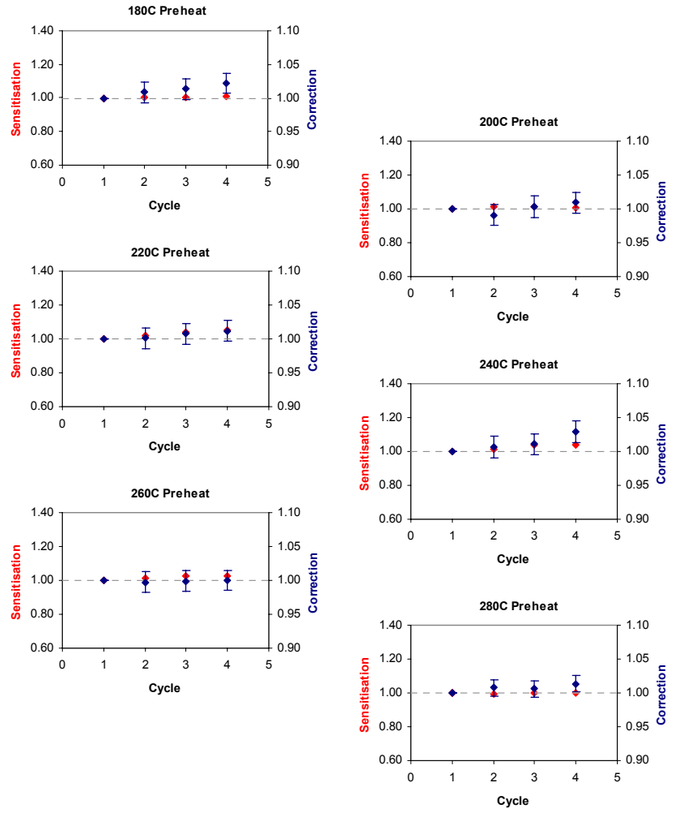

Fig. 3 D_e Preheat Dependence

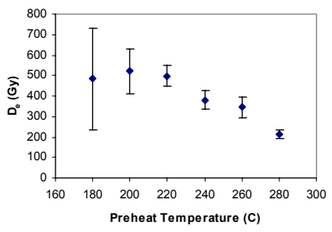

Fig. 4 Dose Recovery

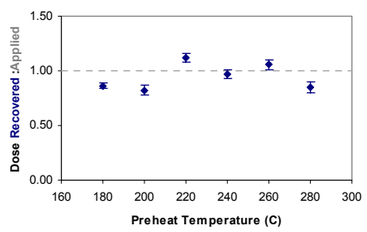

Sample: GL06057

Fig. 5 Inter-aliquot D_e distribution

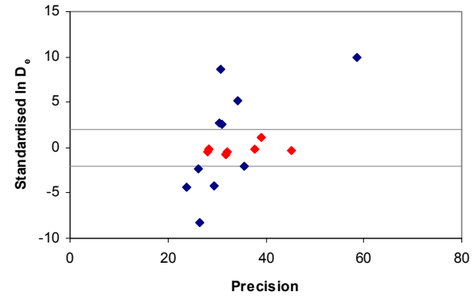

Fig. 6 Signal Analysis

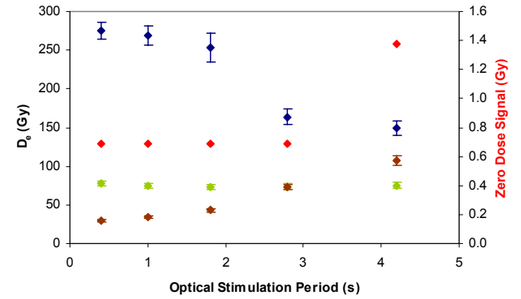

Fig. 7 Th & U Decay Activities

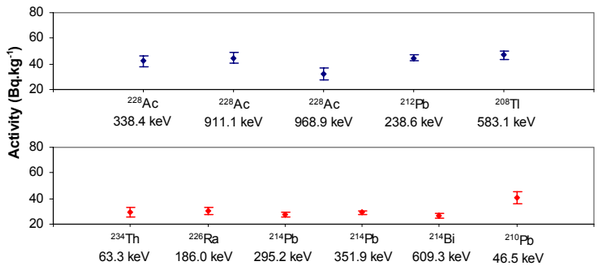

Fig. 8 Age Range

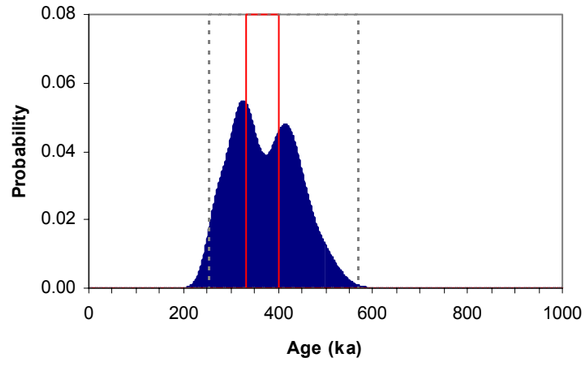

APPENDIX 26: MEASUREMENTS OF SAMPLE GL06058

Fig. 1 Signal Calibration

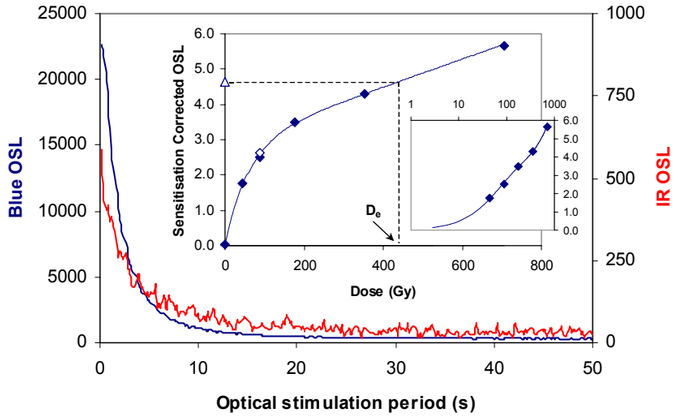

Signal Calibration Natural blue and laboratory-induced infrared (IR) OSL signals. Detectable IR signal decays are diagnostic of feldspar contamination. Inset, the natural blue OSL signal (open triangle) of each aliquot is calibrated against known laboratory doses to yield equivalent dose (D_e) values. Where D_e values are >40 Gy, a **pulsed irradiation** response is shown; pulsed irradiation D_e values are used in age calculations if significantly different from continuous irradiation-based D_e. Where D_e values are >100Gy, a log-linear plot of dose response is shown; D_e can be confidently interpolated if signal response increases with dose.

Irradiation-Preheat Cycling The acquisition of D_e values is necessarily predicated upon thermal treatment of aliquots succeeding environmental and laboratory irradiation. Repeated irradiation and thermal treatment results in aliquot sensitisation, rendering calibration of the natural signal inaccurate. This sensitisation can be monitored and corrected for. The accuracy of correction can be preheat dependent; irradiation-preheat cycling quantifies this dependence for laboratory-induced signals, examining the reproducibility of corrected OSL resultant of repeat laboratory doses.

D_e Preheat Dependence Quantifies the combined effects of thermal transfer and sensitisation on the natural signal. Insignificant adjustment in D_e may reflect limited influence of these effects

Dose Recovery Attempts to replicate the above diagnostic, yet provide improved resolution of thermal effects through removal of variability induced by heterogeneous dose absorption in the environment and using a precise lab dose to simulate natural dose. Based on this and preceding data an appropriate thermal treatment is selected to refine the final D_e value.

Inter-aliquot D_e distribution Provides a measure of inter-aliquot statistical concordance in D_e values derived from **natural** and **laboratory** irradiation. Discordant data (those points lying beyond **±2 standardised ln D_e**) reflects heterogeneous dose absorption and/or inaccuracies in calibration.

Signal Analysis Statistically significant increase in **natural** D_e value with signal stimulation period is indicative of a partially-bleached signal, provided a significant increase in D_e results from **simulated partial bleaching** along with insignificant adjustment in D_e for simulated **zero** and **full bleach** conditions. Ages from such samples are considered maximum estimates.

Th & U Decay Activities Statistical concordance (equilibrium) in the activities of daughter radioisotopes in the Th and U decay series may signify the temporal stability of D_r emissions from these chains. Significant differences (disequilibrium) in activity indicate addition or removal of isotopes creating a time-dependent shift in D_r values and increased uncertainty in the accuracy of age estimates

Age Range The **mean age range** provides an estimate of sediment burial period based on mean D_e and D_r values with associated analytical uncertainties. The probability distribution indicates the inter-aliquot variability in age. The **maximum influence** of temporal variations in D_r forced by minima-maxima variation in moisture content and overburden thickness may prove instructive where there is uncertainty in these parameters, however the combined extremes represented should not be construed as preferred age estimates.

Fig. 2 Irradiation-Preheat Cycling

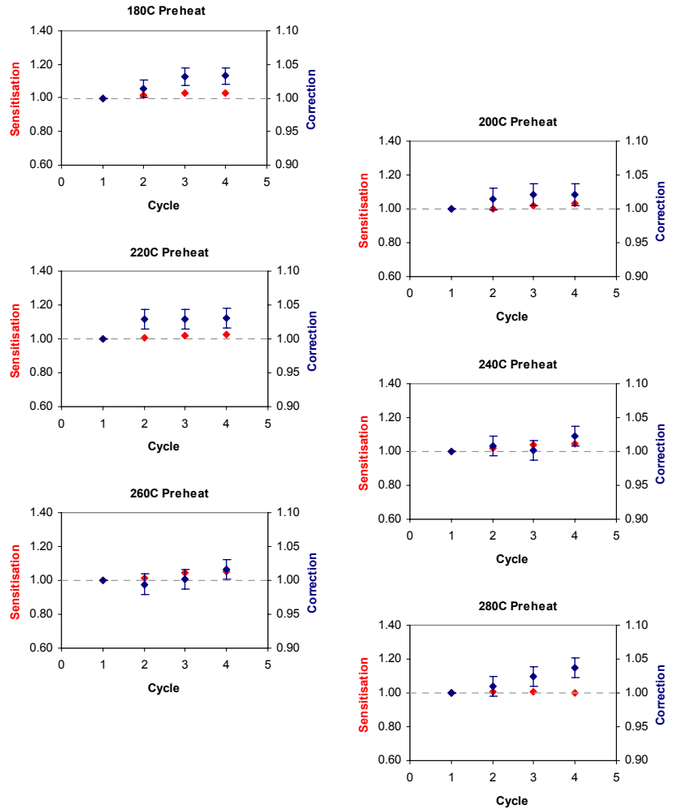

Fig. 3 D_e Preheat Dependence

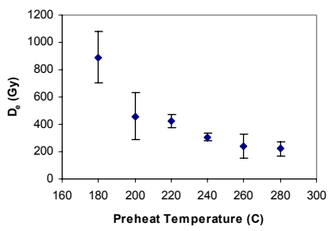

Fig. 4 Dose Recovery

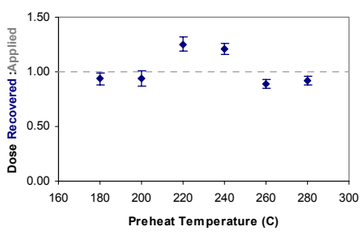

Sample: GL06058

Fig. 5 Inter-aliquot D_e distribution

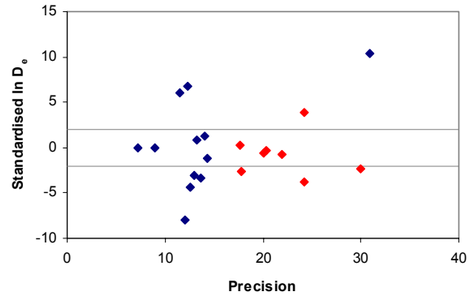

Fig. 6 Signal Analysis

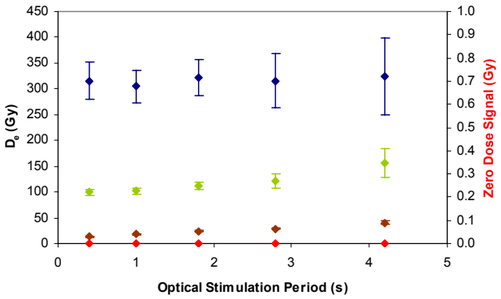

Fig. 7 Th & U Decay Activities

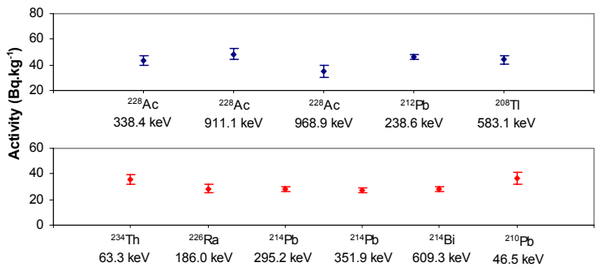
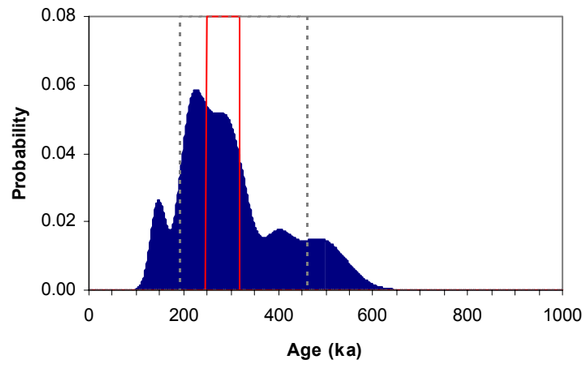
Fig. 8 Age Range